European Seismic Risk Model (ESRM20)

Report

Author(s):
Crowley, Helen; Dabbeek, Jamal; Despotaki, Venetia; Rodrigues, Daniela; Martins, Luis; Silva, Vitor; Romão, Xavier; Pereira, Nuno; Weatherill, Graeme; Danciu, Laurentiu

Publication date:
2021

Permanent link:
https://doi.org/10.3929/ethz-b-000590388

Originally published in:
EFEHR Technical Report 002, https://doi.org/10.7414/EUC-EFEHR-TR002-ESRM20

European Seismic Risk Model (ESRM20)

Helen Crowley, Jamal Dabbeek, Venetia Despotaki, Daniela Rodrigues, Luis Martins, Vitor Silva, Xavier Romão, Nuno Pereira, Graeme Weatherill, Laurentiu Danciu

EFEHR Technical Report 002 V1.0.1

Author Affiliations

Helen Crowley[1], Jamal Dabbeek[1], Venetia Despotaki[2*], Daniela Rodrigues[1*], Luis Martins[2], Vitor Silva[2], Xavier Romão[3], Nuno Pereira[3*], Graeme Weatherill[4], Laurentiu Danciu[5]

[1] EUCENTRE Foundation, Pavia, Italy
[2] GEM Foundation, Pavia, Italy
[3] University of Porto, Porto, Portugal
[4] GFZ Potsdam, Germany
[5] ETH Zurich, Switzerland
** former affiliation*

Citation advice

Crowley H., Dabbeek J., Despotaki V., Rodrigues D., Martins L., Silva V., Romão, X., Pereira N., Weatherill G. and Danciu L. (2021) *European Seismic Risk Model (ESRM20)*, EFEHR Technical Report 002, V1.0.1, 84 pp, https://doi.org/10.7414/EUC-EFEHR-TR002-ESRM20

Table of Contents

Acknowledgments

We would like to thank Domenico Giardini for supporting the need for a community-developed European seismic risk model, and for including such activity as a work package within the SERA project (http://www.sera-eu.org/en/activities/joint-research/). Much of the research that is presented in this report would not have been possible without that support.

The many activities leading towards the release of the European Seismic Risk Model (ESRM20) have also been supported by the RISE, EPOS-IP and EPOS-SP projects (all under the framework of the European Union's Horizon 2020 research and innovation programme). Additional financial support for the associated services has been provided by EPOS (European Plate Observing System), and in particular the Italian division of EPOS (EPOS-Italia). In-kind support has also been provided by GEM (the Global Earthquake Model Foundation).

We are grateful to the following individuals that have contributed to the development of the European Seismic Risk Model v2020 (ESRM20) in various ways, from data provision to workshop participation to website development:

Christoph Adam, Naida Ademovic, Armando Aguilar Melendez, Sinan Akkar, Alexander Allman, Anton Andonov, Drazen Aničić, António Araújo Correia, Josip Atalic, Anže Babič, Paolo Bazzurro, Celine Beauval, Maria Belen Benito Oterino, Rita Bento, Bjarni Bessason, Huseyin Bilgin, Jovana Borozan, Barbara Borzi, Svetlana Brzev, José Miguel Castro, Miguel Castro, Serena Cattari, Francesco Cavalieri, Catarina Costa, Fabrice Cotton, Irina Dallo, James Daniell, Manya Deyanova, Matiaz Dolsek, Kemal Edip, Leandra Erberle, Licia Faenza, Giulia Fagà, Donat Fäh, Marta Faravelli, Gabriele Ferro, Rainer Flesch, Stuart Alexander Fraser, Paolo Gamba, Andrea Giorgi, Cécile Gracianne Hidalgo, Marin Grubišić, Philippe Gueguen, Franco Giullermo, Marijana Hadzima-Nyarko, Ufuk Hancilar, Anna Karatzetzou, Philipp Kästli, Danai Kazantzidou, Alireza Khodaverdian, Fortunat Kind, Indranil Kongar, Sreeram Reddy Kotha, Pauline Kruiver, Olga Ktenidou, Nicolas Kyriakides, Pierre Labbé, Sergio Lagomarsino, Dominik Lang, Damir Lazarević, Anne Lemoine, Wolfgang Lenhardt, Dimitrios Lignos, Paivi Mantyniemi, Michèle Marti, Alberto Michelini, Zoran Milutinović, Amaryllis Mouyiannou, Matteo Nastasi, Cecilia Nievas, Sevgi Ozcebe, Marco Pagani, Athanasios Papadopoulos, Myrto Papaspiliou, Nicole Paul, Florin Pavel, Gordana Pavić, Daniele Perrone, Crescenzo Pettrone, Rui Pinho, Kyriazis Pitilakis, Antonios Pomonis, Nicolas Ponard, Adrien Pothon, Evi Riga, Agathe Roullé, Radmila Šalić, M. Abdullah Sandikkaya, Marta Šavor Novak, Mattias Schmid, John Schneider, Veronika Shendova, Zvonko Sigmund, Michele Simionato, Anselm Smolka, Luis Sousa, Elena Speranza, Alexandru Tiganescu, Dragos Toma-Danila, Paolo Tormene, Bruno Tourlière, Georgios Tsionis, Mario Uroš, Radu Vacareanu, Dimitrios Vamvatsikos, Enes Veliu, Nadja Valenzuela, Susana Vilanova, Stefan Wiemer, Jochen Woessner, Catalina Yepes, Mustafa Tolga Yilmaz, Simona Zaugg, Jure Žižmond, Zeljko Zugic.

We would also like to thank the individuals that anonymously contributed to two surveys, one on a beta version of the maps on the risk.EFEHR platform (risk.efehr.org) and another on the seismic risk index map and poster (to be released in Spring 2022).

Executive Summary

This technical report describes the European Seismic Risk Model (ESRM20), a new, open model of seismic risk that has been supported by the European Union's Horizon 2020 research and innovation programme in the framework of the projects SERA, RISE, EPOS-IP, EPOS-SP, and has been developed in collaboration with the Global Earthquake Model (GEM Foundation).

This report describes the development of the main components of ESRM20 (namely stochastic catalogues and ground motion fields, exposure models and vulnerability models), provides clear indications on where to access the models (and associated source data and tools), explains how the components have been combined in the estimation of key metrics of probabilistic seismic risk, and presents a summary of the risk results. You can directly access all material and products related to ESRM20 by visiting the http://risk.efehr.org website.

The stochastic catalogues and ground motion fields have been computed using the European Seismic Hazard Model (ESHM20), which is summarized herein and described in more detail in Danciu et al. (2021). The European exposure model has been developed using mainly public census data and contains an estimated 143 Million buildings, which contain an average of 460 Million occupants (over a typical 24-hour period), and a total replacement cost (structural, non-structural and contents) of 50 Trillion Euros, of which 66% is from the residential building stock. A total of 512 vulnerability models have been developed to cover the different classes of buildings within the European building stock, using an analytical approach to represent the response of buildings to earthquake ground shaking. A number of tests and consistency checks, including the estimation of losses from recent damaging earthquakes, have been carried out during the development of these components. The table below summarises the links to access the source data and tools, as well as associated maps and web services, for these components:

Component	**Access to Component Data/Tools**	**Access to Component Maps/Web Services**
Source model logic tree	See Danciu et al. (2021)	http://hazard.efehr.org
Ground-motion model logic tree	See Danciu et al. (2021)	http://hazard.efehr.org
Site Response Model	https://gitlab.seismo.ethz.ch/efehr/esrm20_sitemodel	https://maps.eu-risk.eucentre.it/tags/site-response/
Exposure Models	https://gitlab.seismo.ethz.ch/efehr/esrm20_exposure	https://maps.eu-risk.eucentre.it/tags/exposure/
Vulnerability Model	https://gitlab.seismo.ethz.ch/efehr/esrm20_vulnerability	https://vulncurves.eu-risk.eucentre.it/
Scenario Testing	https://gitlab.seismo.ethz.ch/efehr/esrm20_scenario_tests	https://maps.eu-risk.eucentre.it/tags/scenarios/

If you make use of any of these services, please note that they carry a CC-BY license[1] and you should cite the work using the credits/attribution information provided at each of these web links.

[1] https://creativecommons.org/licenses/by/4.0/

The two main risk metrics that can be computed with this first version of the European seismic risk model are economic loss due to direct costs to repair/replace the buildings (residential, commercial and industrial) and loss of life of occupants due to damage/collapse of those buildings. The probability of these losses is accounted for in the risk model, leading to estimations of the average annual losses (i.e. the long-term mean loss per year due to earthquake ground shaking) and losses with specific return periods (i.e. the long-term mean loss value due to earthquake ground shaking that is expected to be equalled or exceeded at least once every X years, where X varies from 50 to 1000).

According to ESRM20, the average annual economic loss in Europe is around 7 Billion EUR, with almost 70% of this loss occurring in Italy, Turkey and Greece. The average annual loss of life is estimated to be around 900 fatalities, with over 75% of those fatalities in Italy and Turkey alone. Mid-rise reinforced concrete frames with infill panels designed to outdated seismic design codes, together with low-rise unreinforced masonry buildings, are the two building classes that contribute most to both economic losses and loss of life in Europe. The model has been tested using a number of empirical loss databases and the initial outcomes are encouraging and provide a sufficient level of confidence in this first version of the model. Nevertheless, continued improvements to the model are expected following this open release, as more feedback and additional testing is provided by the scientific community.

Some precomputed results from ESRM20 are available through maps and web services at the following link: https://maps.eu-risk.eucentre.it/tags/risk/. The OpenQuake-engine input files of the model have been released at the following link for reproducibility of the results presented herein and to allow users to further explore the seismic risk model: https://gitlab.seismo.ethz.ch/efehr/esrm20. If you make use of these files or the information provided in this technical report in any way, please cite as follows:

Crowley H., Dabbeek J., Despotaki V., Rodrigues D., Martins L., Silva V., Romão, X., Pereira N., Weatherill G. and Danciu L. (2021) European Seismic Risk Model (ESRM20), EFEHR Technical Report 002, V1.0.0, https://doi.org/10.7414/EUC-EFEHR-TR002-ESRM20

1 Introduction

1.1 A New Seismic Risk Model for Europe

Whilst there have been many European projects over the past 30 years dealing with aspects of seismic hazard and risk, the SERA project (2017-2020) provided the first opportunity for the scientific community to integrate this research towards the development of a uniform seismic risk model for Europe (denoted ESRM20 herein). This model is now being openly released by the European Facilities for Earthquake Hazard and Risk (EFEHR), a consortium of European organisations aimed at advancing earthquake hazard and risk assessment.

The main components of ESRM20 have been developed by a core team (i.e. the authors of this report), with the input from a large number of people that have contributed in numerous ways[2], including through participation in SERA project workshops, census data retrieval and translation, local expert knowledge on buildings, expert recommendations and feedback on modelling and methodologies, risk results review, specification of user/stakeholder needs, and website/software/web services development. This model is therefore the first attempt at a community-developed seismic risk model for Europe, and through its open and transparent release, an even greater participation is expected for all future versions.

1.2 The Importance of Open Data and Licensing

Since the emergence of the first loss-modelling companies in the 1980's, many of the advances in earthquake loss software and modelling have taken place in the private global finance/insurance sector. In the 1990's the release of the free HAZUS (HAZards United States) software (FEMA, 1999) provided estimates of scenario seismic, flood and wind losses in any community in the U.S., and whilst it was a pioneer in providing transparent loss modelling solutions to the public sector, the software itself was not openly available. In 2007, the Alliance for Global Open Risk Analysis (AGORA) was founded to support the development of open software for risk analysis (Scawthorn, 2008). Soon after, in 2009, the public-private non-profit GEM (Global Earthquake Model) Foundation (www.globalquakemodel.org) was incorporated with a mission to build capacity around the globe to assess and manage risk through open, transparent and collaborative seismic risk assessment data and tools/software. Within a few years a paradigm shift started to take place within the private sector, with increased transparency being demanded of the commercial loss models, leading to initiatives such as the Oasis Loss Modelling Framework (https://oasislmf.org/).

The GEM Foundation recently celebrated the 10-year anniversary of the release of the OpenQuake-engine, an open source software for seismic hazard and risk assessment (Pagani et al., 2014; Silva et al., 2014) that has been used in numerous hazard and loss modelling efforts carried out by both the public and private sector. Examples include the 2013 European seismic hazard model (Woessner et al., 2015), national risk models for Costa Rica (Calderon and Silva, 2018), Iran (Motamed et al., 2017) and Italy (DPC, 2018) and validation of the software used for the seismic hazard assessment of nuclear power plants (Bommer et al., 2013; Tromans et al., 2019). In 2018 the GEM Foundation released the Global Seismic Risk Map (GEM, 2018), developed using a mosaic of individual risk models which were produced as part of regional programmes or bilateral collaborations between GEM and national institutions (Silva et al., 2020). The GEM Foundation has recently started to openly release some of the models that were used to develop the global seismic risk map, thus paving the way for reproducibility of the risk results, a basic and unavoidable principle of modern science (Popper, 2002). Such transparency furthermore ensures

[2] See Acknowledgements for a full list of names. Online version here: http://risk.efehr.org/contributors/

that all aspects of scientific methods and results are understood, available for critique, compliment, or reuse. This not only meets a social imperative, it also allows others to test new questions with existing data, makes it easier to identify and correct errors, and helps unmask academic fraud.

The EFEHR Consortium decided in its first General Assembly in September 2020 to openly release all products associated with the European hazard and risk models. The source data, input models, software and outputs of ESRM20 are thus being openly released with a Creative Commons Attribution 4.0 International license (https://creativecommons.org/licenses/by/4.0/). This license allows re-users to distribute, remix, adapt, and build upon the material in any medium or format, so long as attribution is given to the creator. The license allows for commercial use. Each product of ESRM20 is being released with a clear notice on how it should be cited in order to allow users to easily abide by the license.

1.3 Existing Estimates of European Seismic Risk

In 2015 the United Nations International Strategy for Disaster Risk Reduction (UNISDR) released the Global Assessment Report (GAR, 2015) which used probabilistic seismic risk assessment to estimate the uniform average annual losses (AAL) for a number of perils, including earthquakes, at the global scale. The exposure model was based on a top-down approach, whereby national/regional population, socioeconomic data and building-type information were used as proxies to estimate the spatial distribution of building counts (DeBono and Chatenoux, 2015). A probabilistic seismic hazard model was developed using the NEIC-USGS earthquake catalogue together with hundreds of seismic sources distributed across six tectonic regions (Ordaz et al., 2014). The vulnerability functions were region specific with specific studies being carried out in Asia Pacific and Latin America, whilst in other regions, including Europe, the models from HAZUZ (FEMA, 2004) were used (GAR, 2015). Table 1.1 presents the top ranked countries in Europe according to the GAR (2015) estimated economic AAL.

Corbane et al. (2017) presented a feasibility study for a quantitative European seismic risk assessment using open datasets available across the EU27 countries. The calculated risk was conditional on the 475-year return period hazard on rock provided by the ESHM13 model which was converted to macroseismic intensity based on a number of different ground motion to intensity conversion equations. The exposure model made use of the European gridded building database developed in the NERIES project (and expanded to include Croatia) and the macroseismic method developed by Giovinazzi and Lagomarsino (2004) was used to represent the vulnerability of the buildings. The ranking of the top 10 countries (out of the 27 considered) in terms of the selected risk metric (which it is worth noting is different to the one used to rank the GAR results) is also presented in Table 1.1.

The European results of GEM's Global Seismic Risk Map (v2018.1), introduced previously, was based on an early version of the European Exposure Model developed in the SERA project (see Crowley et al., 2020). The vulnerability model made use of a global set of vulnerability functions (Martins and Silva, 2018; Martins and Silva, 2020), whilst the ESHM13 hazard model (Woessner et al., 2015) was used together with site amplification modelled using topographic slope to approximate V_{S30} (Wald and Allen, 2007). Table 1.1 includes the top ranked countries in Europe according to the estimated economic AAL in GEM's Global Seismic Risk Map (v2018.1).

The top 10 countries in terms of direct economic losses found within the disaster databases from the NatCatService (MunichRe, 2019)[3] and the Centre for Research on the Epidemiology of Disasters (CRED)'s

[3] The list provided in Table 1.1 was provided by the GEM Foundation that has access to the NatCatService data (up to the end of 2018).

EMDAT database (EMDAT, n.d.) have also been added to Table 1.1. It is important to note that these disaster databases cover the entire built environment. Both the NatCatService and EMDAT are based on public sources of economic loss, though the former has been continuously updated which leads to some discrepancies between the values in the two databases.

Table 1.1 shows that Italy, Greece and Belgium are ranked in the top 10 of all of the studies considered herein, and Turkey and Germany are ranked in four of the five studies (with Turkey not having been considered in the study by Corbane et al. (2017) and Germany not showing up in the top 10 countries in the NatCatService database). France and Romania all feature in the numerical loss models, but are not present in the observed disaster databases (most likely due to the limited time frame considered for the latter). Croatia is present in the GEM (2018) model and the two observed disaster databases. Whilst this comparison between the numerical models and the observed data is important for consistency checking purposes, it is clear that around 40 years of damage data is not long enough to provide an unbiased ranking of the European countries in terms of their levels of seismic risk. Nevertheless, this comparison shows that there is a fairly high level of consistency amongst the most 'at risk' countries in Europe. These estimates of seismic risk across Europe can provide a benchmark against which the ESRM20 should be compared, as will be investigated later in this report.

Table 1.1 Ranking of countries based on estimated AAL from GEM 2018.v1 and the GAR, the losses conditional on 475-year return period hazard according to Corbane et al. (2017), and on observed losses from the NatCatService and EMDAT disaster databases. The dark blue coloured cells represent countries that are present in all studies, the light blue cells are present in four out of the five studies and the light grey cells are present in three of the studies.

Estimated economic *AAL*		**Economic losses given 475-year return period hazard**	**Observed economic losses**	
GEM 2018.v1	GAR (2015)	Corbane et al. (2017)*	NatCatService (1980-2017)	EMDAT (1980-2021)
Turkey	Italy	Italy	Italy	Italy
Italy	Greece	Slovakia	Turkey	Turkey
Greece	Germany	Romania	Greece	Greece
Romania	Turkey	Slovenia	Moldova	Croatia
France	United Kingdom	Greece	Spain	Albania
Germany	Switzerland	Germany	Croatia	Spain
Cyprus	France	France	Portugal	Belgium
Bulgaria	Romania	Belgium	Iceland	Serbia
Austria	Netherlands	Bulgaria	Serbia	Portugal
Belgium	Belgium	Hungary	Belgium	Germany

** Note that only the EU27 countries (in 2017) were considered in this study and so Turkey, Switzerland, Croatia, Moldova, Iceland, Serbia and Albania (present in the other studies) were not included*

Whilst much of the data used to develop the GAR (2015), Corbane et al. (2017) and GEM (2018) models is publicly available, it has not been released in a manner that easily enables reproducibility of the results, and thus it is not straightforward to explain the differences in the countries in Table 1.1. On the other hand, by openly releasing ESRM20 in a way that allows full reproducibility, scientific and professional communities will be able to investigate the drivers of risk in different countries, thus allowing the results to be fully understood and explained.

1.4 Outline of Report

This report provides a technical description of the main components of ESRM20 (namely the stochastic catalogues and ground motion fields, the exposure models and the vulnerability models), provides clear indications on where to access the models (and associated source data and tools), explains how the components have been combined in the estimation of key metrics of probabilistic seismic risk, and presents a summary of the risk results. A number of academic papers have been published during the development of the model, and whilst readers will be directed to these manuscripts for further details, where relevant, it should be noted that this technical report provides the latest summary of all final decisions and assumptions of the model.

2 Framework for Regional Seismic Risk Assessment

This Chapter discusses important risk metrics and outlines those that can be computed using this first release of the European Seismic Risk Model. The various options for assessing these seismic risk metrics are defined and the seismic risk framework and software used to produce the selected outputs for ESRM20 is presented.

2.1 Risk Metrics

Earthquakes can cause a number of undesirable outcomes (consequences) when strong ground shaking impacts the built environment such as:

- Disturbance to the occupants of buildings;
- Non-structural damage of the buildings requiring repair;
- Structural damage of the buildings requiring repair or even reconstruction of the building;
- Environmental impact (e.g. embodied energy and carbon during the repair / demolition and building reconstruction);
- Economic loss due to direct costs to repair damage / replace buildings and downtime (i.e. losses incurred whilst the buildings cannot be used);
- Injuries to occupants / passers-by due to damage / collapse of the buildings;
- Loss of life of occupants / passers-by due to damage / collapse of the buildings.

A seismic risk assessment may typically focus on one or two of the above consequences depending mainly on the level of seismic hazard and the performance objectives specified by the key stakeholders. For example, in cases of induced seismicity (often characterised by frequent, low intensity levels of ground shaking) the attention of a governmental regulator might be on disturbance and non-structural damage, whereas in an area of significant tectonic activity the most important consequence for the insurance industry might be economic loss, and for disaster risk managers might be loss of life.

The two main risk metrics that have been selected for this first version of the European seismic risk model are economic loss due to direct costs to repair/replace buildings (residential, commercial and industrial) and loss of life of occupants due to damage/collapse of those buildings. The probability of these losses is accounted for in the risk model, leading to the following key outputs:

- Average annual losses (i.e. the long-term mean loss per year due to earthquake ground shaking);
- Losses with specific return periods (i.e. the long-term mean loss value due to earthquake ground shaking that is expected to be equalled or exceeded at least once every X years, where X varies from 50 to 1000 years);
- Statistics (mean and quantiles) of losses for specific events (e.g. repetition of past damaging earthquakes).

However, it is noted that the components of the risk model that have been released allow users to compute other risk metrics, such as average annual probability of collapse for specific building classes, or to explore the analyses at higher levels of resolution or in more detail, for specific building classes or occupancy classes.

2.2 Seismic Risk Assessment Methodology

In addition to selecting specific consequences upon which the risk assessment should focus, another decision that is needed relates to the hazard that should be used to calculate these consequences. There are three main options available to the risk analyst:

- Scenario-based: the consequences are estimated for a specific earthquake scenario (of given magnitude, location, depth, style of faulting etc.) whose recurrence interval can be obtained from the hazard source model.
- Intensity-based: the consequences are estimated for a level of ground shaking intensity that occurs at a given return period (obtained as an output of a probabilistic seismic hazard assessment, PSHA).
- Frequency-based: the consequences are estimated considering all possible levels of ground shaking intensity and their associated frequencies of occurrence.

A brief summary of each of the three options available to model the hazard is provided below.

2.2.1 Scenario-based risk assessment

For some purposes, such as communication of risk, emergency planning, rapid loss assessment or risk model testing, the assessment of the damage and losses due to a single earthquake scenario is required. The scenario should be defined in terms of moment magnitude, location, depth and might also be constrained in terms of style of faulting, rake, dip etc. Once the scenario has been defined, ground motion models (see Section 3.1.2) are used to estimate the level of shaking at the locations of the buildings in the exposure model. The spatial cross-correlation of the aleatory (random) variability in the ground motion model should ideally be accounted for (see e.g. Weatherill et al., 2015), by repeating the scenario event many times, and producing hundreds of possible realisations of the ground motion over the area of interest. The simulated ground motions at each site in the exposure are input into the relevant vulnerability models and the economic loss is estimated for each realisation. The mean and standard deviation of the loss for the whole exposure model can then be estimated. Scenario-based analyses have been an important component of the ESRM20 framework for the validation of components of the risk model, as will be presented later in this report.

2.2.2 Intensity-based risk assessment

Intensity-based assessments evaluate the probable performance of buildings conditioned on the occurrence of a specific intensity of motion, typically represented by an elastic acceleration response spectrum. In the US, the basic life safety performance objective underlying the ASCE/SEI 7 seismic provisions (i.e. less than a 10% chance of collapse, given the occurrence of the Maximum Considered Earthquake shaking) is an example of the use of an intensity-based hazard representation in a performance objective (ATC, 2018). In Europe, seismic risk assessments have been undertaken considering the ground motions with a 475-year return period (e.g. Corbane et al., 2017), and these can be useful in order to compare the performance of existing buildings with the performance expected of code-conforming buildings. As discussed in FEMA P-58 (ATC, 2018), many stakeholders choose to define the intensity at a specific return period “because they have an intuitive understanding of decision making in this context”. However, it should be noted that the resulting consequences do not necessarily have the same return period as the input hazard, and the only way of estimating the damage or losses with a given return period is through a frequency-based approach, as described in the next section. For this

reason, intensity-based risk assessment is not considered further in this report and has not been used for the computation of ESRM20.

2.2.3 Frequency-based risk assessment

Frequency-based (or time-based) risk assessment considers all of the potential earthquake scenarios (defined in terms of magnitude, location, depth, rupture characteristics) that can impact the site over a given time frame, together with their probability of occurrence. For each event, the probability of exceeding different levels of ground motion is obtained from the aleatory variability of the ground motion model, and this is multiplied by the probability of occurrence of that event. This is repeated and summed for all possible events and leads to a hazard curve which describes the annual probability or frequency of exceedance of given levels of ground motion, at a given site. The convolution of this hazard curve with a vulnerability function leads to a loss curve for a single building (see Fig. 2.1), and the mean of the latter is the average annual loss (AAL):

$$AAL = \sum_{i=1}^{N_s} v_i \int_M \int_R \int_{GM} \int_L P[L > l|gm] f_{GM}(m,r) f_M(m) f_R(r|m) dl\, dgm\, dmdr \qquad (2.1)$$

where Ns is the number of sources, v_i stands for the average rate of magnitude exceedance threshold for source i, $P[L>l|gm]$ is obtained from the vulnerability function, $f_{GM}(m,r)$ is the probability density function of the ground shaking at the location of the building conditional on magnitude m and distance r (and possibly other variables, such as style of faulting or site conditions), $f_M(m)$ is the probability density function of magnitude, $f_R(r|m)$ is the probability density function of the source-to-site distances r conditional on magnitude m (see e.g. Silva, 2018). The AAL of each building can be calculated and summed to get the AAL for a whole group/portfolio of buildings.

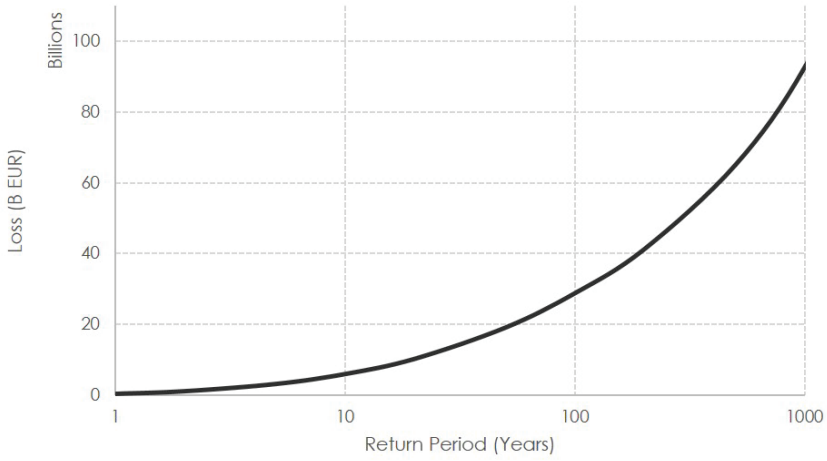

Fig. 2.1 Loss curve (note that these curves are also often presented with the axes inverted and the return period converted to annual probability of exceedance using the Poisson model, leading to what is frequently referred to as an Exceedance Probability (EP) curve)

When a single aggregate loss curve for a group/portfolio of buildings needs to be calculated (rather than just the AAL), it is necessary to consider the joint probability of ground motions at the sites where the buildings are located. The most straightforward way of doing this is by generating a synthetic or stochastic catalogue of events using Monte Carlo simulation (see Chapter 3 for more details), and then ground motions at all sites are simultaneously calculated per event, as described previously for the scenario-based assessment. This method of estimating the hazard is referred to herein as an 'event-

based approach'. The aggregate loss (i.e. the sum of the losses to all buildings at all sites) per event can then be calculated by combining the ground motions with the exposure and vulnerability models. The resulting aggregate loss for each event (often referred to as an event loss table) can then be used for the calculation of several risk metrics, including exceedance probability curves (see Fig. 2.1) and average annual losses (Eq. 2.1).

Each loss in the event loss table is associated with the same annual rate of occurrence, and the annual rate/frequency of exceedance (λ) of each aggregate loss can be calculated by ranking the aggregate losses from the largest to the smallest and computing the number of exceedances of each loss (*l*) divided by the length of the stochastic catalogue (*n*):

$$\lambda(L > l) = \frac{1}{n}\sum_{i=1}^{j} I(L_i > l) \tag{2.2}$$

where $I(L_i>l)$ stands for the number of loss values above *l*, *j* is the total number of losses, L_i stands for the loss caused by event *i*, and *n* represents the length of the stochastic catalogue. The return period is simply the inverse of the annual frequency of exceedance and the annual probability of exceedance can be calculated using the Poisson model. The average annual loss (AAL) can be computed using the following equation:

$$AAL = \frac{1}{n}\sum_{i=1}^{j} L_i \tag{2.3}$$

As the risk metrics being computed for ESRM20 include aggregate values (e.g. the losses to all buildings at national level with a 200-year return period), the hazard needs to be defined using this latter method, i.e. with stochastic catalogues and associated ground motion fields, and so the next Chapter of this report explains how these have been computed.

3 Stochastic Catalogues and Ground-Motion Fields

This Chapter describes the hazard inputs that have been used to calculate the risk metrics of ESRM20, as presented in Chapter 2, and presents some of the intermediate hazard outputs used by the OpenQuake-engine to compute the risk (namely stochastic catalogues).

3.1 Seismogenic Source Model and Ground-Motion Model Logic Trees

Seismic hazard models are made up of two main components: seismogenic source models and ground motion models. Seismogenic sources describe the spatial and temporal distribution of seismicity, typically through one of five different source types: point sources, area sources, simple fault sources, complex fault sources, and characteristic fault sources. The different source types provide flexibility in the modelling of the geographical location, depth, dimensions and rupture characteristics (such as strike, dip and rake) of the earthquake ruptures that can be generated following a given magnitude-frequency distribution. The latter describes the annual rate of earthquakes of different magnitudes, often grouped into bins of magnitude ranges (as illustrated in Fig. 3.1).

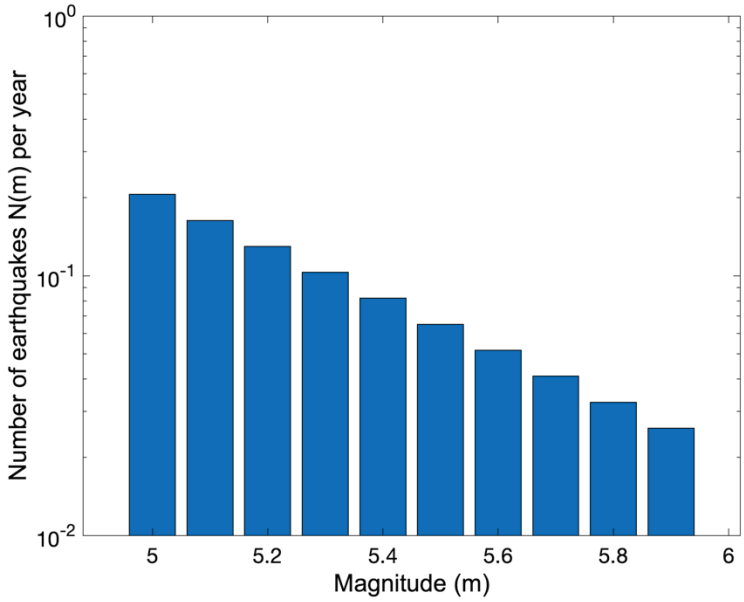

Fig. 3.1 Example of a magnitude-frequency distribution

Ground motion models describe the median and lognormal standard deviation of a range of ground shaking intensity measure levels (e.g. peak ground acceleration, average spectral acceleration) conditional on a number of predictor variables, that are typically the site (e.g. V_{S30}, the average shear wave velocity from the surface to a depth of 30 metres), rupture (e.g. moment magnitude), and distance parameters (e.g. hypocentral distance). Fig. 3.2 shows an example of how the median PGA in various ground motion models scales with moment magnitude (M_w) and attenuates with distance (in this case the so-called Joyner-Boore distance).

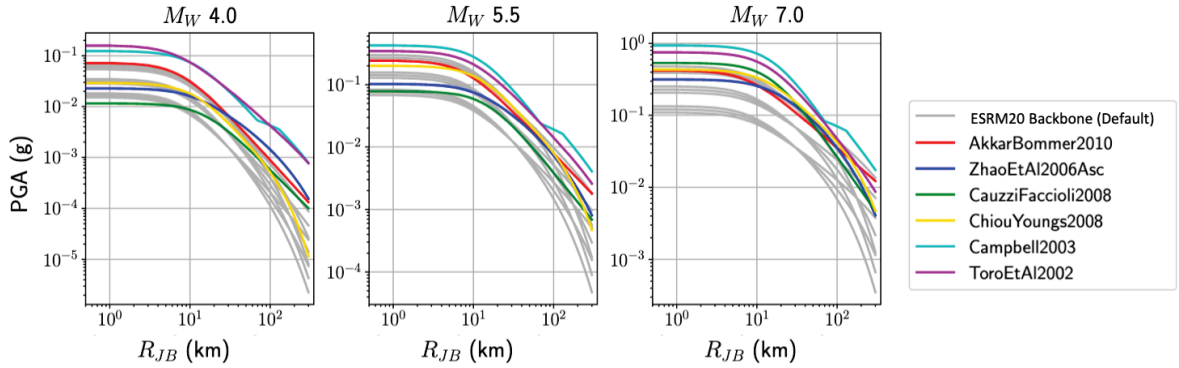

Fig. 3.2 Various ground motion models showing scaling of median PGA with magnitude (M_w) and attenuation with distance (Joyner-Boore distance, R_{JB}) (adapted from Weatherill et al., 2020a)

Both of these components of seismic hazard have sources of epistemic (or modelling) uncertainty and aleatory (random) variability. These two sources of uncertainty are typically propagated in two different ways in the seismic hazard calculations. The aleatory variabilities are included within the models and are integrated within the calculation of mean annual frequency of exceedance of ground motion whereas the epistemic uncertainties are typically represented through logic trees, leading to different percentiles of the mean annual frequency of exceedance of ground motion.

3.1.1 ESHM20 seismogenic source model logic tree

The European Seismic Risk Model has been computed using the latest seismogenic source model for Europe, developed as part of ESHM20 (European Seismic Hazard Model v2020). The reader is referred to Danciu et al. (2021) for more details on the development of this source model. A collapsed version of the ESHM20 source model logic tree has been used for the risk calculations, with two main source branches representing the two source model types: area source model (AS) and seismicity and faults (SEIFA), each with an equal weighting.

Additional epistemic uncertainty related to the source model is not currently modelled in the risk calculations for two main reasons:

- To reduce computational complexity.
- To reduce correlation of the epistemic uncertainty.

As the approach to estimate the risk requires the simulation of a large number of stochastic events and associated ground-motion fields, it is computationally intensive. The model has thus been calibrated in a manner that will allow the calculations to be run in a reasonable timeframe without requiring super-computing resources. Furthermore, it is not currently computationally feasible to run the full ESHM20 source model logic tree in the OpenQuake-engine with uncorrelated branches, and so a collapsed version of the logic tree avoids the potential impact of unexpected/unrealistic correlation of the epistemic uncertainty in the hazard. In a regional hazard model, the epistemic uncertainty in, for example, the activity rate parameters (so-called 'a' and 'b' values) of different sources are not expected to be fully correlated. However, unless uncorrelated logic tree branches are assumed, a given realization of a logic tree that has three branches would have the upper branch activity rates assigned to all sources within that realization. This realization would have more earthquakes than average per year being generated in all sources, and thus higher losses would be assessed everywhere. Hence, until the model can be run with uncorrelated branches, a simplified collapsed logic tree with the mean source model for

each main branch has been adopted. In order not to completely ignore the epistemic uncertainty in the annual frequency of ground motions across sites in Europe, the epistemic uncertainty in the ground motion has been included in the model, as described in the next section.

Future research is necessary to investigate the implications of the assumptions taken herein, and with more computing resources and more time after the open release of the models, research efforts will be focused on running the models with uncorrelated branches in order to identify simplified versions of the source model and ground-motion model logic trees which will lead to similar results to the full logic tree.

3.1.2 ESHM20 ground-motion model logic tree

As discussed in Douglas (2018), the epistemic uncertainty in the logic tree should vary geographically, with higher values found in areas with limited data and lower uncertainty in areas with considerable data. A transparent approach to modelling the epistemic uncertainty in the European ground-motion model, which ensures all branches are mutually exclusive and collectively exhaustive, and which has been used in many site-specific studies for critical facilities, makes use of a so-called backbone approach (Atkinson et al., 2014). In this approach a single ground motion model is calibrated (or selected from the literature) and adjustment factors are applied to this model that quantify the uncertainty in the expected ground motion as a result of the limited knowledge on the seismological properties in a region.

This approach has been adopted for the ESHM20 ground motion logic tree for each of the three main seismotectonic region types in Europe: shallow crustal seismicity (non-craton), seismicity in the stable craton region of northeastern Europe, and subduction and deep seismicity (including the Hellenic, Calabrian, Cypriot and Gibralter arcs, as well as the Vrancea deep seismic zone). In addition, a number of *special cases* are considered in which the main approach is modified, or else decisions are made on the basis of insights and information from other data sets or studies. More details on the logic tree can be found in Danciu et al. (2021), as well as in multiple journal publications that have arisen from this work (Kotha et al., 2020, 2022; Weatherill et al, 2020a; Weatherill & Cotton, 2020).

3.2 Site Response Model

An efficient and practical approach to incorporate site response into the ground-motion modelling of regional risk models uses topography to infer the 30-m averaged shear-wave velocity, V_{S30} (e.g. Wald and Allen, 2007), a parameter that is probably the most widely used to represent site amplification in existing ground-motion models. This approach was explored by Lemoine et al. (2012) and was found to be appropriate within shallow crustal regions for the purposes of regional risk assessment, but did not perform well in stable continental regions. Recent studies have also inferred site properties from quantities including surface geology (Wills and Clahan, 2006; Vilanova et al., 2018), surface morphology (Iwahashi and Pike, 2007), geotechnical descriptors (Seyhan and Stewart, 2014) and hybrid methods (Ahdi et al., 2017).

Topographic slope, inferred V_{S30} (from topographic slope) and geological unit/era have been used as the three main proxies for site response in the European seismic risk model. The site amplification function of the backbone ground motion model for shallow seismicity in active and low seismicity non-cratonic regions in the ESHM20 logic tree (Kotha et al., 2020) has been developed using the regression between the site-to-site variability and topographic slope, with geological unit as a random effect, as described further in Weatherill et al. (2020b) and Weatherill et al. (2022). In both the craton and the subduction/deep seismicity regions, the site amplification terms from the appropriate models (see Section 3.1.2) are directly adopted together with inferred V_{S30} values.

The three main datasets required to prepare the site response input models for ESRM20 are as follows:

- A European map of topographic slope (Fig. 3.3). The Wald and Allen (2007) study that correlated topography with V_{S30} was built on slope calculations based on SRTM30, a 30 arc-seconds (~600 m in central Europe) land topography data set (Farr and Kobrick, 2000). As discussed in Lemoine et al. (2012), topographic slopes derived from land terrain models only (such as SRTM30 land DEM) are associated to artefacts in coastal areas that lead to a number of outliers in the slope values, and it has therefore been decided to instead use the GEBCO_2014 DEM. This is a global terrain model for ocean and land, based on SRTM_Plus (v5) data set (Becker et al., 2009). The slope has been calculated from the DEM using the GMT command "grdgradient" (Wessel and Smith, 1991).

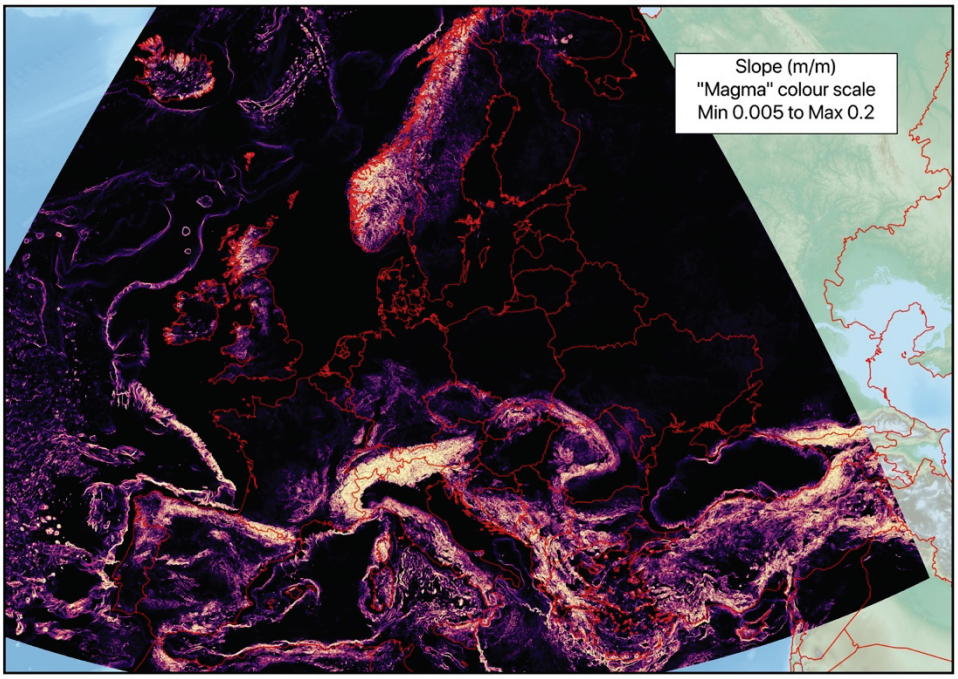

Fig. 3.3 Raster dataset of slope (calculated from the GEBCO_2014 DEM using GMT's grdgradient function)

- The map of topographical slope (Fig. 3.3) has been used to produce a 30 arc-seconds map of inferred V_{S30} using the model by Wald and Allen (2007) (Fig. 3.5).
- A composite map of geological unit/era (Fig. 3.6) at the European scale (covering all countries in the model) has been derived from three existing maps:
    - The geological map at 1:1,500,000 from the European project ProMine (http://promine.gtk.fi/, Cassard et al., 2015).
    - The geological map at 1:1,000,000 from OneGeologyEurope, available from EGDI services (http://www.europe-geology.eu/).
    - The bedrock geological map of Iceland at 1:600,000 available from the Icelandic Institute of Natural History (Johannesson, 2014).

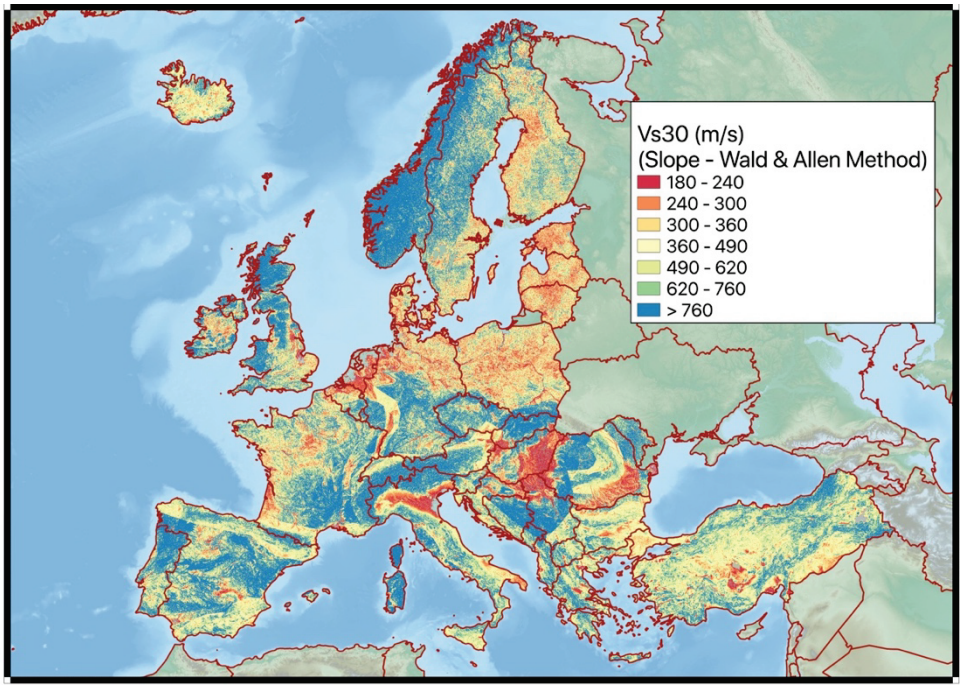

Fig. 3.4 V_{S30} inferred from GEBCO topography/bathymetry using the Wald and Allen (2007) correlation approach

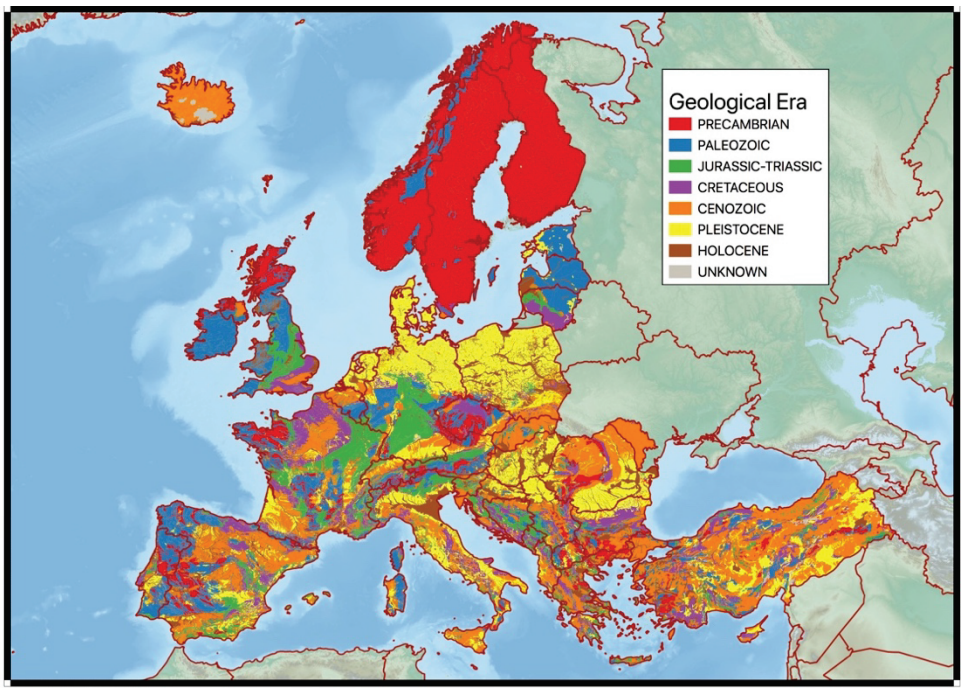

Fig. 3.5 Map of geological era/unit based on harmonizing three datasets across Europe

These datasets can be explored and accessed online here: https://maps.eu-risk.eucentre.it/map/european-site-response-model-datasets.

Using these maps, every cell in Europe on a grid of target resolution of 30 arc-seconds can be assigned a value of slope, inferred V_{S30} and geological unit. Following the sensitivity study undertaken by Dabbeek et al. (2021), the site response input for the risk calculations has been calculated by weighting the 30 arc-seconds maps of slope, topographically inferred V_{S30} and geological unit with a 30 arc-seconds grid

of built-up area density (from Pesaresi et al. 2015). This has been undertaken using the open source 'exposure to site tool' available here: https://gitlab.seismo.ethz.ch/efehr/esrm20_sitemodel.

3.3 Stochastic Catalogues

The OpenQuake-engine (Pagani et al., 2014; Silva et al., 2014) has been used to calculate the seismic risk metrics for Europe (outlined in Chapter 2). The risk calculations have been undertaken with the so-called "eb-risk" calculator of the OpenQuake-engine which uses the hazard library of the OpenQuake-engine (hazardlib) to compute the stochastic catalogues and associated ground motion fields.

This hazard library uses the seismogenic source model to create an earthquake rupture forecast (i.e. a list of all of the possible ruptures that can occur in the region of interest), which is then sampled (with Monte Carlo sampling) to generate a number of stochastic event sets (SES), each with a duration of 1 year. Due to the random nature of the process, a large number of SES is required in order to reach statistical convergence in both the seismic hazard and risk assessments (Silva, 2018), and it has been found that 10,000 are sufficient for adequate convergence of the risk metrics of the European risk model (see Section 2.1). The combination of these stochastic event sets is referred to herein as a *stochastic catalogue*.

The epistemic uncertainty in the seismogenic source models and ground motion models can be propagated through the use of logic trees (Pagani et al., 2014). For the European seismic risk model, 100 branches of the full logic tree (which, as mentioned previously, includes the collapsed seismogenic logic tree and the 5-branch ground motion model logic tree) have been randomly sampled. A 10,000 year stochastic catalogue, and ground motion fields for each event in the stochastic catalogue, is generated for each of the sampled logic tree branches (also referred to as 'realisations'), considering only earthquakes with magnitude above 5.0. Fig. 3.6 shows four of these stochastic catalogues (filtered to show only those events that lead to economic losses greater than 2000 Euros). The ground motion fields consider the tectonic regions and the site response model within 300km of the epicentre of the event and provide the amplified ground motions at the locations in the exposure models. For each event, a sample of the inter-event variability from the ground motion model is applied to all sites, whereas the intra-event variability is sampled at each location in the exposure model. Spatial correlation of the intra-event residuals has not been currently modelled as it increases computational complexity, it does not influence the average annual loss and it has been found not to have a significant impact on the considered return period losses for large-scale risk assessment.

3.4 Online Resources

Users interested in exploring further the hazard inputs to the risk calculations can obtain the final OQ-engine input files here: https://gitlab.seismo.ethz.ch/efehr/esrm20. It is noted that these files differ from the files and inputs used to calculate seismic hazard maps and uniform hazard spectra at specific return periods on 800 m/s reference rock (using a classical PSHA approach) and readers interested in those hazard outputs are referred to Danciu et al. (2021) for more information and for the links to the relevant files and resources. The link above, instead, only provides access to the hazard input models and OQ-engine settings used for the computationally efficient calculation of the selected European seismic risk metrics with an event-based approach.

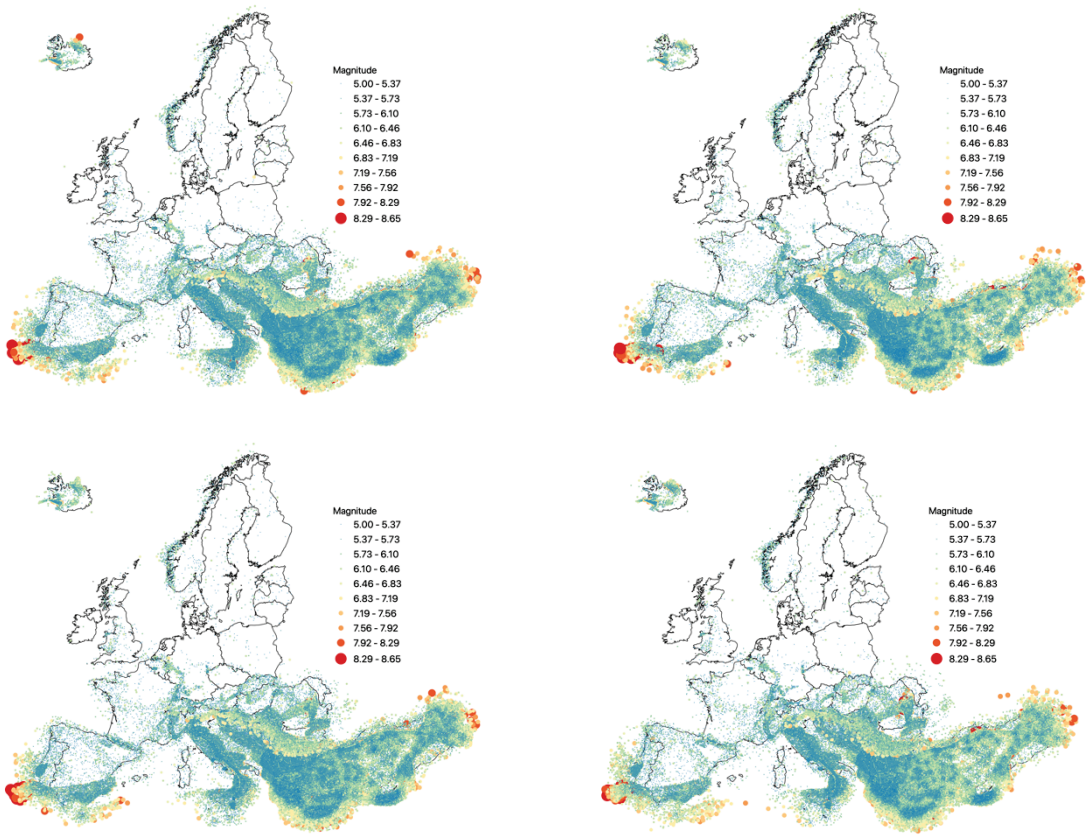

Fig. 3.6 Four of the 100 stochastic catalogues (representing 10,000 years of seismicity) generated for the calculation of risk metrics at the European scale

The seismogenic source model and ground motion model logic tree files are found inside the 'Hazard' folder of the aforementioned repository. Additionally, for further exploration of the model, the following hazard configuration files have been set up inside the 'Configuration_file' folder to allow users to produce stochastic catalogues and ground-motion fields using an event-based approach, as explained in Section 2.2.3: 'config_event_hazard_Group1.ini', 'config _event_hazard_Group2.ini' and 'config _event_hazard_Iceland.ini'. It is noted that, for computational efficiency, two groups of countries are used and Iceland is always run separately, due to its large distance from continental Europe.

These configuration files are set up to calculate stochastic catalogues and associated ground motion fields at the locations of the exposure models using the site response model inside the 'Vs30' folder. As mentioned previously, a tool for users to prepare these site response input files is available at the following repository: https://gitlab.seismo.ethz.ch/efehr/esrm20_sitemodel.

The configuration files are also set up to output hazard maps and hazard curves, computed from the ground motion fields. It is noted that storing the ground motion fields requires a lot of disk space, and users are recommended to adapt the files to only run small regions if they wish to investigate and plot the ground motion fields. Various aspects of the hazard inputs can be modified by users of the models such as the consideration of spatial correlation (by specifying one of the models available in the

OpenQuake-engine). Modellers are referred to the OpenQuake User Manual for instructions on how to make such modifications to the models[4].

3.5 Future Improvements

Further investigations into the most efficient representation of the full hazard logic tree (see Danciu et al., 2021 for more details) will be undertaken in the coming months. This will require the model to be run with uncorrelated logic tree branches, and for comparisons of the losses to be made with 'trimmed' logic trees with correlated branches, such that computationally efficient models are still made available. All future developments to the European seismic hazard model will continue to be propagated to the risk model.

[4] https://docs.openquake.org/manuals/OpenQuake%20Manual%20%28latest%29.pdf

4 Exposure Model

The development of the exposure models for 44 European countries has been described in two peer-reviewed publications: Crowley et al. (2020) and Crowley et al. (2021a). Since these publications were released the models have continued to be developed. Hence, whilst readers are referred to those publications for additional technical details, whilst this Chapter provides a succinct summary of the final data, assumptions and workflow used to develop the exposure models used in ESRM20.

There are three occupancy classes considered in the risk model: residential buildings, commercial buildings and industrial buildings. All of the data used to develop the exposure models has been made available in a GitLab repository: https://gitlab.seismo.ethz.ch/efehr/esrm20_exposure (Crowley et al., 2021b). Note that the version of the exposure data used to develop the models for ESRM20 is v1.0 (which can be accessed by changing the branch of the repository from 'master' to 'v1.0'). The following sections describe the data in this repository and how they have been combined to produce the final exposure models used in ESRM20, which are available from the '/_exposure_models' folder of the aforementioned repository.

4.1 Residential Buildings and Occupants

There are three main approaches that have been adopted to develop the residential exposure models (see Fig. 4.1):

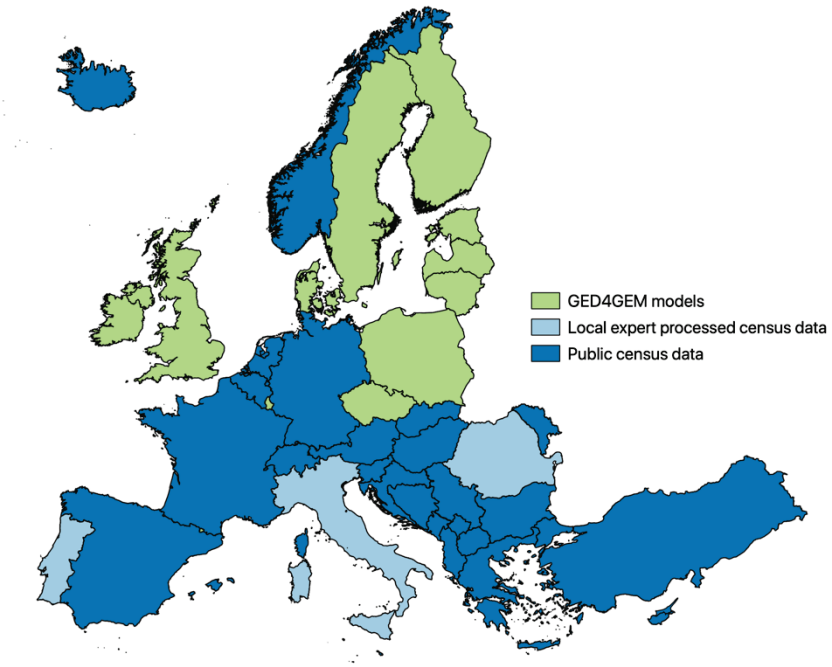

Fig. 4.1 Map classifying the residential model development approach for each country

- For higher hazard countries, public census data has been collected at the highest administrative level available. This includes Albania, Austria, Belgium, Bosnia and Herzegovina, Bulgaria, Croatia, Cyprus, France, Germany, Greece, Hungary, Iceland, Kosovo, Malta, Moldova, Montenegro, Netherlands, North Macedonia, Norway, Serbia, Slovakia, Slovenia, Spain, Switzerland, Turkey.

- In Italy, Portugal and Romania, local researchers have provided a post-processed version of the census data which has been used to develop the final exposure models.
- For lower hazard or very small countries, existing GED4GEM data[5] (Gamba et al., 2014) on the spatial distribution of building classes has been used. This covers Andorra, Czechia, Denmark, Estonia, Finland, Gibraltar, Ireland, Isle of Man, Latvia, Liechtenstein, Lithuania, Luxembourg, Monaco, Poland, Sweden and United Kingdom.

4.1.1 Spatially distributed source data

In the source data folder (/res_exposure_source_data) there is a file for each country with the source data on the number of residential buildings or dwellings and the population in each administrative region (which are typically divided into urban and rural areas). For all GED4GEM countries, and in some other cases where older census data was used, the total number of dwellings has been increased during the model development to match the total number of occupied conventional dwellings provided by EuroStat[6].

For models based on census data, the buildings are described with attributes that vary from country-to-country, with common examples being era of construction and material. The variables available for each country are summarized in the 'European_Exposure_Model_Data_Inputs_Sources.xlsx' file, available inside the sources folder. The GED4GEM source data is in terms of building classes that follow the GEM Building Taxonomy v3.1 (https://github.com/gem/gem_taxonomy; Silva et al., 2021), as the mapping schemes (see the next section) have already been applied. The level of resolution and the reference for each source is provided in the 'European_Exposure_Model_Data_Inputs_Sources.xlsx' file.

4.1.2 Exposure coordinates

A choice was made to keep the level of resolution of the exposure models at the same administrative level at which the data was collected to maintain a close correspondence to the original source data, and to reduce the computational burden that higher resolution models would generate. It was therefore necessary to identify an optimal coordinate at which to model the exposure in each administrative unit that would reduce the potential for bias in the results. Following the sensitivity study undertaken by Dabbeek et al. (2021), each administrative region has been represented by a single coordinate which represents a density-weighted centroid, which is calculated from a 30 arc-seconds grid of built-up area density, interpolated from the 250×250 m resolution built-up area density map (Pesaresi et al., 2015). Dabbeek et al. (2021) disaggregated the exposure models to 30 arc-seconds resolution using the aforementioned dataset and ran the risk assessment with this exposure for the majority of countries in Europe, as a baseline against which other methods with lower levels of resolution could be compared. The use of the aforementioned density-weighted centroid (together with a density-weighted site response model, as presented previously in Section 3.2) led to the lowest bias in the aggregated national and administrative level one losses (for the administrative level-based exposure models), and was thus adopted in the final models.

The aforementioned built-up area density dataset has been openly provided for users of the models that wish to modify the coordinates or spatially disaggregate the data to a higher resolution. This dataset can be downloaded from the '/spatial_disaggregaton' folder and an open source tool to disaggregate the

[5] Available upon request from the GEM Foundation (www.globalquakemodel.org)
[6] https://appsso.eurostat.ec.europa.eu/nui/show.do?dataset=cens_11dwob_r3&lang=en

data to a higher resolution has been developed in collaboration with the GEM Foundation and can be obtained here: https://github.com/GEMScienceTools/spatial-disaggregation.

4.1.3 Mapping schemes

In order to harmonise the description of buildings between countries, and also to describe the buildings in terms of their performance under seismic loading, the buildings in each country are described using building classes that follow the GEM Building Taxonomy v3.1 using the following standard attributes in all cases: i) material of lateral load resisting system (LLRS) (attribute 2), ii) LLRS + seismic code level + lateral force coefficient (attribute 3), and 3) height (attribute 4). These attributes are stored using one of the following string formats:

Material / LLRS + Seismic Code Level + LFC: %f / H: %d
Material / LLRS + Seismic Code Level + LFC: %f / HBET: %d , %d
Material / LLRS + Seismic Code Level + LFC: %f / HBET: %d -

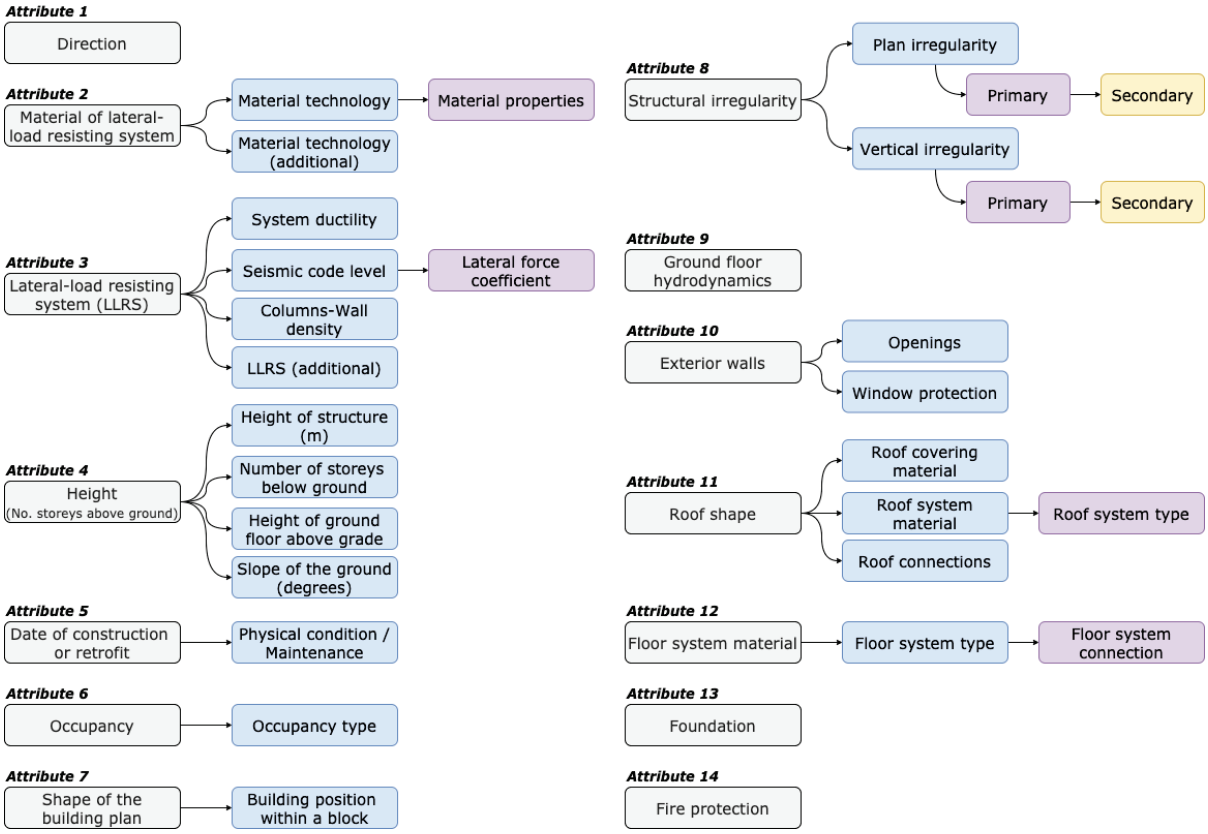

Fig. 4.2 GEM Building Taxonomy v3.1 (https://github.com/gem/gem_taxonomy)

In some countries, additional attributes related to shape of the building plan (attribute 7), structural irregularity (attribute 8), exterior walls (attribute 10), roof shape (attribute 11) and floor system material (attribute 12) were also used to classify the buildings by local engineers. These attributes are reported, in this order, at the end of the string format described above. The building classes in each country have been identified through interaction with local experts, through questionnaires and workshops, and from the academic literature.

In the mapping folder (/res_mapping_schemes), the percentage of buildings in each building class as a function of the available building attributes is presented. These mapping schemes also depend on

whether the building is in an urban or rural area. The seismic design attributes of the engineered building classes have been assigned considering the evolution of seismic design in Europe, as described in Crowley et al. (2021a). Fig. 4.3 presents the distribution of buildings in countries with seismic design according to the four levels considered: CDN (no seismic design, pre-code), CDL (low code), CDM (moderate code) and CDH (high code). Following the assignment of the code level, the lateral force coefficient (i.e. the fraction of weight of the building applied laterally as a force during design) specified in the codes is assigned to the building class, depending on its location.

Table 4.1 presents the years assumed for each design code in each country. The shapefiles that delineate each seismic zone for each code level and provide the lateral force coefficients are available for download in the '/seismic_design_shapefiles' folder. Fig. 4.4 maps the lateral force coefficient values in the shapefiles for the CDL and CDM codes between 1910 and 2000.

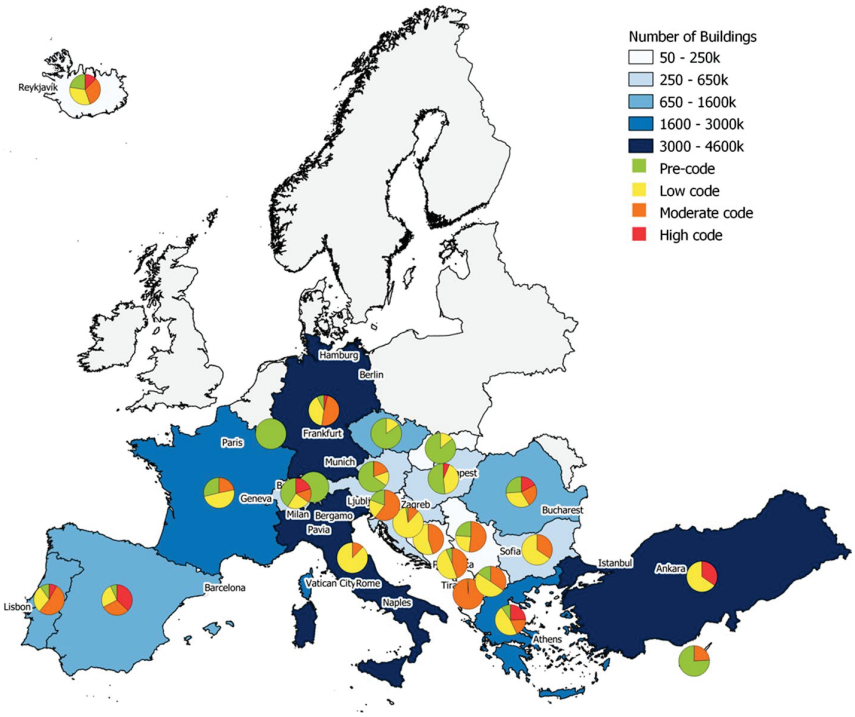

Fig. 4.3 Map with pie-charts for each country showing the percentage of buildings that are pre-code (CDN), low code (CDL), moderate code (CDM) and high code (CDH) (Crowley et al., 2021a)

Table 4.1 Summary of the era considered for each design code level in the European exposure models

Country	**Design Code Level**			
	CDN	CDL	CDM	CDH
Albania	<1978	1978 - 1989	> 1989	
Andorra*				
Austria	< 1979	1979 – 2006		> 2006
Belgium				
Bosnia and Herzegovina	< 1964	1964 – 1981	> 1981	
Bulgaria	< 1957	1957 – 1987	>1987	
Croatia	< 1964	1964 – 1981	> 1981	

Table 4.1 (cont.) Summary of the era considered for each design code level in the European exposure models

Country	Design Code Level			
	CDN	CDL	CDM	CDH
Cyprus	< 1992		>1992	
Czechia*				
Denmark*				
Estonia*				
Finland*				
France	< 1969	1969 – 1991	> 1991	
Germany	< 1957	1957 – 1981	1981 – 2005	> 2005
Gibraltar*				
Greece	< 1959	1959 – 1984	1984 – 1995	> 1995
Hungary	< 1978	1978 – 2006		> 2006
Iceland	< 1958	1958 - 1976	1976 - 2002	> 2002
Ireland*				
Isle of Man*				
Italy	< 1915	1915 – 1996	> 1996	
Kosovo	< 1964	1964 – 1981	> 1981	
Latvia*				
Liechtenstein*				
Lithuania*				
Luxembourg*				
Malta				
Moldova				
Monaco*				
Montenegro	< 1964	1964 – 1981	> 1981	
Netherlands				
North Macedonia	< 1964	1964 – 1981	> 1981	
Norway				
Poland*				
Portugal	< 1958	1958 – 1983	>1983	
Romania	< 1963	1963 – 1978	1978 – 2006	> 2006
Serbia	< 1964	1964 – 1981	> 1981	
Slovakia	< 1988	> 1988		
Slovenia	< 1964	1964 – 1981	> 1981	
Spain	< 1962	1962 – 1994	1994 – 2002	> 2002
Sweden*				
Switzerland	<1970	1970 – 1989	1989 – 2003	> 2003
Turkey	< 1975	1975 - 1997		> 1997
United Kingdom*				

** The exposure models for these countries are based on the GED4GEM data which used mapping schemes from PAGER (Jaiswal and Wald, 2008) and the European NERA project (Crowley et al., 2012), and so the seismic design history of these countries has not been considered further.*

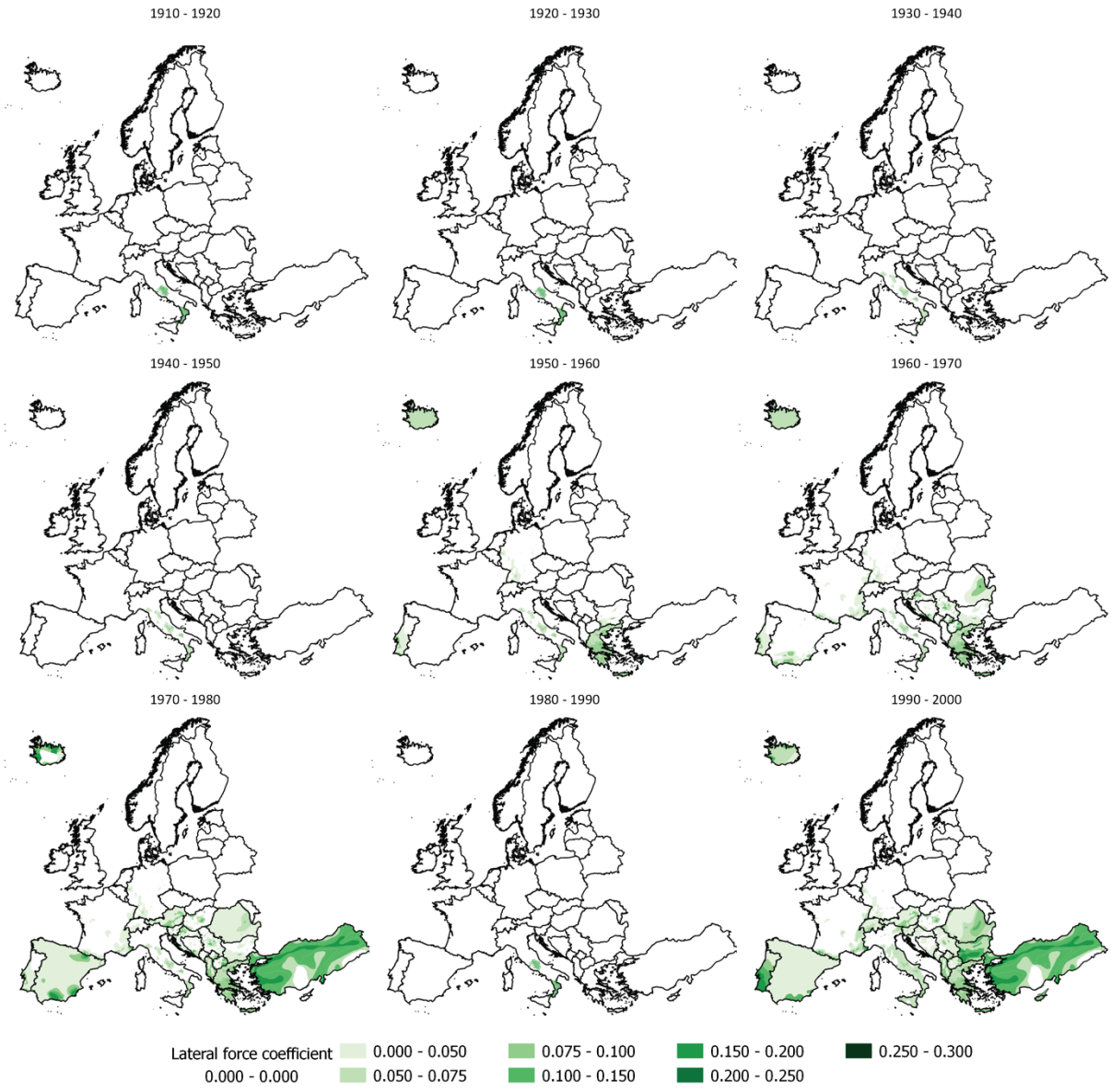

Fig. 4.4 Spatial and temporal evolution of lateral force coefficients in CDL and CDM codes across Europe from 1910 to 2000. These maps can also be viewed through the following interactive viewer: https://maps.eu-risk.eucentre.it/map/european-seismic-design-levels (Crowley et al., 2021a)

For the final exposure models, a simple human-readable simplified taxonomy has also been reported for all building classes, mapping them into one of the classes given in Table 4.2.

4.1.4 Dwellings per building

Some source data is available in terms of dwellings and some source data is available in terms of buildings. In order to have all exposure models represented in terms of both dwellings and buildings, it is necessary to map between the two. Assumptions on the number of dwellings per building for each building class in the exposure model of a given country have thus been made and are reported in the dwellings per building folder (/res_dwelling_per_building).

Table 4.2 Building classes according to the simplified taxonomy

Building Classes - Simplified Taxonomy	
Adobe, low rise	Concrete wall, low rise, high code
Concrete frame with infill panels, high rise, high code	Concrete wall, low rise, low/moderate code
Concrete frame with infill panels, high rise, low/moderate code	Concrete wall, low rise, pre code
Concrete frame with infill panels, high rise, pre code	Concrete wall, mid rise, high code
Concrete frame with infill panels, low rise, high code	Concrete wall, mid rise, low/moderate code
Concrete frame with infill panels, low rise, low/moderate code	Concrete wall, mid rise, pre code
Concrete frame with infill panels, low rise, pre code	Confined or reinforced masonry, low rise
Concrete frame with infill panels, mid rise, high code	Confined or reinforced masonry, mid rise
Concrete frame with infill panels, mid rise, low/moderate code	Steel, low rise
Concrete frame with infill panels, mid rise, pre code	Steel, mid rise
Concrete frame, high rise, low/moderate code	Unknown material, high rise
Concrete frame, high rise, pre code	Unknown material, low rise
Concrete frame, low rise, high code	Unknown material, mid rise
Concrete frame, low rise, low/moderate code	Unreinforced masonry, high rise
Concrete frame, low rise, pre code	Unreinforced masonry, low rise
Concrete frame, mid rise, high code	Unreinforced masonry, mid rise
Concrete frame, mid rise, low/moderate code	Unreinforced masonry, mid rise, high code
Concrete frame, mid rise, pre code	Unreinforced masonry, mid rise, low/moderate code
Concrete wall, high rise, high code	Wood, low rise
Concrete wall, high rise, low/moderate code	Wood, mid rise

4.1.5 Area per dwelling

The assumptions related to the area per dwelling for each building classes are provided for each country in separate files in the area per dwelling folder (/res_dwelling_area). This area is assumed to be the 'useful area' (and thus does not include shared area spaces) for the purposes of assigning reconstruction costs (Section 4.1.6). For each building class, these values are multiplied by the number of dwellings to get the total (surface) area.

4.1.6 Reconstruction costs

The reconstruction costs per square metre (i.e. per useful surface area) for structural and non-structural elements are provided in the 'European_Exposure_Model_Data_Inputs_Sources.xlsx' file for urban areas, rural areas and big cities. The definition of urban/rural as well as the administrative regions that have been assumed to be 'big cities' are also provided therein. These costs have been informed from a variety of sources as presented in Table 4.3, as well as feedback from local experts. Following the identification of typical costs per square metre for a number of countries, the costs for the other countries have been inferred considering the expected relative ranking of residential construction costs between countries in Europe. This ranking has been undertaken using construction cost indices and then a final validation, and subsequent calibration where necessary, of the final reconstruction cost values has been undertaken using the data provided in Paprotny et al. (2019) and COMPASS (2020). These analyses are presented and described further in Appendix A, Section A.1. Minor modifications are finally applied to the reconstruction costs as a function of the main material of construction, by scaling the values as follows: MIX:1.00, MUR:0.95, ADO:0.95, CR:1.05, M:1.05, S:1.00, W:0.95, OT:1.00.

Table 4.3 Sources of reconstruction costs per square metre for residential buildings

Country	Source
Turkey	Turner and Townsend (2019)
Romania	AECOM (2014)
Kosovo	Balkan Insight (n.d.)
Hungary	Daily News Hungary (n.d.)
Poland	Statistica (n.d.)
Cyprus	Kazantzidou et al. (2019)
Portugal	Forum da casa (n.d.)
France	Turner and Townsend (2019); Caseo Professionel (n.d.)
Germany	Kleist et al. (2006); Schmalwasser and Schidlowski (2006); Turner and Townsend (2019)
Liechtenstein	Numbeo (n.d.)
Netherlands	Turner and Townsend (2019)
Belgium	Engel & Völkers (n.d.)
Ireland	Turner and Townsend (2019)
Austria	Turner and Townsend (2019)
Sweden	Turner and Townsend (2019)
Switzerland	Statistica (n.d.)
United Kingdom	Costmodelling Ltd (n.d.)
Isle of Man	Costmodelling Ltd (n.d.)

The structural and non-structural reconstruction cost per square metre is assumed to comprise 80% of the total replacement cost (which includes also the contents). The total replacement cost is divided into structural, non-structural and contents according to the following percentages: 30%, 50%, 20%, respectively.

4.1.7 Occupants

The total population in each administrative region is associated with the residential buildings in that region. This population in each administrative region is distributed as a function of the number of dwellings in each building class, and then the population distribution model from PAGER (Jaiswal and Wald, 2010) is applied to obtain the average number of occupants in residential buildings during the day, night and transit. It is assumed that day represents the time between 10am to 6pm, night is between 10pm to 6am and transit times cover the remaining hours of the day. The average urban and rural area distributions from the PAGER population distribution model have been used. This model is available in the file 'population_distribution_PAGER.xlsx' inside the '/social_indicators' folder.

4.1.8 Calibration and validation data

During the development of the exposure models, the total number of buildings, total number of dwellings and total surface area were checked against calibration data collected for each country and reported in the 'European_Exposure_Model_Data_Inputs_Sources.xlsx' file.

Following the combination of all of the aforementioned datasets to produce the residential exposure models, comparisons and tests with other sources have been undertaken as a final validation of reliability of the models. These checks are presented in Appendix A.

4.2 Commercial Buildings and Occupants

The commercial building stock represents offices, wholesale and retail (trade), and hotels. The data available to develop commercial exposure models varies significantly across Europe, but the main two approaches that have been used can be summarized as follows:

- Data on the number of commercial buildings per sector has been directly obtained from the census or from Eurostat.
- Data on the number of businesses or enterprises per sector has been obtained from the census or from Eurostat and divided by a factor to obtain an estimate of the number of buildings.

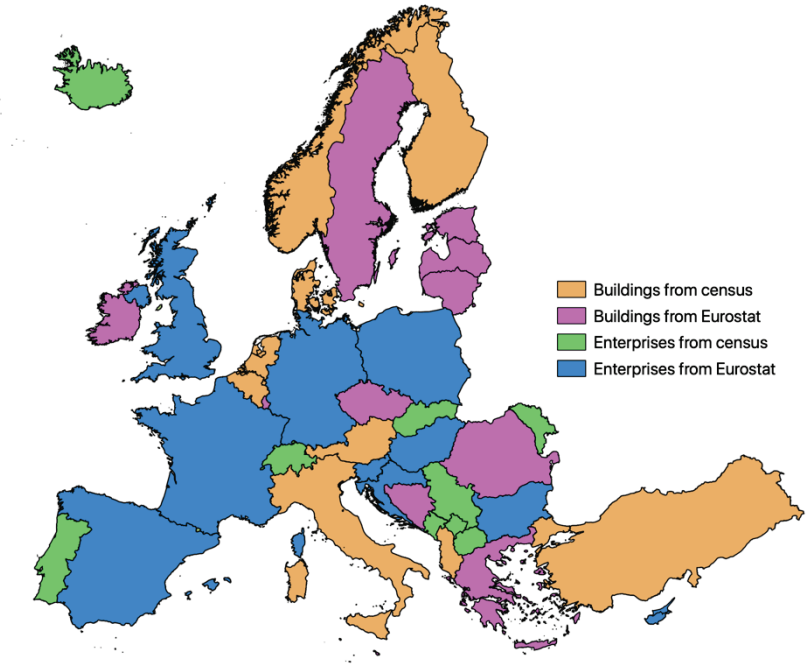

Fig. 4.5 Map classifying the source used for number of commercial buildings per sector for each country

In some cases, this data was already distributed across various administrative regions in the country. When there was no spatial distribution of this data, the labour force distribution from the census has been used to spatially distribute the number of buildings.

4.2.1 Spatially distributed source data

In the source data folder (/com_exposure_source_data) there is a file for each country with the processed source data with the number of commercial buildings in each administrative region. The level of resolution and the reference for each source is provided in the 'European_Exposure_Model_Data_Inputs_Sources.xlsx' file.

4.2.2 Exposure coordinates

The same assumptions reported in Section 4.1.2 have been taken to assign the coordinates of each administrative region.

4.2.3 Mapping scheme

Unlike the residential source data, the commercial source data does not include any information on the attributes of the buildings. Hence, the mapping schemes for commercial buildings simply represent the expected distribution of commercial buildings between different building classes (described using the GEM Building Taxonomy v3.1). In many cases the distribution of residential buildings has been used as a starting point for the mapping scheme, and building classes that are not typically used in the commercial building stock (such as adobe buildings) have been removed, and the percentages redistributed. In the mapping folder (/com_mapping_schemes), the percentage of buildings in each building class for each country is provided in separate files.

The lateral force coefficients have been assigned to the building classes using the same method presented previously in Section 4.1.3 and the same simplified taxonomy classes are considered.

4.2.4 Area per building class

The assumptions related to the area per building for each building classes is provided for each country in separate files in the area per building class folder (/com_building_area). Initial reasonable assumptions are taken for each building class, and then these areas are typically iterated upon until the total floor area matches the calibration data reported in the sources Excel sheet (see Section 4.2.7).

4.2.5 Reconstruction costs

The reconstruction costs per square metre (i.e. per useful surface area) for structural and non-structural elements are provided in the 'European_Exposure_Model_Data_Inputs_Sources.xlsx' file for offices, wholesale and retail (trade), and hotels. These costs have been obtained for office buildings from a variety of sources as presented in Table 4.4, as well as feedback from local experts. Unless otherwise provided by local experts, the costs of reconstruction of hotels has been taken as 5% higher than office buildings and the cost for retail buildings has been taken as 75% of office buildings. Following the identification of typical costs per square metre for a number of countries, the costs for the other countries have been inferred considering the expected relative ranking of non-residential construction costs between countries in Europe. This ranking has been undertaken using construction cost indices and then a final validation, and subsequent calibration where necessary, of the final reconstruction cost values has been undertaken using the data provided in COMPASS (2020). This data has also been used to check the assumption mentioned above on the relative costs of offices and hotels. These analyses are presented and described further in Appendix A, Section A.1. Minor modifications are finally applied to the reconstruction costs as a function of the main material of construction, by scaling the values as follows: MIX:1.00, MUR:0.95, ADO:0.95, CR:1.05, M:1.05, S:1.00, W:0.95, OT:1.00.

The structural and non-structural reconstruction cost per square metre is assumed to comprise 50% of the total replacement cost (which includes also the contents). The total replacement cost is divided into structural, non-structural and contents according to the following percentages: 20%, 30%, 50%, respectively.

Table 4.4 Sources of reconstruction costs per square metre for office buildings

Country	Source
Turkey	Turner and Townsend (2019)
Hungary	Conseil Européen des Economistes de la Construction (n.d.)
Czechia	Conseil Européen des Economistes de la Construction (n.d.)
France	Turner and Townsend (2019); Conseil Européen des Economistes de la Construction (n.d.); Statistica (n.d.)
Germany	Turner and Townsend (2019); Conseil Européen des Economistes de la Construction (n.d.); Statistica (n.d.)
Netherlands	Turner and Townsend (2019); Conseil Européen des Economistes de la Construction (n.d.); Statistica (n.d.)
Ireland	Turner and Townsend (2019); Conseil Européen des Economistes de la Construction (n.d.); Statistica (n.d.)
Austria	Turner and Townsend (2019)
Denmark	Conseil Européen des Economistes de la Construction (n.d.)
Finland	Conseil Européen des Economistes de la Construction (n.d.)
Sweden	Turner and Townsend (2019)
Switzerland	Turner and Townsend (2019); Conseil Européen des Economistes de la Construction (n.d.); Statistica (n.d.)
United Kingdom	Turner and Townsend (2019); Conseil Européen des Economistes de la Construction (n.d.); Statistica (n.d.)

4.2.6 Occupants

For this first version of exposure models, a simplifying assumption has been taken that the same number of people live and work within the same administrative unit, and thus the movement of people from their place of residence to place of work is not currently modelled. It is assumed that 40% of the working population are employed in the commercial sector (which is based on Eurostat statistics[7]). The population in each admin unit is distributed as a function of the area of commercial buildings per building class, multiplied by 0.4 and then the PAGER population distribution model (Jaiswal and Wald, 2010) for non-residential buildings is applied to obtain the average number of occupants in commercial buildings during the day, night and transit times.

4.2.7 Calibration and validation data

During the development of the exposure models, the total floor area of offices, wholesale and retail and hotels were checked against calibration data collected for each country and reported in the 'European_Exposure_Model_Data_Inputs_Sources.xlsx' file.

Following the combination of all of the aforementioned datasets to produce the commercial exposure models, comparisons and tests with other sources have been undertaken as a final validation of the reliability of the models. These checks are presented in Appendix A.

[7] https://ec.europa.eu/eurostat/web/products-datasets/product?code=nama_10_a64_e

4.3 Industrial Buildings and Occupants

The industrial buildings in the model cover the building stock that houses the following industries: mining/quarrying, manufacturing and construction. The total number of industrial buildings in each country was obtained following one of the following three methods:

- The total number of enterprises in each country across these industries was obtained from various sources (reported in the European_Exposure_Model_Data_Inputs_Sources.xlsx' file) and one enterprise was assumed to represent one building.
- The total number of industrial buildings was obtained from the census or other European sources.
- The total area of industrial buildings (see below) was divided by an average area per building (obtained from neighbouring countries).

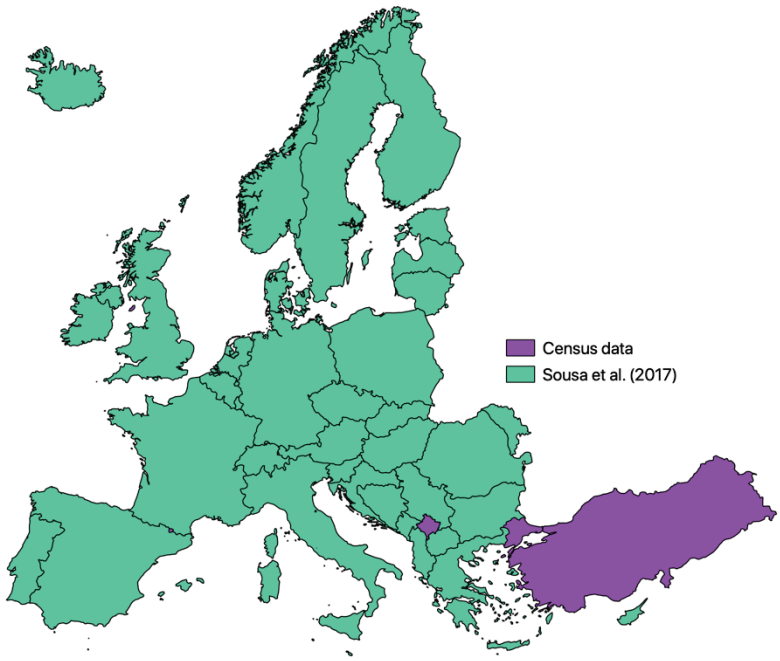

Fig. 4.6 Map classifying the approach used for spatially distributing industrial buildings for each country

The number of industrial buildings was then distributed spatially within the country using one of the following processes (Fig. 4.6):

- For a number of European countries, it has been possible to use the 30 arc-seconds grid of surface area of industrial buildings from Sousa et al. (2017). This has been obtained by combining OpenStreetMap data with CORINE land use maps (https://land.copernicus.eu/pan-european/corine-land-cover).
- Where the latter data was not available, census data was used to distribute the buildings, either using data on the distribution of businesses, or distribution of employees in the considered industrial sectors.
- For Turkey, the distribution of number of industrial buildings across admin regions was already available in the census.

4.3.1 Spatially distributed source data

In the source data folder (/ind_exposure_source_data) there is a file for each country with the processed source data with the number of industrial buildings in each location. In the cases where the data has been distributed according to the 30 arc-seconds grid from Sousa et al. (2017), each row/location represents a grid cell in the country. For the cases where the data was instead distributed using census data, each row represents an administrative region (which is reported in the file). The level of resolution and the reference for each source is provided in the 'European_Exposure_Model_Data_Inputs_Sources.xlsx' file.

4.3.2 Exposure coordinates

For the exposure models based on the 30 arc-seconds grid from Sousa et al. (2017), the coordinates of each location represent the centroid of each grid cell. For models based on census data, the same assumptions reported in Section 4.1.2 have been taken to assign the coordinates of each administrative region.

4.3.3 Mapping scheme

Unlike the residential source data, the industrial source data does not include any information on the attributes of the buildings. Hence, the mapping schemes for industrial buildings simply represent the expected distribution of industrial buildings between different building classes (described using the GEM Building Taxonomy v3.1). Various sources from the academic literature, as well as expert judgment, has been used to develop these distributions. The year of construction of industrial buildings is not available and so the level of seismic design has been based on judgement. The lateral force coefficient has not been applied to the buildings, as it is assumed that these buildings have a lower level of design compared to residential and commercial buildings. The same simplified taxonomy classes as those presented in Section 4.1.3 are considered.

4.3.4 Area per industrial building

The assumptions related to the average area per building/facility for industrial buildings is provided for each country in the 'European_Exposure_Model_Data_Inputs_Sources.xlsx' file. For the countries where the total industrial surface area is available from Sousa et al. (2017), this value is obtained by dividing this total area by the total number of industrial buildings. In other countries this area has been based on expert judgment and checked against similar or neighbouring countries.

4.3.5 Reconstruction Costs

The reconstruction costs per square metre (i.e. per useful surface area) for structural and non-structural elements are provided in the 'European_Exposure_Model_Data_Inputs_Sources.xlsx' file for industrial buildings. The costs have been assumed to be 50% of the reconstruction costs of commercial offices. This assumption has been validated using data provided in COMPASS (2020), as presented in Appendix A, Section A.1. Minor modifications are finally applied to the reconstruction costs as a function of the main material of construction, by scaling the values as follows: MIX:1.00, MUR:0.95, ADO:0.95, CR:1.05, M:1.05, S:1.00, W:0.95, OT:1.00.

The structural and non-structural reconstruction cost per square metre is assumed to comprise 40% of the total replacement cost (which includes also the contents). The total replacement cost is divided into structural, non-structural and contents according to the following percentages: 15%, 25%, 60%, respectively.

4.3.6 Occupants

For this first version of exposure models, a simplifying assumption has been taken that the same number of people live and work within the same administrative unit, and thus the movement of people from their place of residence to place of work is not currently modelled. It is assumed that 40% of the working population work in the industrial sector (which is based on Eurostat statistics[2]).

The total population in each admin unit is distributed as a function of the area of industrial buildings per building class, multiplied by 0.4 and then the PAGER population distribution model (Jaiswal and Wald, 2010) for non-residential buildings is applied to obtain the average number of occupants in industrial buildings during the day, night and transit times. It is worth noting that due to the high resolution of the industrial exposure in many countries, there are a number of administrative regions that do not have industrial buildings and thus it is apparent that the current methodology is likely to be underestimating the occupants in industrial buildings (as the movement of people is not currently considered).

4.3.7 Validation data

No calibration data was used during the development of the industrial building exposure models, but comparisons and tests with other sources have been undertaken as a final validation of reliability of the models, as described in Appendix A.

4.4 Uncertainty in European Exposure

Some of the sources of uncertainty in the exposure models can be categorized as epistemic since with additional knowledge they could be reduced or even neglected. For example, the variability in the probabilities associated with each building class in the mapping schemes can be considered epistemic. This source of variability could be reduced by collecting additional ground truth information in order to understand to which building classes each combination of attributes actually corresponds. Alternatively, this source of variability can be propagated to the exposure results by considering different mapping schemes, each one defined by a different expert or set of experts, though recent studies have suggested that the impact of this epistemic uncertainty on the total losses is negligible (Kalakonas et al., 2020). This latter study did, however, demonstrate the importance of the epistemic uncertainty in the spatial resolution of the exposure on the losses. As discussed in Section 4.1.2, the location of the coordinates of the European exposure models have been defined to reduce the bias in the losses (at least in terms of national and administrative level 1 aggregate losses), whilst maintaining the original resolution of the data and ensuring the run-times of the calculations are reasonable for reproducibility of the models without the need for supercomputing resources. Nevertheless, as also presented in Section 4.1.2, open source tools have been made available that can allow users of the exposure models to disaggregate the exposure models to much higher spatial resolutions should they wish to explore this issue further.

Other parameters required for the derivation of exposure models can be considered as random variables (i.e. aleatory variability), for the purposes of propagating their dispersion to the risk results. These include the average area per dwelling, the average reconstruction cost per square metre, and the number of dwellings per building class. Although the variability of these parameters has not been thoroughly investigated in the past, it is possible to define some parametric distributions based on existing data for some European countries.

To this end, a large amount of data has been collected for five European countries characterized by moderate to high seismic hazard: Portugal, Spain, Italy, Greece, and Slovenia. It is fundamental to ensure that the data covers the entire country and it is defined at a small administrative division. This approach avoids the underestimation of the dispersion, which could arise from significant spatial aggregation (and thus averaging) of each parameter. One of the most reliable and comprehensive sources of information

for this type of data is the National Statistical Office from each country. For the definition of the variability in the average area per dwelling, information concerning the useful floor space per dwelling was collected at the smallest administrative level for all five countries. The evaluation of the distribution of this parameter indicates an average coefficient of variation of 21%. For example, the statistical analysis for Portugal indicated a value of 21.2% while Greece led to a value of 20.5%.

The National Statistical Offices also provide information regarding the construction costs for each country. However, this information was only available at the national level or at the first administrative division. Such level of aggregation does not allow modelling the variability in the construction costs within each country. As an alternative, for each country, 200 construction costs were randomly collected from real estate agencies for residential buildings, for three development types: cities, urban areas, and rural areas. Clearly the costs from real estate agencies reflect the commercial value and not the construction costs, though while the latter is preferable it is not readily available and thus an assumption has been made that the two are highly correlated. However, the purpose of this exercise is solely to evaluate the variability in the costs, and not the average costs. This set of values were used to estimate a coefficient of variation for each development type, leading to values of 39%, 53%, and 37% for cities, urban areas, and rural areas, respectively. These results indicate a similar dispersion in the costs for cities and rural areas, which is somehow expected as the building classes do not differ significantly within each: new construction in cities is mostly represented by modern mid- to high-rise reinforced concrete buildings while in rural areas low-rise masonry or single- dwelling reinforced concrete continue to be the main construction type. On the other hand, urban areas can be characterized by a wide range of building classes, spanning from costly modern high-rise buildings to cost-efficient housing, thus leading to a greater coefficient of variation.

The aleatory variabilities reported above are not currently propagated in the risk model as this is not currently possible with the OpenQuake-engine, but the impact could be explored further in the future.

4.5 Summary of European Exposure

The final exposure models contain an estimated 143 Million buildings, which have an average of 460 Million occupants (over a typical 24-hour period), and a total replacement cost (structural, non-structural and contents) of 50 Trillion Euros, of which 66% is from the residential building stock.

Table 4.5 presents a summary of the number, average number of occupants (over a 24-hour period) and total replacement cost of buildings in each country in the European exposure models. The distribution of the number of residential, commercial and industrial buildings in each country is then plotted in Fig. 4.7. Additional plots in terms of replacement cost and occupants are provided in Appendix B. These figures show that the majority of the building stock in all countries is residential, though the contribution of the commercial and industrial buildings become relatively more important when the occupants and total replacement costs are considered. Table 4.6 presents the distribution of building classes across all European exposure data (according to the simplified taxonomy – see Section 4.1.3) in terms of number of buildings, occupants (average of a 24-hour period) and total replacement cost. This data is then plotted for the top 10 building classes in terms of number of buildings in Fig. 4.8, and in terms of total replacement cost and occupants in Appendix B. These figures show the dominance of unreinforced masonry in the building stock, especially when the number of buildings is considered, though it should be considered that the reinforced concrete buildings have been separated into a number of separate classes. If all reinforced concrete building classes are combined, it is found that they contribute the most in terms of occupants and total replacement cost, but not in terms of number of buildings, which is still dominated by unreinforced masonry.

Table 4.5 Summary of the number, average number of occupants (over a 24-hour period) and total replacement cost of buildings (residential, commercial and industrial) in the European exposure models

Country	Number of buildings (thousands)	Occupants (average) (thousands)	Replacement cost (M EUR)
Albania	644	2043	30365
Andorra	18	56	8331
Austria	2316	6572	1086647
Belgium	3847	8439	1297493
Bosnia and Herzegovina	1099	2487	62981
Bulgaria	2193	5104	290548
Croatia	1670	2961	157490
Cyprus	287	625	90447
Czechia	2373	7824	616284
Denmark	1687	4274	876430
Estonia	235	971	63904
Finland	1339	4064	606109
France	15347	47581	7448179
Germany	19935	58029	10651811
Gibraltar	6	25	3484
Greece	3352	7743	608960
Hungary	2824	7270	528346
Iceland	74	262	62178
Ireland	1929	3619	508573
Isle of Man	20	60	8244
Italy	12188	43803	5262975
Kosovo	292	1348	20031
Latvia	383	1397	95219
Liechtenstein	14	27	11205
Lithuania	599	2050	160848
Luxembourg	131	464	82029
Malta	117	376	30247
Moldova	813	1968	43351
Monaco	10	29	6857
Montenegro	165	476	15490
Netherlands	5498	12875	2596802
North Macedonia	494	1523	41134
Norway	1761	3888	878738
Poland	7025	27916	1445547
Portugal	3629	6865	706579
Romania	5507	13818	337233
Serbia	2341	5164	227816
Slovakia	996	4021	287869
Slovenia	512	1497	84052
Spain	10013	32897	3738161
Sweden	2379	7576	1318713
Switzerland	1874	6083	1294150
Turkey	9160	61765	822174
United Kingdom	15475	49256	5548205

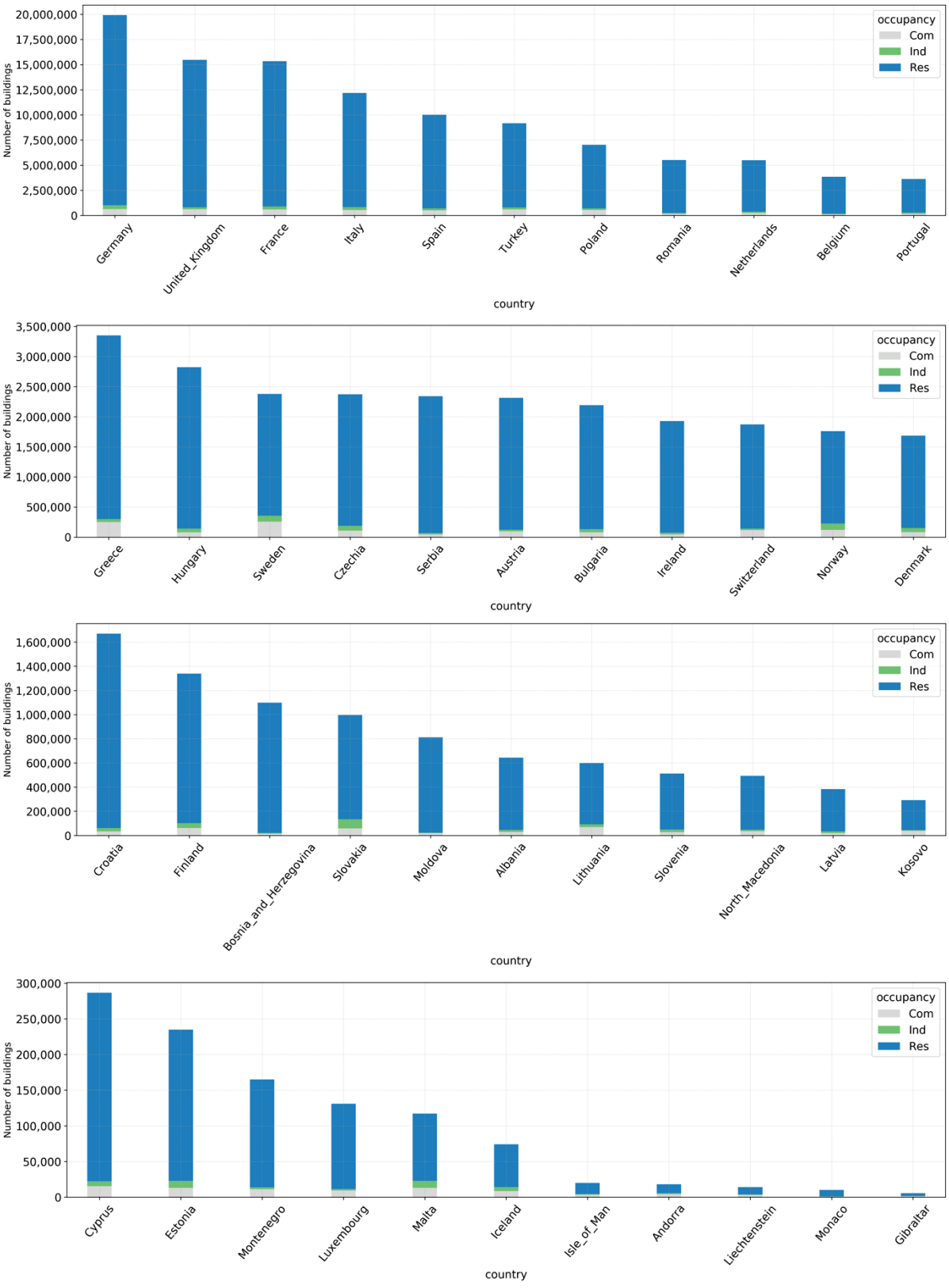

Fig. 4.7 Number of buildings in each country, and distribution between residential (Res), industrial (Ind) and commercial (Com) occupancy classes

Table 4.6 Summary of the distribution of building classes (according to the simplified taxonomy – see Section 4.1.3) in terms of number of buildings, occupants (average of a 24 hour period) and total replacement cost in the European exposure model

Simplified Taxonomy	Number of buildings	Occupants (average)	Total Replacement cost
Unreinforced masonry, low rise	49.7%	29.1%	26.5%
Concrete frame with infill panels, mid rise, low/moderate code	3.0%	10.2%	9.4%
Concrete frame with infill panels, low rise, low/moderate code	9.3%	6.9%	8.0%
Concrete frame with infill panels, mid rise, pre code	5.3%	7.4%	7.8%
Concrete wall, mid rise, pre code	3.6%	6.9%	7.0%
Steel, low rise	0.9%	4.2%	6.2%
Wood, low rise	8.2%	4.1%	5.2%
Concrete wall, mid rise, low/moderate code	1.0%	4.2%	5.0%
Concrete frame, low rise, pre code	0.4%	1.7%	2.9%
Concrete frame, low rise, low/moderate code	0.7%	2.2%	2.9%
Confined or reinforced masonry, low rise	6.7%	3.7%	2.7%
Concrete frame with infill panels, low rise, pre code	2.0%	2.0%	2.2%
Unreinforced masonry, mid rise	1.0%	2.0%	1.9%
Steel, mid rise	0.3%	1.0%	1.7%
Concrete wall, mid rise, high code	0.8%	4.8%	1.4%
Unreinforced masonry, mid rise, low/moderate code	0.4%	0.8%	1.4%
Concrete frame, mid rise, pre code	0.1%	0.6%	1.1%
Wood, mid rise	0.4%	0.7%	1.0%
Concrete frame with infill panels, mid rise, high code	0.2%	0.7%	1.0%
Concrete frame with infill panels, low rise, high code	0.9%	0.6%	0.8%
Concrete wall, low rise, pre code	0.6%	0.4%	0.7%
Concrete frame with infill panels, high rise, low/moderate code	0.1%	0.7%	0.6%
Confined or reinforced masonry, mid rise	0.4%	0.9%	0.6%
Concrete wall, low rise, low/moderate code	1.3%	1.3%	0.4%
Concrete frame, mid rise, low/moderate code	0.1%	0.5%	0.3%
Concrete frame, high rise, low/moderate code	0.0%	0.2%	0.2%
Adobe, low rise	1.9%	1.0%	0.2%
Concrete frame, low rise, high code	0.0%	0.1%	0.2%
Concrete wall, low rise, high code	0.7%	0.6%	0.1%
Concrete wall, high rise, low/moderate code	0.0%	0.1%	0.1%
Concrete frame with infill panels, high rise, pre code	0.0%	0.1%	0.1%
Concrete frame, high rise, pre code	0.0%	0.1%	0.1%
Concrete frame with infill panels, high rise, high code	0.0%	0.1%	0.1%
Concrete wall, high rise, high code	0.0%	0.0%	0.0%
Unreinforced masonry, mid rise, high code	0.0%	0.0%	0.0%
Unknown material, low rise	0.0%	0.0%	0.0%
Unreinforced masonry, high rise	0.0%	0.0%	0.0%
Concrete frame, mid rise, high code	0.0%	0.0%	0.0%
Unknown material, high rise	0.0%	0.0%	0.0%
Unknown material, mid rise	0.0%	0.0%	0.0%

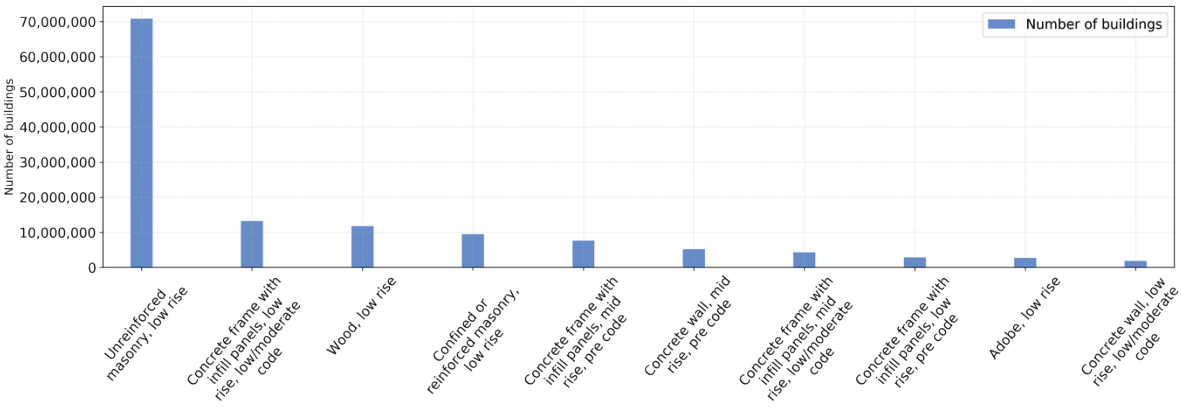

Fig. 4.8 Top 10 building classes (according to the simplified taxonomy) in the European exposure model in terms of number of buildings

4.6 Online Resources

As presented in the previous sections, the data used to develop the exposure models, as well as the final models themselves are available from the following GitLab repository: https://gitlab.seismo.ethz.ch/efehr/esrm20_exposure. Version 1.0 of this repository has been used for the results presented herein.

These exposure models contain a number of fields that are not used by the OpenQuake-engine for running the risk calculations, and so users interested in running calculations with these exposure models can obtain the OQ-engine input files here: https://gitlab.seismo.ethz.ch/efehr/esrm20/-/tree/main/Exposure.

A number of GIS layers and maps of the exposure models have been prepared and are available to view, query and download (with web services) though a web-based geo-viewer: https://maps.eu-risk.eucentre.it/tags/exposure/.

4.7 Future Improvements

From next year the 2021 census data is expected to become available in many European countries. This data will need to be downloaded and postprocessed for the updating of the exposure models. This will lead to the need for a more detailed assessment of the introduction of modern seismic design codes (CDH) in each European country, and the mapping of associated seismic zonation maps and the calculation of lateral force coefficients.

By releasing the models and assumptions publicly, additional feedback from the scientific community is expected. This feedback will be actively sought, in particular on the mapping schemes used in each country, not necessarily to better represent the epistemic uncertainty in this aspect of the model, but to reduce any bias that might currently be included due to inaccuracies in the building classes present in each country for different occupancy classes. As described in the previous section, the aleatory variability in the exposure models could also be explored for future updates to the European seismic risk calculations.

Improvements to the modelling of occupants within the buildings during different times of the day, week and season, accounting also for the migration of people from their place of residence to place of work, or for tourism, will be investigated in the future using data sets such as those from the ENACT project (https://ghsl.jrc.ec.europa.eu/enact.php).

Within the European Horizon 2020 RISE project (www.rise-eu.org), an effort led by GFZ Potsdam is being undertaken to develop a high-resolution Global Dynamic Exposure (GDE) model. The GDE aims to describe exposure on the building level by employing a fully open big-data approach including open geographic data such as OpenStreetMap, open remote-sensing data, machine learning, and other open data like cadastral data-services. The GDE provides a server infrastructure to automatically compute exposure indicators for ~375 million buildings at a global scale (a number which is growing by approx. 150,000 buildings daily as more buildings are mapped in OpenStreetMap). Some of these indicators are shown on the OpenBuildingMap (http://www.openbuildingmap.org) and its 3D version (http://obm3d.gfz-potsdam.de). Currently within the RISE project, the high-resolution building data from GED is being combined with the European exposure models presented herein to produce a high-resolution European exposure model. Further advances in this direction are expected in the coming years.

5 Vulnerability Model

This Chapter describes the development of vulnerability models for the estimation of economic losses (from repair, replacement and reconstruction due to direct damage) and loss of life. All of the data used to develop the vulnerability models has been made available with a CC-By license in a GitLab repository: https://gitlab.seismo.ethz.ch/efehr/esrm20_vulnerability. Note that the version of the vulnerability data used to develop the models for ESRM20 is v2.1 (which can be accessed by changing the branch of the repository from 'master' to 'v2.1'). The following sections describe the data in this repository and how they have been combined to produce the final fragility and vulnerability models used in ESRM20.

5.1 Capacity Curves for European Building Stock

Capacity curves provide a description of the lateral strength and deformation capacity of buildings or building classes, and are often transformed to the ADRS (acceleration displacement response spectrum) format for the purposes of developing fragility functions.

For ESRM20, capacity curves for a large range of building classes are needed to cover the varying construction types in Europe (as included within the European exposure models described in Chapter 4). The GEM Building Taxonomy v3.1 (https://github.com/gem/gem_taxonomy) has been used to define the vulnerability classes of European buildings with the attributes summarised below:

- Materials. CR: reinforced concrete, MR: reinforced masonry, MCF: confined masonry, MUR: unreinforced masonry, MUR-ADO: adobe, MUR-CB99: concrete block masonry, MUR-CL99: clay brick masonry, MUR-STDRE: dressed stone masonry, MUR-STRUB: rubble stone masonry, S: steel, W: wood/timber.
- Lateral load resisting systems. LDUAL: dual frame-wall system, LFINF: infilled frame, LWAL: load bearing wall, LFM: moment frame, LFBR: braced frame.
- Code Level or Ductility. CDN: absence of seismic design, CDL: low code level (designed for lateral resistance using allowable stress design), CDM: moderate code level (designed for lateral resistance with modern limit state design), CDH: high code level (designed for lateral resistance coupled with target ductility requirements and capacity design), DNO: non-ductile, DUL: low ductility, DUM: moderate ductility, DUH: high ductility.
- Height. H: number of storeys.
- Lateral Force Coefficient. The value of the lateral force coefficient, i.e. the fraction of the weight that was specified as the design lateral force in the seismic design code (see Code Level), expressed in % (currently applied to reinforced concrete moment and infilled frames only).

Following their use in the calculation of their Global Seismic Risk Map (GEM, 2018), the GEM Foundation has released a global database of capacity curves (Martins and Silva, 2020) which have been derived through the compilation of data coming from research studies and experimental campaigns. Within ESRM20, these capacity curves have been used to represent the European CR_LDUAL, CR_LWAL, MCF, MR, MUR, S and W typologies with different heights and ductility levels, for a total of 248 vulnerability classes.

As part of the European SERA project (www.sera-eu.org), a detailed set of capacity curves for European reinforced concrete infilled frames (CR_LFINF) and moment frames (CR_LFM) has been recently developed (Romão et al., 2019). A total of 264 reinforced concrete classes have been identified by combining different numbers of storeys (1 to 6), seismic design code levels (no code: CDN, low code: CDL, moderate code: CDM, high code: CDH) and lateral force coefficient levels (0, 5, 10, 15, 20, 25, 30 % of the weight of the structure). Buildings of design class CDN were typically designed to older codes

(from before the 1960's) that used allowable stresses and very low material strength values and considered predominantly the gravity loads. Buildings of design class CDL were designed considering the seismic action by enforcing values of the seismic coefficient, β (referred to herein as lateral force coefficient). Structural design for these codes was typically based on material-specific standards that used allowable stress design or a stress-block approach. Seismic design including modern concepts of ultimate capacity and partial safety factors (limit state design) was the basis of the CDM category of codes. The seismic action was also accounted for in the design by enforcing values for the lateral force coefficient, β. Finally, the CDH class refers to modern seismic design principles that account for capacity design and local ductility measures, similar to those available in Eurocode 8 (CEN, 2004). As described in Section 4.1.3, seismic zonation maps associated with the seismic design codes employed in Europe over the last century have been used to identify the lateral force coefficient of the reinforced concrete frame building classes in the exposure models.

The capacity curves for the 264 vulnerability classes were developed through simulated design of prototype frames (see e.g. Borzi et al., 2008; Verderame et al., 2010) and then nonlinear analysis has been undertaken to obtain the backbone capacity curves of these frames. Up to 300 capacity curves have been simulated per class by modifying the geometrical and material properties of the prototype frames, and thus accounting for the building-to-building variability in the simulated design. Fig. 5.1 shows, as an example, the median capacity curves for reinforced concrete frames with masonry infills not designed with seismic loads (i.e. CDN).

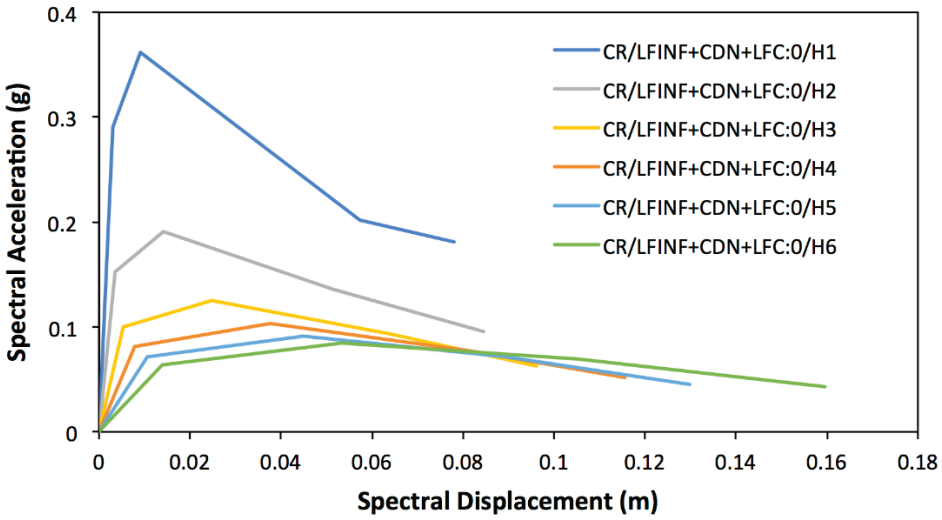

Fig. 5.1 Median capacity curves for reinforced concrete infilled frame buildings with no seismic design (CDN) from one to six storeys

All of the median capacity curves for the 512 vulnerability classes are publicly available on the following GitLab repository: https://gitlab.seismo.ethz.ch/efehr/esrm20_vulnerability (Romão et al. 2021).

5.2 Vulnerability Modelling

5.2.1 Vulnerability Modellers' Toolkit

The fragility functions of these European vulnerability classes have been computed using the Vulnerability Modeller's Toolkit, a resource that has been developed and released by the GEM Foundation in collaboration with members of the European risk community (Martins et al., 2021). This toolkit is a set of Python scripts that read the capacity curves, produce SDOF hysteretic models, launch

OpenSeesPy[8] to run nonlinear dynamic analysis, apply linear censored regression to the cloud of nonlinear responses, and compute fragility functions for different damage states, based on the user-defined damage state thresholds. A graphical user interface is provided with the toolkit and includes a set of default assumptions, allowing less experienced users to interact with the VMTK. Experienced users are instead encouraged to make use of Python's scripting capabilities to explore all the features of the VMTK source code and to contribute to future releases of the toolkit. The complete toolkit, including source code and GUI, is currently hosted in a publicly available GitHub repository. https://github.com/GEMScienceTools/VMTK-Vulnerability-Modellers-ToolKit.

5.2.2 Fragility Functions

The median capacity curves in Romão et al. (2021) have been read by the VMTK's 'nlth_on_sdof.py' script which has been used to produce SDOF models using the Pinching4 hysteresis curve of OpenSeesPy. Pinghing4 is a uniaxial material that represents a 'pinched' load-deformation response and exhibits degradation under cyclic loading. In addition to the response envelope (taken from the capacity curves), the hysteretic properties given in Table 5.1 have been assumed for the SDOF models for the different material types. The cyclic degradation of the strength and stiffness (i.e. Degradation = True) is modelled for the CR (CDL, CDN, DUL), MUR, MCF (DUL) and MR (DUL) typologies through unloading stiffness degradation, reloading stiffness degradation, and strength degradation. Mass proportional damping is used with different damping ratios for each typology. Typically, masonry is assigned 10% damping, confined masonry is 7.5%, reinforced concrete and wood is 5%, and steel is 3%. The nlth_on_sdof.py' script runs nonlinear dynamic analysis using each SDOF and a set of records. A database of recordings has been compiled for the nonlinear dynamic analyses using records with PGA above 0.05g in the Engineering Strong Motion (ESM, Luzi et al 2016; Luzi et al. 2020) and NGA (Chiou et al. 2008) databases. Records have then been selected from this database to match a range of intensity measure bins (represented by PGA) with maximum scaling factors that ranged from 1.5 (for the lower intensity bins) to 3.5 (for the highest intensity bins).

The final scripts used to develop the models are available on the aforementioned GitLab repository (Romão et al. 2021) for full reproducibility of the models.

Table 5.1 Adopted parameters of the Pinching4 hysteresis model (from the simpleSDOF4.tcl model provided in Vamvatsikos, 2011)

Parameters of Pinching4*	**Degradation = True**	**Degradation = False**
rdispP/N, fForceP/N, uForceP/N	0.5, 0.25, 0.05	0.5, 0.25, 0.5
gK1 gK2 gK3 gK4 gKLim	0, 0.1, 0, 0, 0.2	0,0,0,0,0
gD1 gD2 gD3 gD4 gDLim	0, 0.1, 0, 0, 0.2	0,0,0,0,0
gF1 gF2 gF3 gF4 gFLim	0, 0.4, 0, 0.4, 0.9	0,0,0,0,0
gE	10	10
dmgType	energy	energy

** See https://openseespydoc.readthedocs.io/en/latest/src/Pinching4.html?highlight=pinching4 for definition of the parameters*

The 'fragility_censored_cloud_analysis.py' script in the VMTK uses the nonlinear response outputs from each dynamic analysis together with damage thresholds to apply linear censored regression

[8] https://openseespydoc.readthedocs.io/en/latest/index.html

Four different intensity measure types have been used in the censored regression: PGA, Sa(0.3), Sa(0.6) and Sa(1.0). Plots of response displacement versus input spectral acceleration have been produced for all classes and a minimum displacement (10% of the yield displacement) has been reduce the influence of the low levels of linear response on the regression. Censored regression (see e.g. Crowley et al., 2017; Stafford, 2018) is applied by considering a censored displacement of 1.5 times the ultimate displacement (i.e. the final displacement in the capacity curve). The reasoning for considering a censored regression method lies in the fact that in numerical analyses, convergence can still be attained for levels of displacement that are incompatible with structural stability. This occurs mainly due to limitations in numerical modelling and it can introduce a bias in the best-fit curve. Fig. 5.2 shows an example of the regression plots for one of the building classes for each intensity measure type.

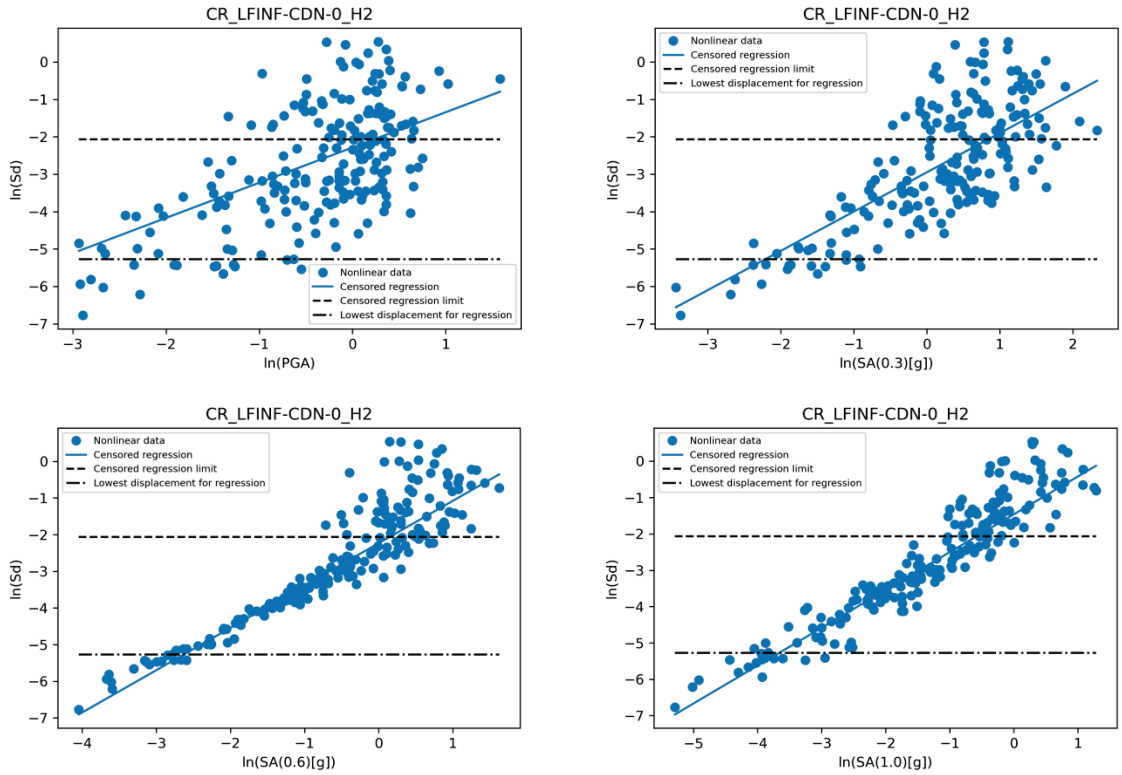

Fig. 5.2 Regression plots showing the response of an SDOF (based on the two storey capacity curve shown in Fig. 5.1 and the Pinching4 hysteresis parameters with degradation given in Table 5.1) and the censored linear regression using a lower limit displacement

The final intensity measure for each building typology is taken as that with the lowest lognormal dispersion in the fragility function, given that this is related to efficiency (i.e. low dispersion in the nonlinear response, given the intensity measure). Also, it has been found by checking the sufficiency (i.e. conditional independence of the distribution of nonlinear response, given IM, on other parameters of the ground motion) of the different intensity measures that the most efficient is typically also sufficient. Some recent studies have shown that the higher the efficiency, the higher the sufficiency of the intensity measure (e.g. Bradley et al. 2010). Others have cautioned that the typical checks for sufficiency (e.g. Luco and Cornell, 2007) only provide evidence rather than proof of sufficiency and that it should be ensured that the intensity measure is also efficient to ensure that the additional parameters really are having a significant influence on the response (Kazantzi and Vamvatsikos, 2015). Hence, the assumption that the most efficient intensity measure is also sufficient is deemed a simple and appropriate approach when developing hundreds of fragility functions for regional scale application.

A script is provided in the GitLab repository to compute the fragility functions (lognormal distributions) from the outputs of the nonlinear regression (esrm20_fragility_postprocess.py) for different damage states, based on user-defined damage state thresholds. For the European fragility functions, the damage thresholds presented in Fig. 5.3 have been assumed, where Sd_y represents the yield displacement and Sd_u represents the ultimate (final) displacement in the capacity curve. Four damage states are delineated with these thresholds: DS1 (slight), DS2 (moderate), DS3 (extensive) and DS4 (complete). It is worth noting here that a simple assumption has been made in this first set of vulnerability models for Europe that the damage state represents the combined state of damage to structural and non-structural elements and contents.

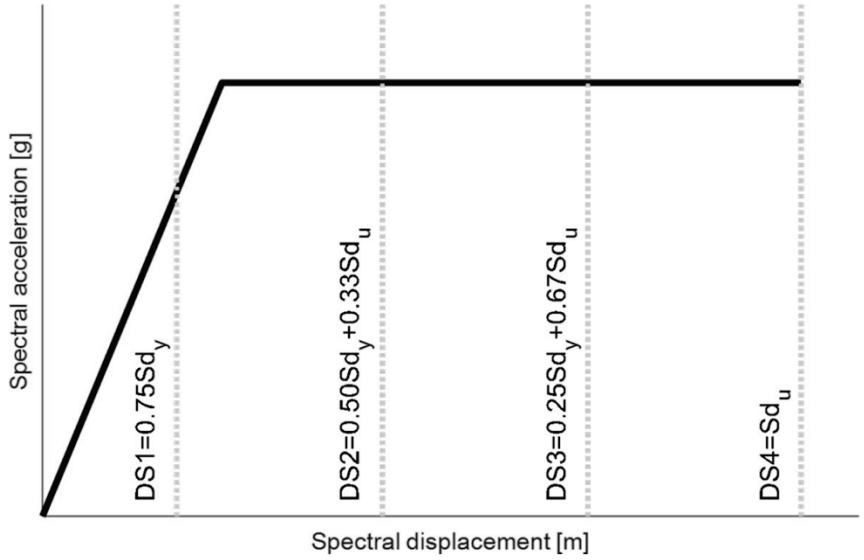

Fig. 5.3 Damage thresholds assumed in the development of the fragility functions (Martins and Silva, 2020)

In order to account for the building-to-building variability, which is not accounted for given the use of the median capacity curves, a separate study to produce fragility functions using all available capacity curves for the CR/LFINF and CR/LFM typologies has been undertaken. This study showed that the mean fragility functions based on all of the capacity curves of a given typology had very similar medians to the fragility functions based on the median capacity curves. However, the dispersion was, as expected, slightly higher. It was found that the additional dispersion required to account for building-to-building variability was around 0.3, and this is therefore combined with the dispersion obtained with the median capacity curves through the square-root-sum-of-squares to produce the final fragility functions in the aforementioned script. Other studies have also found similar additional uncertainty due to geometric and material variation within a given class of buildings (e.g. Grant et al., 2021).

For illustration and comparison purposes, Fig. 5.4 shows the fragility functions in terms of Sa(0.3s) that have been obtained with the capacity curves presented in Fig. 5.1. It is recalled that the intensity measure used in the final risk analyses for these classes is not Sa(0.3s), but varies from PGA (for one storey) to Sa(1.0s) (for six storeys). This plot has been produced using the vulnerability viewer that has been prepared for viewing and comparing fragility and vulnerability functions: https://vulncurves.eu-risk.eucentre.it/. The lognormal fragility functions for all classes and for all intensity measures as well as the final selected intensity measure type can be downloaded from the aforementioned tool, or can be obtained from the aforementioned GitLab repository (file 'esrm20_fragility_various_IM_lognormal.xlsx').

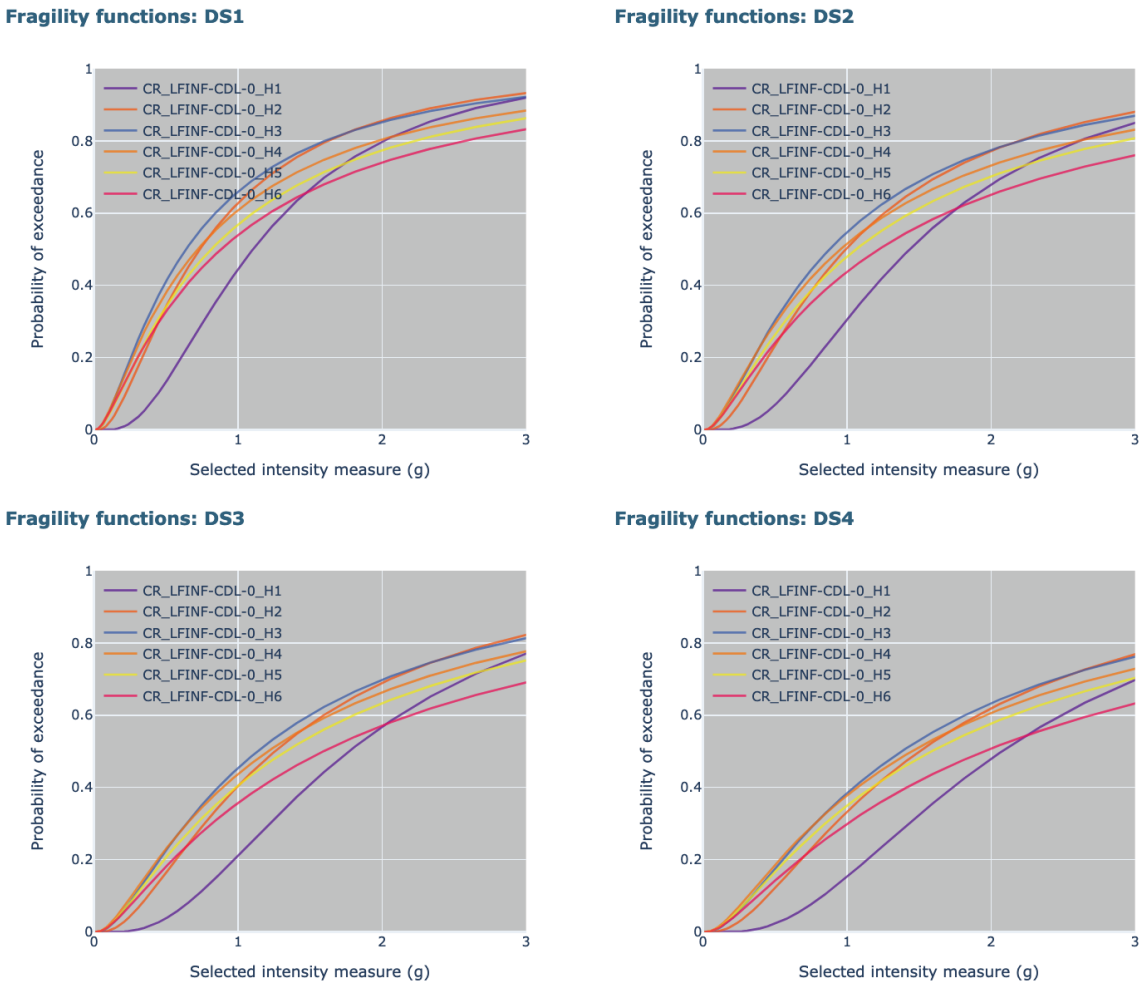

Fig. 5.4 Fragility functions calculated using the capacity curves presented in Fig. 5.1, where DS1 = slight damage, DS2 = moderate damage, DS3 = extensive damage and DS4 = complete damage (from https://vulncurves.eu-risk.eucentre.it/)

5.3 Vulnerability Functions for Economic Losses

The fragility functions are converted into vulnerability models using damage-loss models which provide damage ratios for each damage state (slight, moderate, extensive and complete). For losses due to damage, the following damage ratios (which represent the ratio of cost of repair to cost of replacement) have been adopted: 0.05 (slight damage), 0.15 (moderate damage), 0.6 (extensive damage), 1.0 (complete damage). These values are based on a review of recent European damage-loss models (Cosenza et al., 2018; Di Ludovico et al., 2021; De Martino et al., 2017; Erdik et al., 2021; Akkar, 2021; Tyangunov et al., 2006). One thing that is important to note is that these damage ratios are assumed to represent the cost of damage as a proportion of the total replacement cost, which covers structural, non-structural and contents, as fragility models for each component have not yet been developed.

For a range of intensity measure levels, the probability of occurrence of each damage state is obtained from the fragility functions, multiplied by the damage ratios and summed, leading to a mean loss ratio (MLR). The uncertainty in the loss ratio is assumed to follow a beta model and the standard deviation (σ) has been computed using the method presented in Silva (2019):

$$\sigma = \sqrt{MLR(-0.7 - 2 \cdot MLR + \sqrt{6.8 \cdot MLR + 0.5})} \quad (5.1)$$

5.4 Vulnerability Functions for Loss of Life

For loss of life, the model uses a number of factors obtained from both past observations and expert judgment, including: the likelihood that a completely damaged building will collapse to the extent that it could cause loss of life (currently taken as an average of 1.0% based on the data from recent earthquakes: Antonios Pomonis, personal communication), a collapse factor (which is based on expert judgment and varies from 0.5 to 5 as a function of the building class), the probability of entrapment given collapse (Reinoso et al. 2017), and the probability of loss of life given entrapment (Reinoso et al. 2017). Different entrapment ratios for day and night are assumed, with higher values for the latter given the increased time required for people to wake up and escape from a collapsing building. Also, an increase in the entrapment ratio with number of storeys has been implemented for the day-time entrapment rates. The loss of life given entrapment has been obtained from the data in Table 2 of Reinoso et al. (2017) where a clear distinction between buildings with less than and more than 5 storeys was observed and has thus been applied herein. Table 5.2 presents the assumed entrapment values, and all parameters of the damage-loss model are provided in the 'fatality_damage_model_ESRM20.xlsx' file in the GitLab repository.

Table 5.2 Adopted entrapment-related parameters of the fatality model

Number of storeys	P-entrapment (day)	P-entrapment (night)	P-loss-life|entrapment
1	0.25	0.95	0.4
2	0.5	0.95	0.4
3-4	0.75	0.95	0.4
>5	0.95	0.95	0.7

The fatality vulnerability models are obtained by simply multiplying the complete damage fragility functions by 1.0%, the collapse factor and the values presented in Table 5.2. It is noted that the uncertainty in the mean loss ratios for loss of life is not currently included in the vulnerability models. Given that the final risk metrics are based on mean values, this assumption does not influence the final results. Users of the models that wish to explore the uncertainties and fractiles of loss further can include an estimate of the uncertainty in the loss ratio in the input vulnerability models by specifying the standard deviation and associated distribution (beta or lognormal) in the OpenQuake input files.

5.5 Validation

Simple validation checks are undertaken to ensure the median and dispersion values of the fragility functions are within sensible ranges, and to compare with existing functions from the literature. A database of existing models that can be used for this purpose has been made available on the GitLab repository: 'European_Building_Vulnerability_Database.xlsx'.

For the vulnerability models, these have been compared with national empirical models, in terms of macroseismic intensity (MMI), released by PAGER (Jaiswal et al., 2009; Jaiswal and Wald, 2013). A mean vulnerability function for a number of countries has been calculated through an exposure-weighted combination of the vulnerability models of all the building classes in the country. For economic loss the weighting has been based on the total replacement cost per typology, whereas for loss of life the average occupants have been used. The vulnerability models for Sa(0.3) have been used, and the spectral ordinates have been converted to macroseismic intensity using the Faenza and Michelini (2010) model (with the associated uncertainty in the conversion represented by mean and +/1 standard deviation

vulnerability curves). It is assumed, for the purposes of these simple comparisons, that MMI and MCS (used in the Faenza and Michelini model) are equivalent. Fig. 5.5 shows this comparison in terms of economic loss vulnerability for Greece, Romania, Italy and Turkey, and Fig. 5.6 shows this comparison in terms of fatality/loss of life vulnerability.

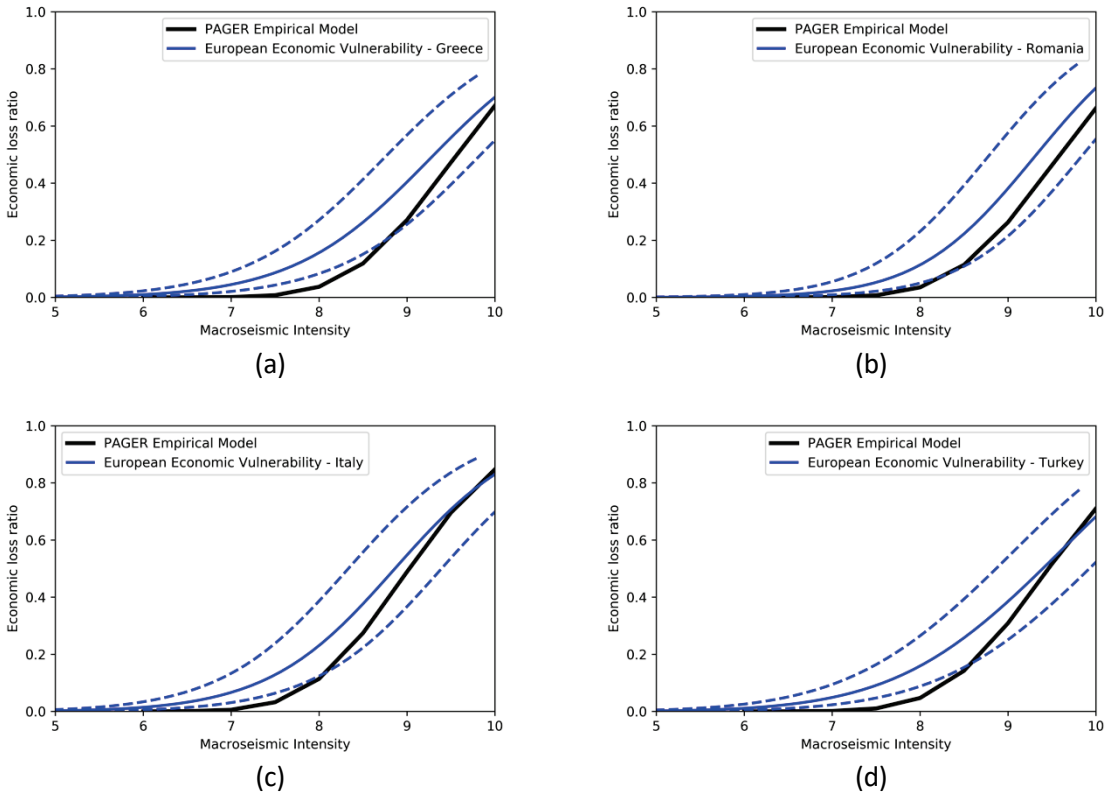

Fig. 5.5 Comparison of national empirical vulnerability models for economic losses from PAGER (Jaiswal and Wald, 2013) with national average vulnerability models produced using the models developed herein, and converted to macroseismic intensity. The dotted lines show the mean and +/1 standard deviation due to the uncertainty in the conversion of spectral acceleration to macroseismic intensity.

These figures show that the analytical models developed herein for economic losses compare very well with these empirical models for all countries considered. On the other hand, there is a larger difference in the models for fatalities, which is expected given that fatalities are much rarer and the empirical data is only based on a few events per country and is highly influenced by aspects such as the time of day of the event and number of people inside the buildings at the time of the earthquake. Another issue with this comparison for fatalities is that only a few building classes in a few locations of these countries have actually caused fatalities, whereas the national models developed from the analytical models are weighted by all building classes in the country. Hence, these comparisons alone are not sufficient to test the validity of the models and further tests are required.

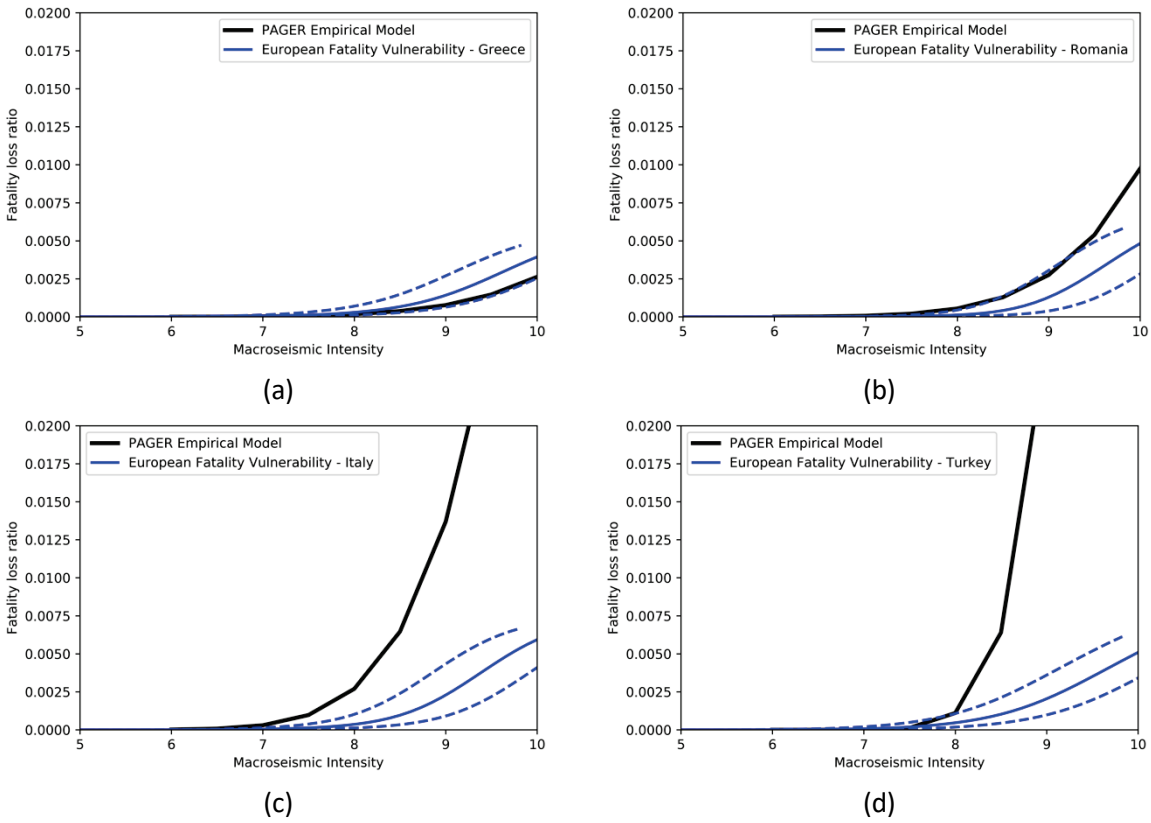

Fig. 5.6 Comparison of national empirical vulnerability models for fatalities from PAGER (Jaiswal et al., 2009) with national average vulnerability models produced using the models developed herein, and converted to macroseismic intensity. The dotted lines show the mean and +/1 standard deviation due to the uncertainty in the conversion of spectral acceleration to macroseismic intensity.

Additional tests have been undertaken to compare the losses predicted by the analytical models with past losses observed in recent damaging earthquakes in Europe (Crowley et al., 2021c). A total of 48 scenarios above magnitude 5 in Europe since the 1980's have been considered, and two approaches to represent the ground motion fields have been considered. The first uses scenario rupture models together with the European ground motion and site response models (see Chapter 3) for each event. The second makes use of ShakeMaps published for these events, either by USGS (https://earthquake.usgs.gov/data/shakemap/) or, for those in Italy and neighbouring countries, from INGV (http://shakemap.rm.ingv.it/shake4/). These ground motions are then combined with the current exposure and vulnerability models in the OpenQuake-engine to estimate direct economic losses and number of fatalities. The uncertainty in the ground motions is considered in these analyses by producing at least 100 different ground-motion fields. The losses from each ground motion field can then be used to obtain the mean, median and any other fractile loss (such as the 5th and 95th percentile). These losses are then compared with the reports on economic losses and fatalities. Fatality and economic loss data can be openly obtained from various databases including the Centre for Research on the Epidemiology of Disasters (CRED)'s EMDAT database (EMDAT, n.d.) and NOAA's Significant Earthquake Database (NGDC/WGS, n.d.). In the plots shown in Fig. 5.7 below, the data from CRED's EMDAT database (EMDAT, n.d.) has been used and is compared with the mean loss for each event (shown by a circle), together with the bounds given by the 5th and 95th percentile loss. A best-fit linear curve (shown by the black line) has also been fit to the modelled data.

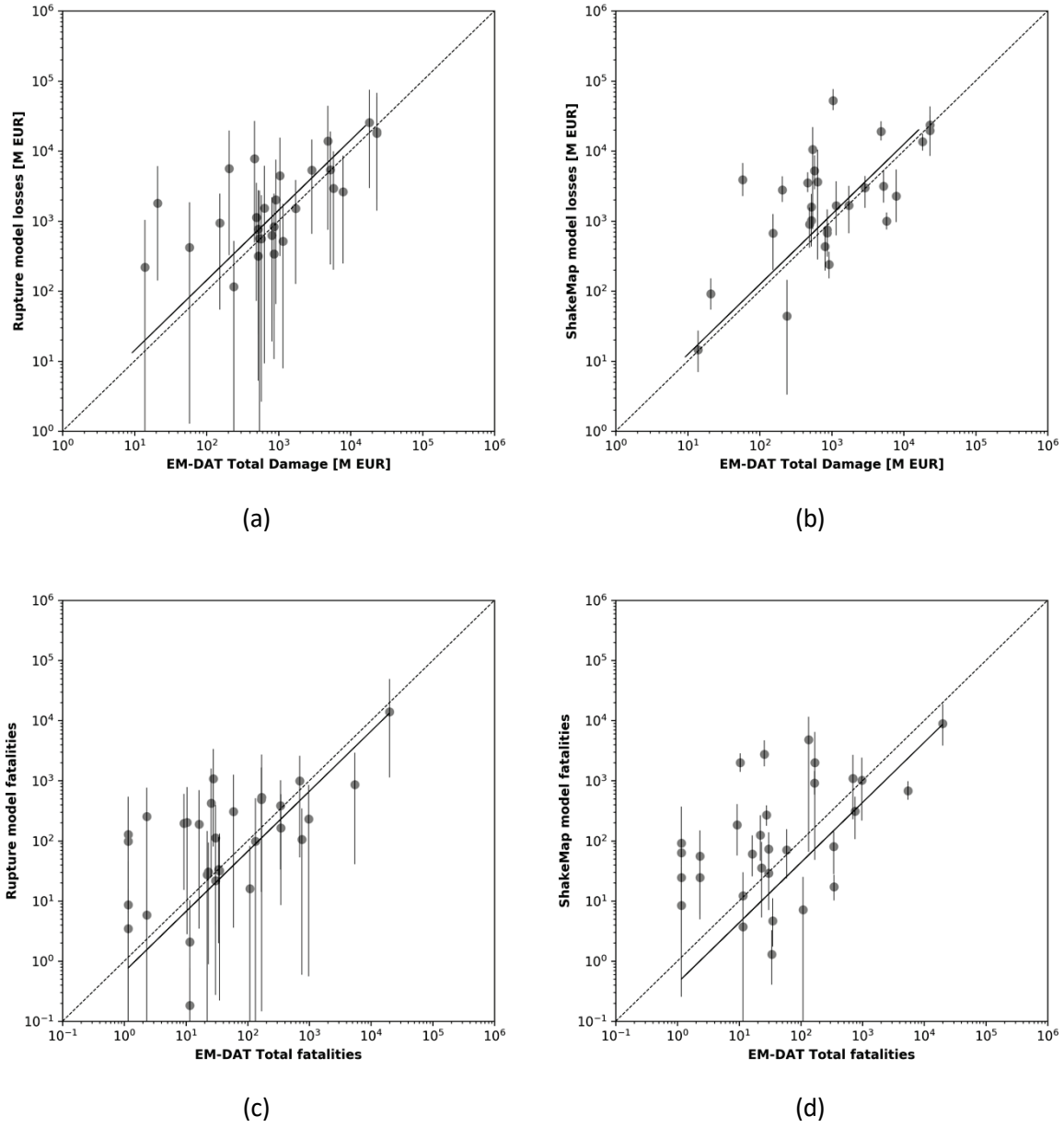

Fig. 5.7 Comparison of observed (horizontal axis) and modelled (vertical axis) losses (a) economic losses based on rupture model, (b) economic losses based on ShakeMap model, (c) fatalities based on rupture model, (d) fatalities based on ShakeMap model (Crowley et al., 2021c)

The observed economic losses in the plots have been inflated to the 2020 value using the Consumer Price Index (CPI) values reported by EM-DAT. The best-fit lines show there is a slight bias in the results, with modelled economic losses being slightly higher on average than the observed losses. For the fatalities, there appears to be a slight underestimation of the modelled losses, which could be due to changes in construction since the time of the event (and an almost 'natural selection' of the most vulnerable or fatal buildings in earthquake-hit areas).

The large uncertainties in the rupture models are evident from this plot, but the uncertainty bounds also illustrate that the combination of ground motion uncertainty, exposure and vulnerability leads, in the majority of cases, to a range of feasible losses that encompass the observed losses (i.e. those cases where the uncertainty bounds cross the 1:1 line). The uncertainties in the losses from the ShakeMaps are much lower (due to the constraints on ground motion provided by the recordings or macroseismic

intensity), and thus should provide a better picture of the performance of the exposure and vulnerability models, which although are seen to produce limited bias in the losses on average, can lead to losses that are quite different from the observations in individual cases. Appendix A, Section A.2 presents the same plots per country for Italy, Greece and Turkey, for which there have been sufficient events over the past 40 years. Very limited bias in the results is observed in the economic losses in Italy and in both the economic losses and fatalities in Turkey, whilst an overestimation of losses is observed in Greece, and an underestimation of fatalities is seen in Italy. Whilst these results are useful to test the models and should be kept in mind when evaluating the losses from the European risk model (presented in Chapter 6), it is worth considering that there are also a lot of uncertainties in the observed losses used in these tests (e.g. the total economic losses after an event are difficult to define and might not represent the same assets considered in the European risk model, fatalities are often misreported, and past losses have been inflated to today's value without explicitly considering the changes in the built environment).

5.6 Online Resources

As introduced in Fig. 5.4, a web app is available that allows users to view and compare the fragility and vulnerability functions for all of the vulnerability classes and to download Excel sheets with all of the models, and can be accessed here: http://vulncurves.eu-risk.eucentre.it/.

All of the inputs, scripts and outputs presented in this Chapter can be downloaded from the following GitLab repository: https://gitlab.seismo.ethz.ch/efehr/esrm20_vulnerability/-/tree/v2.1 (Romão et al., 2021). The final fragility and vulnerability models are provided in three Excel sheets (for all intensity measure types and for the 'Final' types used in the risk model).

These vulnerability models are also available in the .xml format used by the OpenQuake-engine for running the risk calculations here: https://gitlab.seismo.ethz.ch/efehr/esrm20/-/tree/main/Vulnerability. This repository also contains an additional file that is required to run the risk calculations, which is the mapping between the building classes in the exposure models and the vulnerability classes for which vulnerability models have been developed ('esrm20_exposure_vulnerability_mapping.csv').

The scenarios and all input files used to validate the models (see Section 5.5) have all be made available at the following GitLab repository: https://gitlab.seismo.ethz.ch/efehr/esrm20_scenario_tests.

5.7 Future Improvements

There are a number of possible improvements to the vulnerability models, some of which are already planned:

- Fragility and vulnerability models using a simulated-design approach could be developed for more building classes.
- Separate fragility models could be provided for structural, non-structural and contents, and these could be combined with appropriate damage-loss models to produce vulnerability models that account for the loss to each component separately.
- Demand surge could be included in the damage-loss model to account for larger losses in the more damaging events.
- Expansion of the models to include other consequences: for example, injuries, homelessness, downtime.

6 Seismic Risk Model Results

This Chapter summarises the main risk results that have been post-processed at national level for the 44 European countries and presents some of the validation results carried out as a consistency check of the model. These results have been run with version 3.13.0-git16dd69ecea of the OpenQuake-engine which has been installed from source on a server cluster with the following characteristics: 3+1 worker nodes M630 (Intel Xeon E5 20c/40t, 128 GB of RAM each). With these computational resources, it takes about 14 hours to run the risk model for the whole of Europe.

6.1 Summary of Risk Results

The national average annual losses for each country in Europe are summarized in Table 6.1. It is noted that the average annual loss ratio (AALR) represents the average annual loss divided by the total replacement cost of the buildings. Fig. 6.1 and Fig. 6.2 present the average annual losses (economic and loss of life, respectively) for each country, and the proportion for each occupancy class (residential, industrial and commercial). These results show that the majority of the losses, both economic and loss of life, are within the residential building stock, and the commercial and industrial building stock has a larger impact on the economic losses than on loss of life. Italy has by far the highest AAL in terms of economic losses in Europe, whereas Turkey has the highest AAL in terms of loss of life. In terms of relative losses, Turkey is at the top of the list, closely followed by Albania, Cyprus and Romania. A more detailed view of how these risk metrics vary across Europe (at administrative level 1 resolution) is provided in the maps in Fig. 6.3 to Fig. 6.5.

Table 6.1 Summary of the average annual loss metrics for each country

Country	AAL (Economic loss, M EUR)	AALR (Economic loss, ‰)	AAL (loss of life)
Albania	39	1.270	12
Andorra	<1	0.021	<1
Austria	113	0.104	4
Belgium	35	0.027	2
Bosnia and Herzegovina	14	0.226	3
Bulgaria	128	0.442	11
Croatia	70	0.444	8
Cyprus	114	1.260	4
Czechia	1	0.002	<1
Denmark	1	0.001	<1
Estonia	<1	0.001	<1
Finland	<1	<0.001	<1
France	171	0.023	5
Germany	260	0.024	5
Gibraltar	<1	0.045	<1
Greece	591	0.971	33
Hungary	27	0.050	1
Iceland	10	0.155	<1
Ireland	<1	<0.001	<1
Isle of Man	<1	0.000	<1
Italy	3303	0.628	128
Kosovo	5	0.251	2

Country	AAL (Economic loss, M EUR)	AALR (Economic loss, ‰)	AAL (loss of life)
Latvia	<1	0.002	<1
Liechtenstein	<1	0.037	<1
Lithuania	<1	0.001	<1
Luxembourg	1	0.007	<1
Malta	1	0.043	<1
Moldova	8	0.176	1
Monaco	1	0.141	<1
Montenegro	6	0.419	1
Netherlands	37	0.014	1
North Macedonia	18	0.450	4
Norway	2	0.003	<1
Poland	2	0.001	<1
Portugal	76	0.108	4
Romania	402	1.190	86
Serbia	45	0.195	4
Slovakia	11	0.039	1
Slovenia	31	0.367	3
Spain	280	0.075	10
Sweden	1	0.001	<1
Switzerland	55	0.043	2
Turkey	1179	1.430	569
United Kingdom	14	0.002	<1

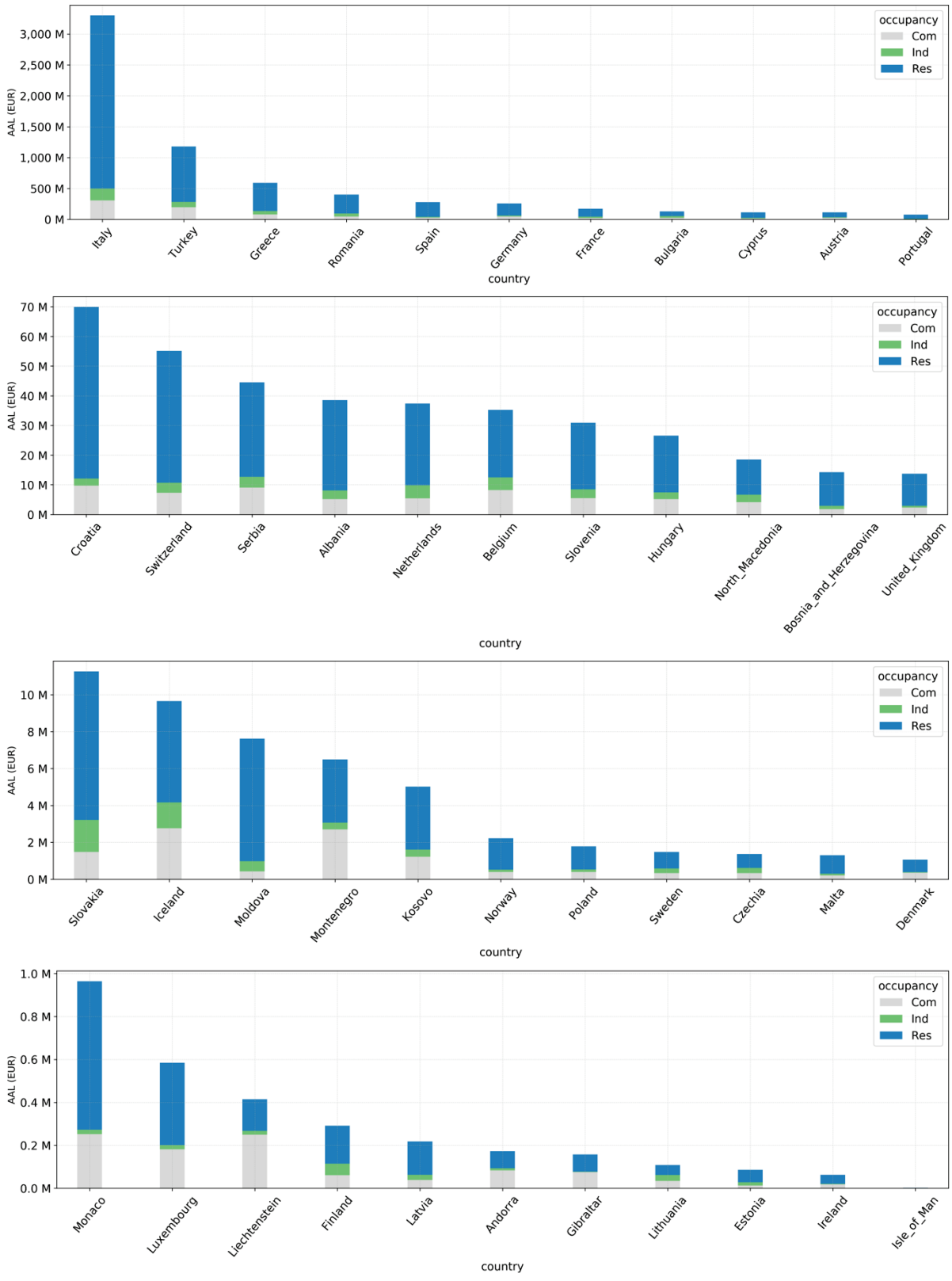

Fig. 6.1 AAL (economic) in each country, and distribution between residential (Res), industrial (Ind) and commercial (Com) occupancy classes

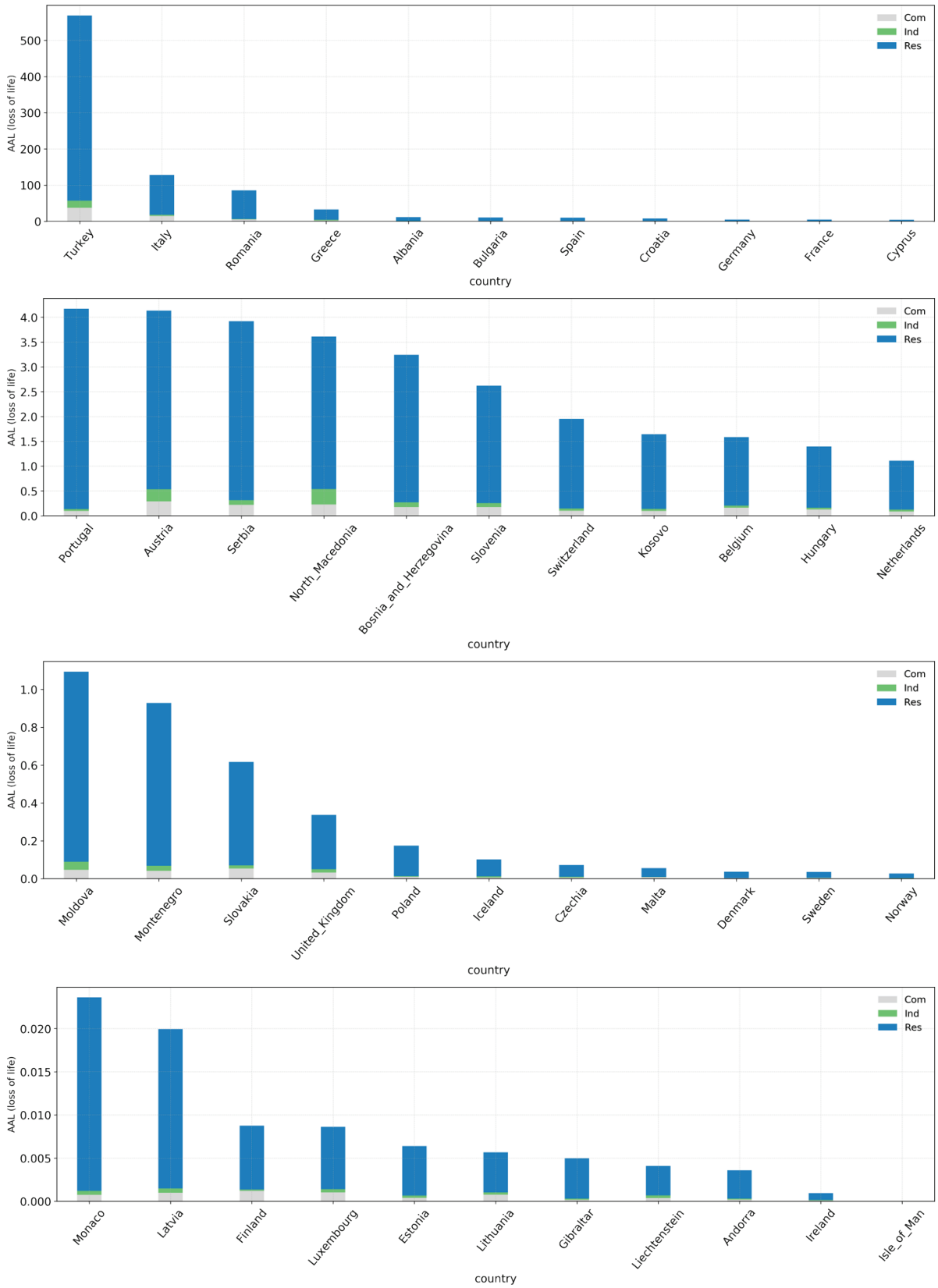

Fig. 6.2 AAL (loss of life) in each country, and distribution between residential (Res), industrial (Ind) and commercial (Com) occupancy classes

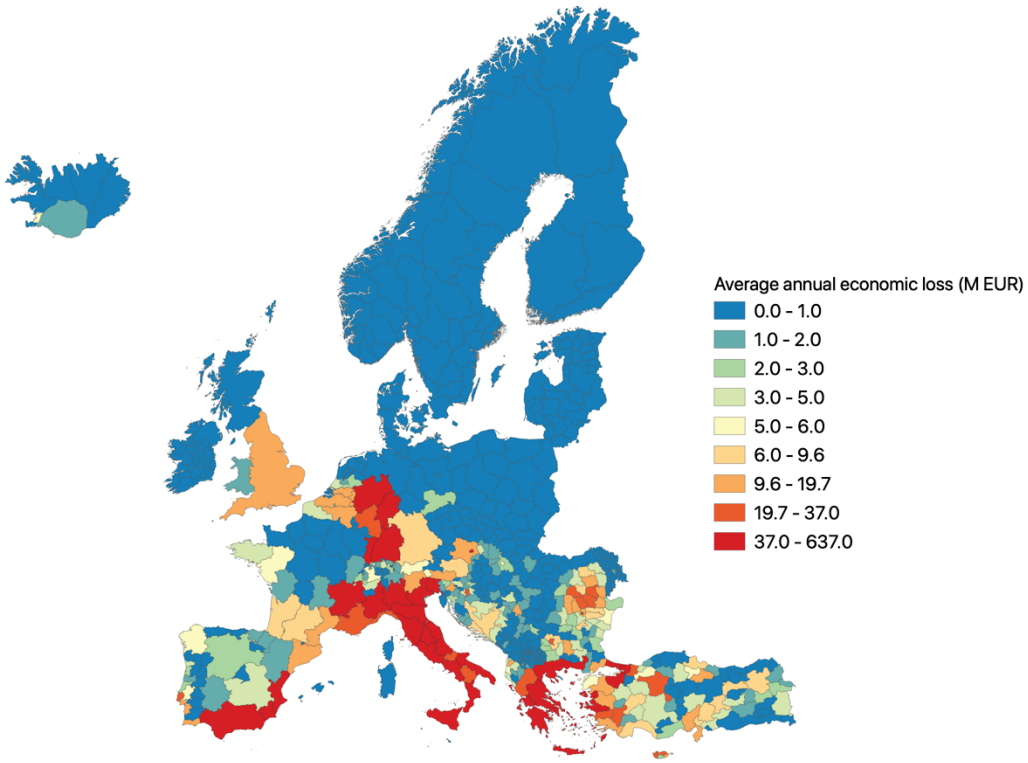

Fig. 6.3 Map of the average annual economic loss across Europe at administrative level 1

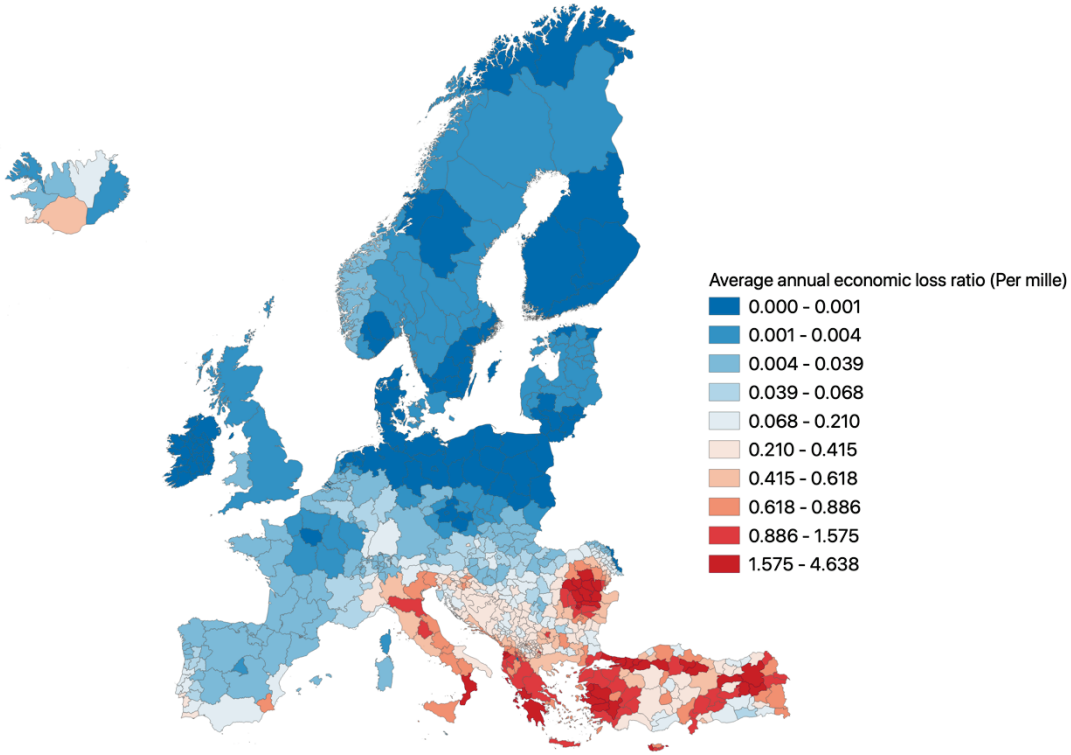

Fig. 6.4 Ma of the average annual loss economic loss ratio across Europe at administrative level 1

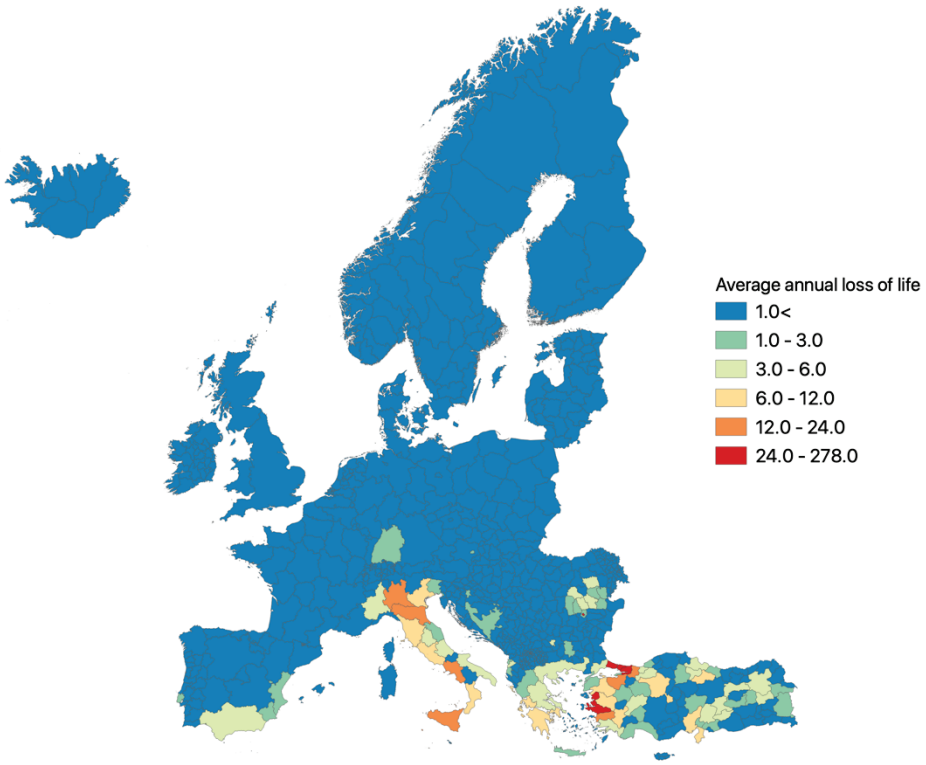

Fig. 6.5 Map of the average annual loss of life across Europe at administrative level 1

Table 6.2 shows the distribution of AAL (both economic and loss of life) across Europe according to the simplified taxonomy. These results show that mid-rise reinforced concrete frames with infill panels with older seismic design (CDL or CDM), and low-rise unreinforced masonry buildings are the two building classes that contribute most to both economic losses and loss of life in Europe. One thing that might seem unusual with these results is that these seismically designed reinforced concrete buildings contribute more to the losses than pre-code (CDN) buildings. The main reason for this is that the losses are predominantly from areas of high hazard where there is a history of damaging earthquakes. In these areas, the first generations of seismic design codes were introduced much earlier than in other parts of Europe, and often this introduction occurred during the 60's and 70's when a large proportion of the current reinforced concrete building stock was being constructed.

Table 6.2 Summary of the distribution of building classes (according to the simplified taxonomy – see Section 4.1.3) in terms of European AAL (economic and loss of life)

Simplified Taxonomy	**AAL (Economic loss)**	**AAL (Loss of life)**
Concrete frame with infill panels, mid rise, low/moderate code	28.8%	57.7%
Unreinforced masonry, low rise	28.4%	16.1%
Concrete frame with infill panels, low rise, low/moderate code	14.2%	5.6%
Unreinforced masonry, mid rise	5.1%	2.9%
Confined or reinforced masonry, low rise	2.8%	1.4%
Concrete frame with infill panels, mid rise, pre code	2.4%	2.2%
Concrete frame, low rise, low/moderate code	2.3%	1.5%
Confined or reinforced masonry, mid rise	2.2%	1.9%
Concrete wall, mid rise, low/moderate code	2.1%	1.2%
Concrete frame with infill panels, low rise, pre code	1.8%	1.0%
Concrete frame, low rise, pre code	1.7%	0.2%
Adobe, low rise	1.5%	3.6%

Table 6.2 (cont.) Summary of the distribution of building classes (according to the simplified taxonomy – see Section 4.1.3) in terms of European AAL (economic and loss of life)

Simplified Taxonomy	AAL (Economic loss)	AAL (Loss of life)
Concrete wall, mid rise, high code	1.4%	1.7%
Steel, low rise	0.9%	0.0%
Concrete frame, mid rise, low/moderate code	0.7%	1.8%
Concrete wall, mid rise, pre code	0.6%	0.1%
Concrete wall, low rise, low/moderate code	0.6%	0.3%
Concrete frame, mid rise, pre code	0.5%	0.2%
Wood, low rise	0.4%	0.1%
Concrete frame with infill panels, high rise, low/moderate code	0.4%	0.2%
Unreinforced masonry, mid rise, low/moderate code	0.3%	0.1%
Concrete frame with infill panels, mid rise, high code	0.2%	0.0%
Steel, mid rise	0.2%	0.0%
Concrete frame with infill panels, low rise, high code	0.1%	0.0%
Concrete wall, low rise, high code	0.1%	0.1%
Concrete wall, low rise, pre code	0.1%	0.0%
Concrete frame, high rise, low/moderate code	0.1%	0.1%
Concrete frame, low rise, high code	0.1%	0.0%
Wood, mid rise	0.0%	0.0%
Concrete frame with infill panels, high rise, pre code	0.0%	0.0%
Concrete frame, high rise, pre code	0.0%	0.0%
Concrete wall, high rise, low/moderate code	0.0%	0.0%
Concrete wall, high rise, high code	0.0%	0.0%
Unreinforced masonry, high rise	0.0%	0.0%
Unreinforced masonry, mid rise, high code	0.0%	0.0%
Unknown material, low rise	0.0%	0.0%
Concrete frame with infill panels, high rise, high code	0.0%	0.0%
Unknown material, mid rise	0.0%	0.0%
Unknown material, high rise	0.0%	0.0%
Concrete frame, mid rise, high code	0.0%	0.0%

Finally, the loss curves showing the return periods of total economic loss (Billion EUR) for each country in the model are presented in Fig. 6.6. These curves show the aggregated loss to all buildings (residential, commercial and industrial) within the country for the following return periods: 50, 100, 200, 500 and 1000 years.

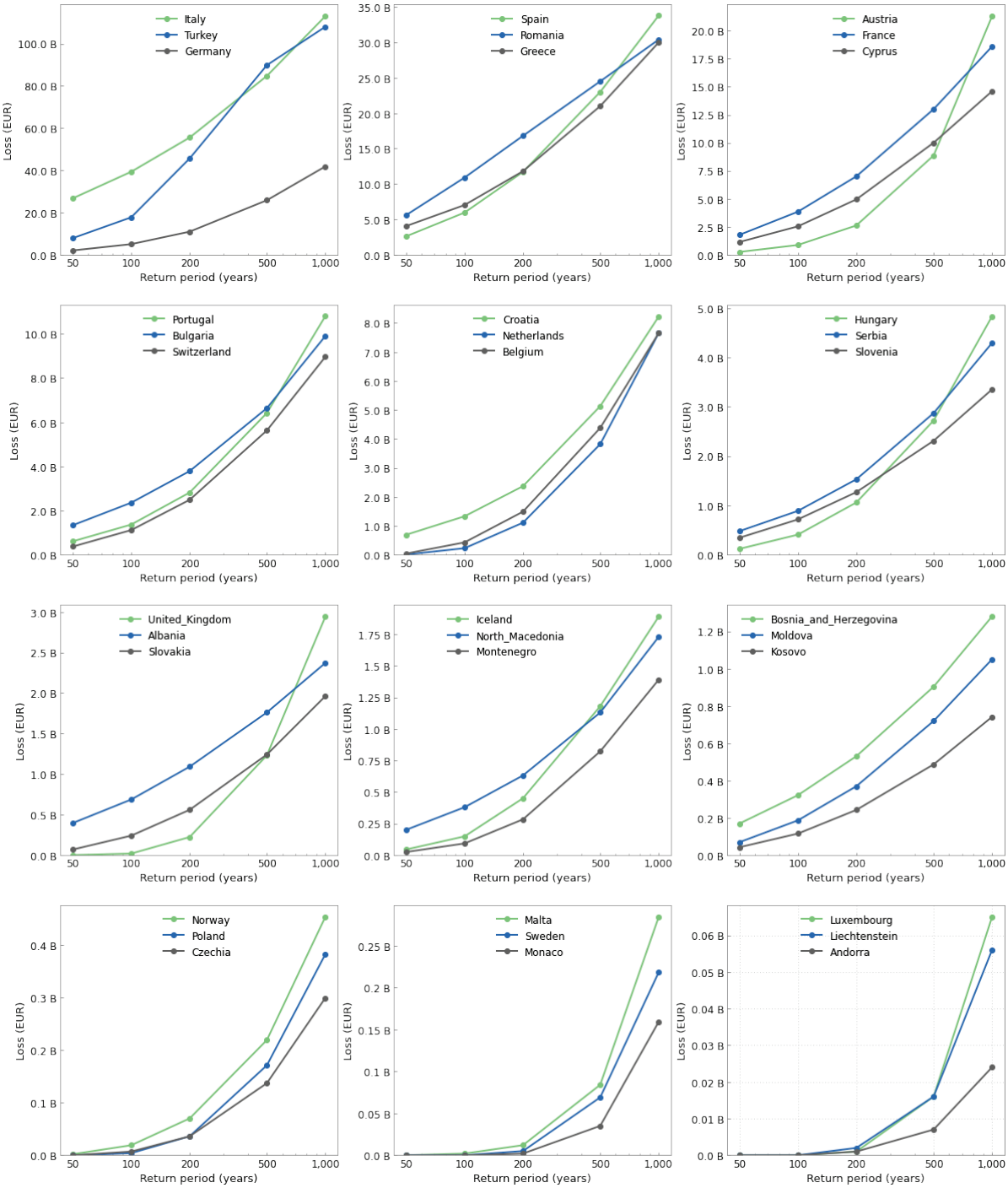

Fig. 6.6 Loss curves showing the return periods of total economic loss (Billion EUR) for each country in the model

6.2 Validation

The empirical average annual loss (AAL) for economic losses and loss of life for Europe and for countries with more than 5 damaging/fatal events since 1980 have been computed from Munich Re's NatCatService (MunichRe, 2019)[9] and EMDAT (EMDAT, n.d.). The date for the period 1980-2017 has

[9] The data for the plots in this section was provided by the GEM Foundation that has access to the NatCatService data (up to the end of 2018).

been obtained from the NatCatService database, whereas the data from the past 100 years (1920-2020) has been extracted for loss of life. In order to get fairly stable estimates of average annual losses, it is necessary to use a long period of time. However, the further back in time, the less representative the losses are of what would happen today under the same levels of seismicity. This is believed to be even more important for economic loss, and so only data since 1980 has been used. The results are presented in Table 6.3 and Table 6.4, respectively, and compared with the equivalent values from ESRM20.

Table 6.3 Empirical average annual loss (AAL) for economic losses compared with the values from ESRM20

	NatCatService (1980-2017)[1] (AAL, economic, M EUR)	**NatCatService (1980-2017)[2] (AAL, economic, M EUR)**	**EMDAT (1980-2020)[1] (AAL, economic, M EUR)**	**ESRM20 (AAL, economic, M EUR)**
Europe	3111	4341	4166	7055
Italy	1831	2322	2130	3303
Turkey	535	1087	810	1179
Greece	297	321	276	591

[1] *inflation adjusted using national Consumer Price Index (CPI),*
[2] *normalized based on national Gross Domestic Product (GDP)*

Table 6.4 Empirical average annual loss (AAL) for loss of life compared with the values from ESRM20

	EMDAT (1920-2020) AAL (Loss of Life)	**ESRM20 AAL (Loss of Life)**
Europe	969	903
Italy	86	128
Turkey	827	569
Greece	13	33

The same data has been used to plot empirical loss curves, by ranking the losses in the databases from largest to smallest, and assigning an annual rate of 1 divided by the length of time of the database (i.e. 37 years for economic loss and 100 years for loss of life). These empirical loss curves have then been compared with the loss curves for the whole of Europe from the model (Fig. 6.7 for economic loss and Fig. 6.8 for loss of life). For the modelled loss curves, the epistemic uncertainty in the loss curves has been presented by showing the loss curves for each of the 100 samples of the logic tree (see Section 3.3): these are represented in grey in the figures, and the mean loss curve is shown in black.

Table 6.5 presents a similar table to the one presented at the beginning of this report in Chapter 1, but now the results of ESRM20 have been added. These results show that the order of the top 3 countries in Europe (in terms of economic losses) agree with both empirical loss databases. It is also notable that Belgium is in the top 10 of the other models/databases, but not in ESRM20. It is interesting to note that Spain, which is not in the top 10 of GEM 2018.v1 or GAR15, is found in ESRM20 and both of the empirical loss databases.

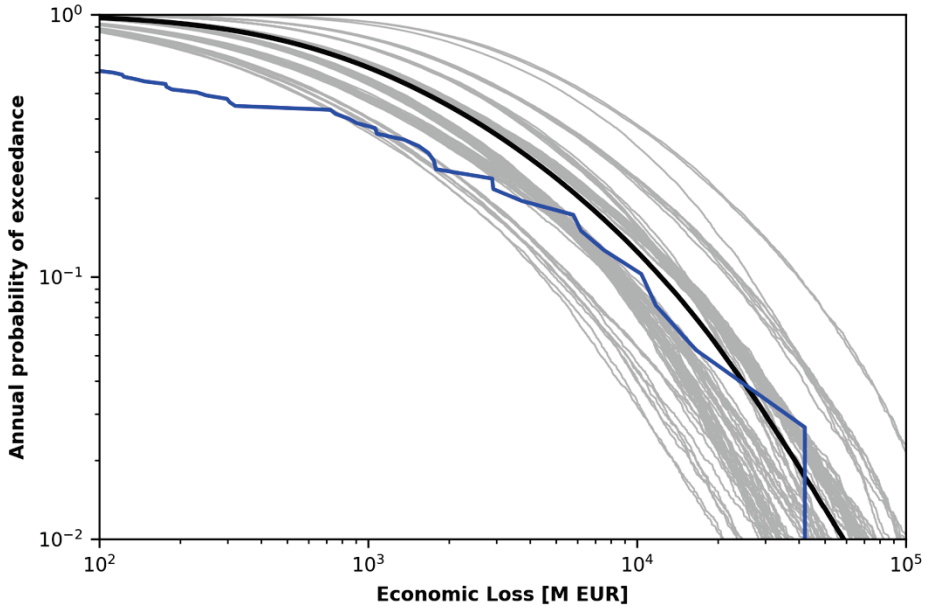

Fig. 6.7 Empirical loss curve for Europe in terms of economic loss using data from NatCatService for the past 37 years (GDP weighted data) (blue curve) compared with the modelled loss curves: each branch of the logic tree shown in grey and the mean loss curve is shown in black

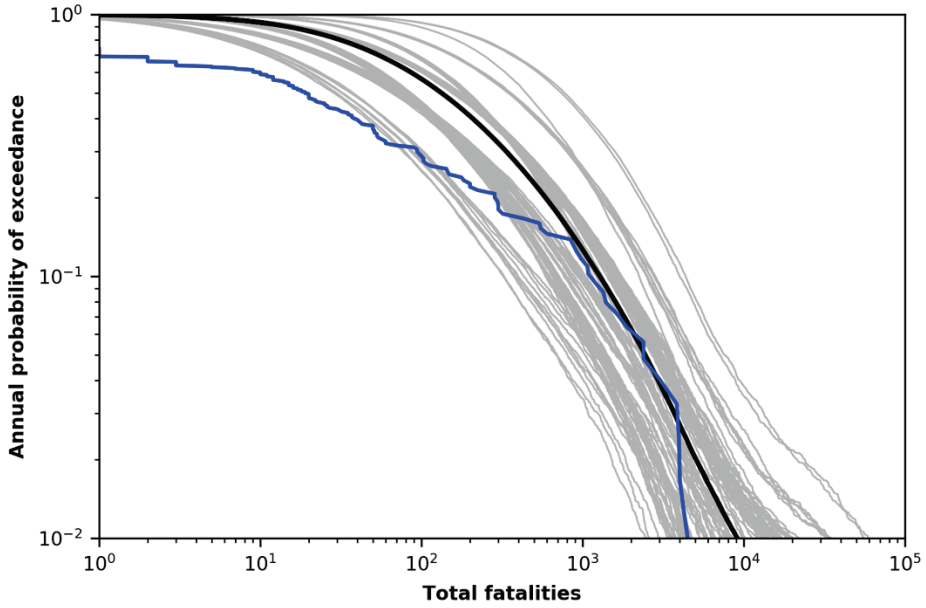

Fig. 6.8 Empirical loss curve in terms of loss of life using data from EM-DAT for the past 100 years (blue curve) compared with the modelled loss curves: each branch of the logic tree shown in grey and the mean loss curve is shown in black

Table 6.5 Ranking of countries based on estimated AAL from ESRM20, GEM 2018.v1 and the GAR15, and on observed losses from the NatCatService and EMDAT disaster databases. The dark blue coloured cells represent countries that are present in all studies, the light blue cells are present in four out of the five studies and the light grey cells are present in three of the studies.

Estimated economic *AAL*			**Observed economic losses**	
ESRM20	**GEM 2018.v1**	**GAR (2015)**	**NatCatService (1980-2017)**	**EMDAT (1980-2021)**
Italy	Turkey	Italy	Italy	Italy
Turkey	Italy	Greece	Turkey	Turkey
Greece	Greece	Germany	Greece	Greece
Romania	Romania	Turkey	Moldova	Croatia
Spain	France	United Kingdom	Spain	Albania
Germany	Germany	Switzerland	Croatia	Spain
France	Cyprus	France	Portugal	Belgium
Bulgaria	Bulgaria	Romania	Iceland	Serbia
Cyprus	Austria	Netherlands	Serbia	Portugal
Austria	Belgium	Belgium	Belgium	Germany

Table 6.6 presents a comparison of the values of AAL (economic) in ESRM20, GEM 2018.v1 and the GAR15. The latter two are in USD, but the exchange rate has been between 1.06 and 1.23 since the time these models were released. The total average annual loss in the GAR15 is 24,113 M USD, which is at least 5 times higher than the average losses reported in Europe over the past 37 years. On the other hand, the total average annual loss in GEM 2018.v1 is around 8,864 M USD, and is thus much closer to the empirical losses and to the total losses in ESRM20. A more detailed comparison with GEM 2018.v1, focusing on the top 10 countries in ESRM20 (which contribute to around 85% of the total loss in Europe), shows that the losses in Spain and Italy are over 30% higher in ESRM20 and the losses in Turkey, France, Cyprus are over 30% lower, whereas the difference in all other countries is within 30%. The main reason for these differences is likely to be in the recent updates to the European seismic hazard model, and interested users can now explore further these differences thanks to the open release of all the products, as discussed in the Introduction.

Table 6.6 Comparison of the average annual economic loss values from ESRM20, GEM 2018.v1 and the GAR15

Country	**GAR15 (M USD)**	**GRM18 (M USD)**	**ESRM20 (M EUR)**
Albania	47	34	39
Andorra	<1	<1	<1
Austria	525	123	113
Belgium	190	117	35
Bosnia and Herzegovina	15	18	14
Bulgaria	83	135	128
Croatia	153	116	70
Cyprus	29	153	114
Czechia	150	7	1
Denmark	3	11	1
Estonia	1	1	<1
Finland	1	1	<1

Table 6.6 (cont.) Comparison of the average annual economic loss values from ESRM20, GEM 2018.v1 and the GAR15

Country	GAR15 (M USD)	GRM18 (M USD)	ESRM20 (M EUR)
France	501	338	171
Germany	2350	194	260
Gibraltar	3	0	<1
Greece	5109	733	591
Hungary	123	30	27
Iceland	32	30	10
Ireland	13	<1	<1
Isle of Man	N/A	<1	<1
Italy	9773	2105	3303
Kosovo	N/A	11	5
Latvia	<1	1	<1
Liechtenstein	10	1	<1
Lithuania	1	1	<1
Luxembourg	13	2	1
Malta	13	2	1
Moldova	12	35	8
Monaco	5	2	1
Montenegro	238	14	6
Netherlands	23	88	37
North Macedonia	26	36	18
Norway	10	14	2
Poland	189	16	2
Portugal	7	69	76
Romania	256	424	402
Serbia	33	55	45
Slovakia	61	26	11
Slovenia	159	61	31
Spain	72	88	280
Sweden	5	8	1
Switzerland	787	100	55
Turkey	2200	3607	1179
United Kingdom	892	57	14

6.3 Online Resources

Users interested in repeating the European seismic risk calculations can obtain the final OQ-engine input files here: https://gitlab.seismo.ethz.ch/efehr/esrm20. It is noted that v1.0 of this repository (which can be accessed by changing the 'main' branch to the tag v1.0) has been used to produce the results presented in this report. The 'Configuration_file' folder contains the main files needed to run the models. The hazard configuration files in this folder have been described previously (see Section 3.4). Instead, to run the risk calculations only the three 'ebrisk' files are needed. Europe has been divided up into three groups to run the risk calculations (for computational reasons), but users that are interested in only

running the calculations for specific countries can modify one of these files to call only the 'site_model_file' and 'exposure_file' for the country of interest.

Two .csv files with a summary outputs of the risk calculations at country and admin level 1 have been uploaded to this repository, to the 'Risk' folder. Any additional outputs of interest to users that are not able to rerun the model can be made available upon request[10].

A number of GIS layers and maps of the outputs of the risk models (country level and admin level 1 results) have been prepared and are available to view, query and download (with web services) though a web-based geo-viewer: https://maps.eu-risk.eucentre.it/tags/risk/.

6.4 Future Improvements

In addition to updating the models based on improvements and potential bug fixes to each of the components, as described previously in this report, there are some modifications to the mechanics of the risk calculations that might be implemented in the future. These include improvements to the OpenQuake-engine to include correlation of inter-event variability between intensity measure types are expected. Currently, each building class that has a different intensity measure type, either PGA, SA(0.3), SA(0.6) or SA(1.0), and thus has an independent sample of the inter-event variability. This modification will not affect the average annual losses presented herein, but will influence the very low and very high return period losses, that are affected by correlation in the model.

The European Seismic Risk Model will continue to be updated in the coming years based on all the future improvements outlined in this report, and also following feedback that is encouraged from the scientific and professional risk communities.

[10] Please send an email to efehr.risk@sed.ethz.ch

References

AECOM (2014) *The blue book,* Available at: https://www.aecom.com/ca/wp-content/uploads/2015/10/Blue-Book-2014.pdf (accessed 9 October 2020).

Ahdi S.K., Stewart J.P., Ancheta T.D., Kwak D.Y. and Mitra D. (2017) "Development of VS Profile Database and Proxy-Based Models for Vs30 Prediction in the Pacific Northwest Region of North America," *Bulletin of the Seismological Society of America*, 107(4), pp. 1781-1801.

Akkar S. (2021) *Earthquake Physical Risk/Loss Assessment Models and Applications: A Case Study on Content Loss Modeling Conditioned on Building Damage*, In: Akkar S., Ilki A., Goksu C., Erdik M. (eds) Advances in Assessment and Modeling of Earthquake Loss. Springer Tracts in Civil Engineering. Springer, Cham. https://doi.org/10.1007/978-3-030-68813-4_10

ATC (2018) *Guidelines for Performance-Based Seismic Design of Buildings*, FEMA P-58-6, Applied Technology Council, Redwood City (CA), USA.

Atkinson G.M., Bommer J.J. and Abrahamson N.A. (2014) "Alternative approaches to modeling epistemic uncertainty in ground motions in probabilistic seismic-hazard analysis," *Seismological Research Letters*, 85(6), pp. 1141-1144, https://doi.org/10.1785/0220140120.

Balkan Insight (n.d.) Available at: https://balkaninsight.com/2008/12/03/kosovo-builders-reap-huge-profits/ (accessed 9 October 2020).

Becker J.J., Sandwell D.T., Smith W.H.F., Braud J., Binder B., Depner J.L., ... and Ladner R. (2009) "Global bathymetry and elevation data at 30 arc seconds resolution: SRTM30_PLUS," *Marine Geodesy*, 32(4), pp. 355- 371.

Bommer J., Strasser F.O., Pagani M. and Monelli D. (2013) "Quality assurance for Logic-Tree implementation in probabilistic seismic hazard analysis for nuclear applications: A practical example," *Seismological Research Letters*, 84 (6), pp. 938-945.

Borzi B., Crowley H. and Pinho R. (2008) "Simplified pushover-based vulnerability analysis for large-scale assessment of RC buildings," *Engineering Structures*, 30, pp. 804-820.

Bradley B.A., Dhakal R.P., MacRae G.A. and Cubrinovski M. (2010) "Prediction of spatially distributed seismic demands in specific structures: Ground motion and structural response," *Earthquake Engineering and Structural Dynamics*, 39, pp. 501-520.

Calderon A. and Silva V. (2018) "Probabilistic seismic risk assessment for Costa Rica," *Bulletin of Earthquake Engineering*, https://doi.org/10.1007/s10518-018-0499-1.

Caseo Professionel (n.d.) Available at: http://www.caseo-professionnels.com/articles/co%C3%BBt-de-la-construction-au-m%C2%B2-en-france (accessed 9 October 2020).

Cassard C., Bertrand G., Billa M., Serrano J.J. Tourlière B., Angel J.M. and Gaál G. (2015) *ProMine Mineral Databases: New Tools to Assess Primary and Secondary Mineral Resources in Europe*, *In: 3D, 4D and Predictive Modelling of Major Mineral Belts in Europe*, Chapter: 2, Publisher: Springer, Editors: P. Weihed.

Chiou B., Darragh R., Gregor N. and Silva W. (2008) "NGA project strong-motion database," *Earthquake Spectra*, 24, pp. 23–44.

COMPASS (2020) *2020 Global Construction Costs Yearbook,* COMPASS International Inc*,* Available at: https://compassinternational.net/product/global-construction-costs/

Conseil Européen des Economistes de la Construction (n.d.) Available at: https://www.ceecorg.eu/wp-content/uploads/2020/05/CEEC-Office-Cost-Model-2010-2019-EN.pdf (accessed 9 October 2020).

Corbane C., Hancilar U., Ehrlich D. and De Groeve T. (2017) "Pan-European seismic risk assessment: a proof of concept using the Earthquake Loss Estimation Routine (ELER)," *Bulletin of Earthquake Engineering*, 15(3), pp. 1057-1083.

Cosenza E., Del Vecchio C., Di Ludovico M., Dolce M., Moroni C., Prota A. and Renzi E. (2018) "The Italian guidelines for seismic risk classification of constructions: technical principles and validation," Bulletin of Earthquake Engineering, 16, pp. 5905–5935, https://doi.org/10.1007/s10518-018-0431-8.

Costmodelling Ltd. (n.d.) Available at: http://costmodelling.com/building-costs (accessed 9 October 2020).

Crowley H., Özcebe S., Spence R., Foulser-Piggott R., Erdik M. and Alten K. (2012) "Development of a European building inventory database," *Proceedings of 15th World Conference on Earthquake Engineering*, Lisbon, Portugal.

Crowley H., Polidoro B., Pinho R. and van Elk J. (2017) "Framework for developing fragility and consequence models for local personal risk," *Earthquake Spectra*, 33(4), pp.1325–1345.

Crowley H., Despotaki V., Rodrigues D., Silva V., Toma-Danila D., Riga E., Karatzetsou A., Sousa L., Ozcebe S., Zugic Z. and Gamba P. (2020) "Exposure model for European Seismic Risk Assessment," *Earthquake Spectra*, https://doi.org/10.1177/8755293020919429.

Crowley H., Despotaki V., Silva V., Dabbeek J., Romão X., Pereira N., Castro J.M., Daniell J., Veliu E., Bilgin H., Adam C., Deyanova M., Ademović N., Atalic J., Riga E., Karatzetzou A., Bessason B., Shendova V., Tiganescu A., Toma-Danila D., Zugic Z., Akkar S., Hancilar U. (2021a) "Model of Seismic Design Lateral Force Levels for the Existing Reinforced Concrete European Building Stock", *Bulletin of Earthquake Engineering*, https://doi.org/10.1007/s10518-021-01083-3.

Crowley H., Despotaki V., Rodrigues D., Silva V., Costa C., Toma-Danila D., Riga E., Karatzetzou A., Fotopoulou S., Sousa L., Ozcebe S., Gamba P., Dabbeek J., Romão X., Pereira N., Castro J.M., Daniell J., Veliu E., Bilgin H., Adam C., Deyanova M., Ademović N., Atalic J., Bessason B., Shendova V., Tiganescu A., Toma-Danila D., Zugic Z., Akkar S., Hancilar U. (2021b). *European Exposure Model Data Repository (v1.0),* Data set, Zenodo, http://doi.org/10.5281/zenodo.4062044.

Crowley H., J. Dabbeek, L. Danciu, P. Kalakonas, E. Riga, V. Silva, E. Veliu, G. Weatherill (2021c). *Earthquake Scenario Loss Testing Repository* (*v1.0)*, Data set, Zenodo, https://doi.org/10.5281/zenodo.5728008

Dabbeek J., Crowley H., Silva V., Weatherill G., Paul N., Nievas C. (2021) "Impact of exposure spatial resolution on seismic loss estimates in regional portfolios," *Bulletin of Earthquake Engineering*, https://doi.org/10.1007/s10518-021-01194-x

Daily News Hungary (n.d.) Available at: https://dailynewshungary.com/hungarian-home-construction-costs-climb-almost-8-pc-in-2017/ (accessed 9 October 2020).

Danciu L., Nandan, S., Reyes C., Weatherill G., Beauval C., Rovida A., Vilanova, S., Sesetyan K., Bard P-Y., Cotton F., Wiemer S. and Giardini D. (2021) *The 2020 update of the European Seismic Hazard Model: Model Overview*, EFEHR Technical Report 001.

De Bono A. and Chatenoux B. (2015) *A Global Exposure Model for GAR 2015*, Geneva: UNEP/Grid- Geneva, UNISDR, Available at: GAR 2015 Background Papers for Global Risk Assessment, https://www.preventionweb.net/english/hyogo/gar/2015/en/home/documents.html#working_papers (accessed 21 November 2021).

De Martino G., Di Ludovico M., Prota A., Moroni C., Manfredi G. and Dolce M. (2017) "Estimation of repair costs for RC and masonry residential buildings based on damage data collected by post-earthquake visual inspection," Bulletin of Earthquake Engineering, 15, pp. 1681-1706, https://doi.org/10.1007/s10518-016-0039-9.

Di Ludovico M., De Martino G., Prota A., Manfredi G. and Dolce M. (2021) *Damage Assessment in Italy, and Experiences After Recent Earthquakes on Reparability and Repair Costs*, In: Akkar S., Ilki A., Goksu C., Erdik M. (eds) Advances in Assessment and Modeling of Earthquake Loss. Springer Tracts in Civil Engineering. Springer, Cham. https://doi.org/10.1007/978-3-030-68813-4_4.

Douglas, J. (2018) *Capturing Geographically-Varying Uncertainty in Earthquake Ground Motion Models or What We Think We Know May Change*, Recent Advances in Earthquake Engineering in Europe, Editor: Kyriazis Pitilakis, Chapter 6, pp. 153-181.

DPC (2018) *National risk assessment, Overview of the potential major disasters in Italy: seismic, volcanic, tsunami, hydro-geological/hydraulic and extreme weather, droughts and forest fire risks*, Technical report by the Presidency of the Council of Ministers Italian Civil Protection Department, Rome, Italy.

Engles & Völkers (n.d.) Available at: https://www.engelvoelkers.com/en-be/belgium/blog/construction-or-renovation-decoding-two-solutions/ (accessed 9 October 2020).

EMDAT (n.d.) *International Disasters Database of the Centre for Research on the Epidemiology of Disasters*, Available at: https://www.emdat.be/ (accessed 15 September 2021).

Erdik M. (2021) *Earthquake Risk Assessment from Insurance Perspective*, In: Akkar S., Ilki A., Goksu C., Erdik M. (eds) Advances in Assessment and Modeling of Earthquake Loss. Springer Tracts in Civil Engineering. Springer, Cham. https://doi.org/10.1007/978-3-030-68813-4_6

Faenza L. and Michelini A. (2010) "Regression analysis of MCS intensity and ground motion parameters in Italy and its application in ShakeMap," *Geophysical Journal International*, 180(3), pp. 1138–1152.

Farr T.G. and Kobrick M. (2000) "Shuttle Radar Topography Mission produces a wealth of data," *EOS Transactions*, American Geophysical Union, 81(48), pp. 583-585.

FEMA (1999) *HAZUS99 – Earthquake Loss Estimation Methodology: User's Manual*, Federal Emergency Management Agency, Washington, DC.

Forum da casa (n.d.) Available at. https://forumdacasa.com/discussion/53535/orientacao-valor-medio-construcao-2018/ (accessed 9 October 2020).

Gamba P., Cavalca D., Jaiswal K., Huyck C. and Crowley H. (2014) "The GED4GEM project: Development of a global exposure database for the global earthquake model initiative," *Proceedings of the 15th World Conference on Earthquake Engineering*, Lisbon, Portugal.

GEM (2018) *Global earthquake maps*, Available at: www.globalquakemodel.org/gem (accessed 6 December 2018).

Giovinazzi S., Lagomarsino S. (2004) "A macroseismic model for the vulnerability assessment of buildings," *Proceedings of 13th World Conference on Earthquake Engineering*, Vancouver, Canada.

Global Assessment Report (GAR) (2015) *UNISDR 2015 Global Assessment Report*, Available at: www.preventionweb.net/english/hyogo/gar/2015 (accessed 21 November 2021).

Grant D.N., Dennis J., Stuart R., Milan G., McLennan D., Negrette P., da Costa R. and Palmieri M. (2021) "Explicit modelling of collapse for Dutch unreinforced masonry buildng typology fragility functions," Bulletin of Earthquake Engineering, 19, pp. 6697-6519, https://doi.org/10.1007/s10518-020-00923-y

Iwahashi J. and Pike R.J. (2007) "Automated classifications of topography from DEMs by an unsupervised nested-means algorithm and a three-part geometric signature," *Geomorphology*, 86(3-4), pp. 409-440.

Jaiswal K.S. and Wald D.J. (2008) *Creating a global building inventory for earthquake loss assessment and risk management* US Geological Survey Open-File Report 1160.

Jaiswal K., Wald D. and Hearne M. (2009) *Estimating casualties for large worldwide earthquakes using an empirical approach*, US Geological Survey Open-File Report 1136.

Jaiswal K. and Wald D. (2010) "Development of a semi-empirical loss model within the USGS Prompt Assessment of Global Earthquakes for Response (PAGER) System," *Proceedings of the 9th US and 10th Canadian Conference on Earthquake Engineering: Reaching Beyond Borders*, Toronto, Canada.

Jaiswal K. and Wald D. (2013) "Estimating Economic Losses from Earthquakes Using an Empirical Approach," *Earthquake Spectra*, 29(1), pp. 309-324.

Jóhannesson H. (2014) *Geological Map of Iceland*. Bedrock Geology. Scale: 1:600 000 Edition: Revised edition 2014, 2nd edition Náttúrufræðistofnun Íslands – Icelandic Institute of Natural History.

Kalakonas P., Silva V., Mouyiannou A. and Rao A. (2020) "Exploring the impact of epistemic uncertainty on a regional probabilistic seismic risk assessment model," *Natural Hazards*, https://doi.org/10.1007/s11069-020-04201-7.

Kazantzi A.K. and Vamvatsikos D. (2015) "Intensity measure selection for vulnerability studies of building classes," *Earthquake Engineering and Structural Dynamics*, 44, pp. 2677-2694.

Kazantzidou-Firtinidou D., Kyriakides N. and Chrysostomou (2019) "Earthquake risk assessment for Cyprus," *Proceedings of 2nd International Conference on Natural Hazards and Infrastructure*, ICONHIC 2019, Chania, Greece.

Kleist L., Thieken A.H., Köhler P., Müller M., Seifert I., Borst D. and Werner U. (2006) "Estimation of the regional stock of residential buildings as a basis for a comparative risk assessment in Germany," Natural Hazards and Earth System Sciences, https://doi.org/10.5194/nhess-6-541-2006.

Kotha S.R., Weatherill G., Bindi D. and Cotton F. (2020) "A regionally-adaptable ground-motion model for shallow crustal earthquakes in Europe," *Bulletin of Earthquake Engineering*, 18, pp. 4091–4125, https://doi.org/10.1007/s10518-020-00869-1

Kotha S.R., Weatherill G., Bindi D. and Cotton F. (2022) "Near-source Magnitude Scaling of Spectral Accelerations: Analysis and Update of the Kotha et al. (2020) Model." *Bulletin of Earthquake Engineering*, *under review*

Lemoine A., Douglas J. and Cotton F. (2012) "Testing the applicability of correlations between topographic slope and Vs30 for Europe," *Bulletin of the Seismological Society of America*, 102(6), pp. 2585-2599.

Luco N. and Cornell A. (2007) "Structure-Specific Scalar Intensity Measures for Near-Source and Ordinary Earthquake Ground Motions," *Earthquake Spectra*, 23(2), pp. 357–392.

Luzi L., Puglia R., Russo E., D'Amico M., Felicetta C., Pacor F., Lanzano G., Çeken U., Clinton J., Costa G., Duni L., Farzanegan E., Gueguen P., Ionescu C., Kalogeras I., Özener H., Pesaresi D., Sleeman R., Strollo A., Zare M. (2016) "The Engineering Strong-Motion Database: A platform to access pan-European accelerometric data," *Seismological Research Letters*, 87(4), pp. 987-997, http://doi.org/10.1785/0220150278.

Luzi L., Lanzano G., Felicetta C., D'Amico M.C., Russo E., Sgobba S., Pacor F., ORFEUS Working Group 5 (2020) *Engineering Strong Motion Database (ESM)* (Version 2.0), Istituto Nazionale di Geofisica e Vulcanologia (INGV), https://doi.org/10.13127/ESM.

Martins L. and Silva V. (2018) "A Global Database of Vulnerability Models for Seismic Risk Assessment," *Proceedings of the 16th European Conference on Earthquake Engineering*, Thessaloniki, Greece.

Martins L. and Silva V. (2020) "Development of a fragility and vulnerability model for global seismic risk analyses," *Bulletin of Earthquake Engineering*, https://doi.org/10.1007/s10518- 020-00885-1

Martins L., Silva V., Crowley H. and Cavalieri F. (2021) "Vulnerability Modeller's Toolkit, an Open-Source Platform for Vulnerability Analysis," *Bulletin of Earthquake Engineering,* https://doi.org/10.21203/rs.3.rs-458348/v1

Motamed M., Calderon A., Silva V. and Costa C. (2018) "Development of a probabilistic earthquake loss model for Iran," *Bulletin of Earthquake Engineering*, 17, pp. 1795–1823, https://doi.org/10.1007/s10518-018-0515-5.

MunichRe (2019) *NatCatService - Natural catastrophe statistics online*, Available upon request at: https://natcatservice.munichre.com/.

National Geophysical Data Center / World Data Service (NGDC/WDS): NCEI/WDS Global Significant Earthquake Database. NOAA National Centers for Environmental Information. doi:10.7289/V5TD9V7K (accessed 21 November 2021)

Ordaz M., Cardona O.D., Salgado-Gálvez M.A., Bernal-Granados G.A., Singh S.K. and Zuloaga-Romero D. (2014) "Probabilistic seismic hazard assessment at global level," *International Journal of Disaster Risk Reduction,* 10(B), pp. 419–427.

Numbeo (n.d.) Available at: https://www.numbeo.com/cost-of-living/compare_countries_result.jsp?country1=Switzerland&country2=Liechtenstein (accessed 9 October 2020).

Pagani M., Monelli D., Weatherill G., Danciu L., Crowley H., Silva V., Henshaw P., Butler L., Nastasi M., Panzeri L., Simionato M. and Vigano D. (2014) "OpenQuake engine: An open hazard (and risk) software for the global earthquake model," *Seismological Research Letters,* 85(3), pp. 692–702, https://doi.org/10.1785/0220130087.

Paprotny D., Kreibich H., Morales-Nápoles O., Terefenko P. and Schröter K. (2019) "Estimating exposure of residential assets to natural hazards in Europe using open data," *Natural Hazards and Earth Systems Science*, DOI: https://doi.org/10.5194/nhess-2019-313.

Pesaresi M, Ehrilch D, Florczyk AJ, Freire S, Julea A, Kemper T, Soille P, Syrris V (2015) *GHS built-up grid, derived from Landsat, multitemporal (1975, 1990, 2000, 2014),* European Commission's Joint Research Centre, Available at: http://data.europa.eu/89h/jrc-ghsl-ghs_built_ldsmt_globe_r2015b (accessed 24 April 2019).

Popper, K. (2002) *The Logic of Scientific Discovery,* Rutledge classic, 545 pp.

Reinoso E., Jaimes M.A. and Esteva L. (2017) "Estimation of life vulnerability inside buildings during earthquakes," *Structure and Infrastructure Engineering*, https://doi.org/10.1080/15732479.2017.1401097.

Romão X., Castro J.M., Pereira N., Crowley H., Silva V., Martins L. and Rodrigues D. (2019) *European physical vulnerability models*, SERA Deliverable D26.5, Available at: http://static.seismo.ethz.ch/SERA/JRA/SERA_D26.5_Physical_Vulnerability.pdf.

Romão X., Pereira N., Castro J.M., Crowley H., Silva V., Martins L., and De Maio F. (2021) *European Building Vulnerability Data Repository (v2.1)*, Data set, Zenodo, https://doi.org/10.5281/zenodo.4062410.

Scawthorn C. (2008) "Opening Risk Analysis," *Proceedings of 14th World Conference on Earthquake Engineering*, Beijing, China, October 2018.

Schmalwasser O. and Schidlowski M. (2006) "Measuring Capital Stock in Germany, Slightly abridged version of a paper published in the journal Wirtschaft und Statistik 11/2006," Available at: https://www.destatis.de/EN/Methods/WISTAScientificJournal/Downloads/capital-stock-germany-112006.html (accessed 21 November 2021).

Seyhan E. and Stewart J.P. (2014) "Semi-empirical nonlinear site amplification from NGA-West2 data and simulations," *Earthquake Spectra*, 30(3), pp. 1241-1256.

Sousa L., Silva V., Bazzurro P. (2017) "Using open-access data in the development of exposure data sets of industrial buildings for earthquake risk modeling," *Earthquake Spectra*, 33, pp. 63–84, https://doi.org/10.1193/020316eqs027m.

Silva, V. (2018) "Critical Issues on Probabilistic Earthquake Loss Assessment," *Journal of Earthquake Engineering*, 22 (9), pp. 1683-1709, DOI: https://doi.org/10.1080/13632469.2017.1297264..

Silva V. (2019) "Uncertainty and correlation in seismic vulnerability functions of building classes," *Earthquake Spectra*, 35(4), pp. 1515-1539.

Silva V., Crowley H., Pagani M., Monelli D. and Pinho R. (2014) "Development of the OpenQuake engine, the Global Earthquake Model's open-source software for seismic risk assessment," *Natural Hazards,* 72(3), pp. 1409–1427, DOI: https://doi.org/10.1007/s11069-013-0618-x.

Silva V., Amo-Oduro D., Calderon A., Costa C., Dabbeek J., Despotaki V., Martins L., Pagani M., Rao A., Simionato M., Viganò D., Yepes-Strada C., Acevedo A., Crowley H., Horspool N., Jaiswal K., Journeay M., Pittore M. (2020) "Development of a global seismic risk model," *Earthquake Spectra*, https://doi.org/10.1177/8755293019899953

Silva V., Brzev S., Scawthorn C., Yepes-Estrada C., Dabbeek J. and Crowley H. (2021) "A Building Classification System for Multi-Hazard Risk Assessment," *International Journal of Disaster Risk Science*, under review.

Stafford, P. J. (2008) "Conditional prediction of absolute durations," *Bulletin of Seismological Society of America*, 98, pp. 1588–1594.

Statistica (n.d.) Available at: https://www.statista.com/statistics/872802/building-costs-per-square-meter-by-residential-building-type-poland-europe/ (accessed 9 October 2020).

Statistica (n.d.) Available at: https://www.statista.com/statistics/892504/building-costs-per-square-meter-by-residential-building-type-switzerland/ (accessed 9 October 2020).

Statistica (n.d.) Available at: https://www.statista.com/statistics/898188/cost-of-building-in-selected-european-cities/ (accessed 9 October 2020).

Tromans I.J., Aldama-Bustos G., Douglas J., Lessi-Cheimariou A., Hunt S., Daví M., Musson R.M.W., Garrard G., Strasser F.O. and Robertson C. (2019) "Probabilistic seismic hazard assessment for a new-build nuclear power plant site in the UK," *Bulletin of Earthquake Engineering*, 17, pp. 1–36, https://doi.org/10.1007/s10518-018-0441-6.

Turner & Townsend (2018) *International construction market survey 2019* Available at: www.turnerandtownsend.com/media/3352/international-construction-market-survey-2018.pdf

Tyagunov S., Grünthal G., Wahlström R., Stempniewski L. and Zschau J. (2006) "Seismic risk mapping for Germany," *Natural Hazards and Earth System Sciences*, 6, pp. 573-586.

Vamvatsikos D. (2011) *Software – earthquake, steel dynamics and probability*, viewed January 2021, http://users.ntua.gr/divamva/software.html

Verderame G.M., Polese M., Marinello C. and Manfredi G. (2010) "A simulated design procedure for the assessment of seismic capacity of existing reinforced concrete buildings," *Advances in Engineering Software*, 41(2), pp. 323-335.

Vilanova, S.P., Narciso, J., Carvalho, J.P., Lopes, I., Quinta-Ferreira, M., Pinto, C.C., ... and Nemser, E.S. (2018) "Developing a Geologically Based Vs30 Site-Condition Model for Portugal: Methodology and Assessment of the Performance of Proxies," *Bulletin of the Seismological Society of America*, 108(1), pp. 322-337.

Wald D.J. and Allen T.I. (2007) "Topographic Slope as a Proxy for Seismic Site Conditions and Amplification", *Bulletin of the Seismological Society of America*, 97, pp. 1379-1395.

Weatherill G.A. and Cotton F (2020) "A ground motion logic tree for seismic hazard analysis in the stable cratonic region of Europe: regionalization, model selection and development of a scaled backbone approach," *Bulletin of Earthquake Engineering*, 18, pp. 6119 – 6148.

Weatherill G., Kotha S-R., Cotton F. (2020a) "A regionally adaptable "scaled backbone" ground motion logic tree for shallow seismicity in Europe: application to the 2020 European seismic hazard model," *Bulletin of Earthquake Engineering*, 18, pp. 5087 – 5117.

Weatherill G., Silva V., Crowley H. and Bazzurro P. (2015) "Exploring the impact of spatial correlations and uncertainties for portfolio analysis in probabilistic seismic loss estimation," *Bulletin of Earthquake Engineering*, https://doi.org/10.1007/s10518-015-9730-5.

Weatherill G., Kotha S-R. and Cotton F. (2020b) "Re-thinking site amplification in regional seismic risk assessment," *Earthquake Spectra*, https://doi.org/10.1177/8755293019899956

Weatherill G.A., Crowley H., Roullé A., Toulière B., Lemoine A., Gracianne Hidalgo C., Kotha S.R., Cotton F. (2022) "Modelling site response at regional scale for the 2020 European Seismic Risk Model (ESRM20)," *Bulletin of Earthquake Engineering*, under preparation.

Wessel P. and Smith W.H.F, (1991) "Free software helps map and display data," *EOS Transactions*, American Geophysical Union, 72(41), pp. 445–446, https://doi.org/10.1029/90EO00319.

Wills C.J. and Clahan K.B. (2006) "Developing a map of geologically defined site-condition categories for California," *Bulletin of the Seismological Society of America*, 96, pp. 1483–1501.

Woessner J., Danciu L., Giardini D., Crowley H., Cotton F., Grünthal G., Valensise G., Arvidsson R., Basili R., Bermircioglu M.B., Hiemer S., Meletti C., Musson R.W., Rovida A.N., Sesetyan K., Stucchi M. and the SHARE Consortium (2015) "The 2013 European seismic hazard model—Key components and results," *Bulletin of Earthquake Engineering,* 13, pp. 3553–3596, https://doi.org/10.1007/s10518-015-9795-1.

Appendix A: Additional Material Related to Validation of Models

A.1 Exposure Models

As discussed in Chapter 3, a number of calibration and validation checks of the exposure models have been undertaken. For the reconstruction costs per square metre (i.e. per useful surface area) for structural and non-structural elements, the absolute values for each country have been compared against the values for residential buildings from Paprotny et al. (2019), and against the residential, commercial and industrial values from COMPASS (2020). These comparisons were undertaken to aid the finalization of the model values in each country, and the final comparisons are shown in Figures A.1 to A.5.

Other data source that were used to check the reconstruction costs, and in particular the ranking of countries, are presented in Table A.1. These include construction cost indices (residential, non-residential) as well as a proposed grouping of countries in terms of construction costs.

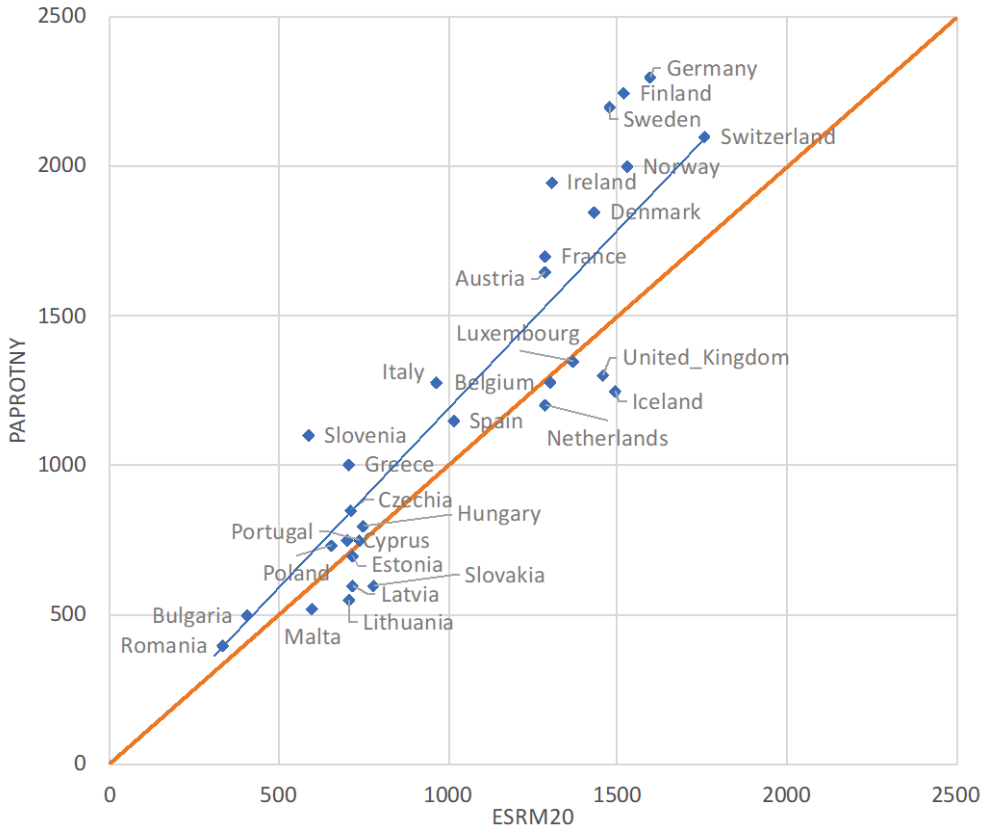

Fig A.1 Comparison of residential reconstruction cost per square metre in Paprotny et al. (2019) and ESRM20

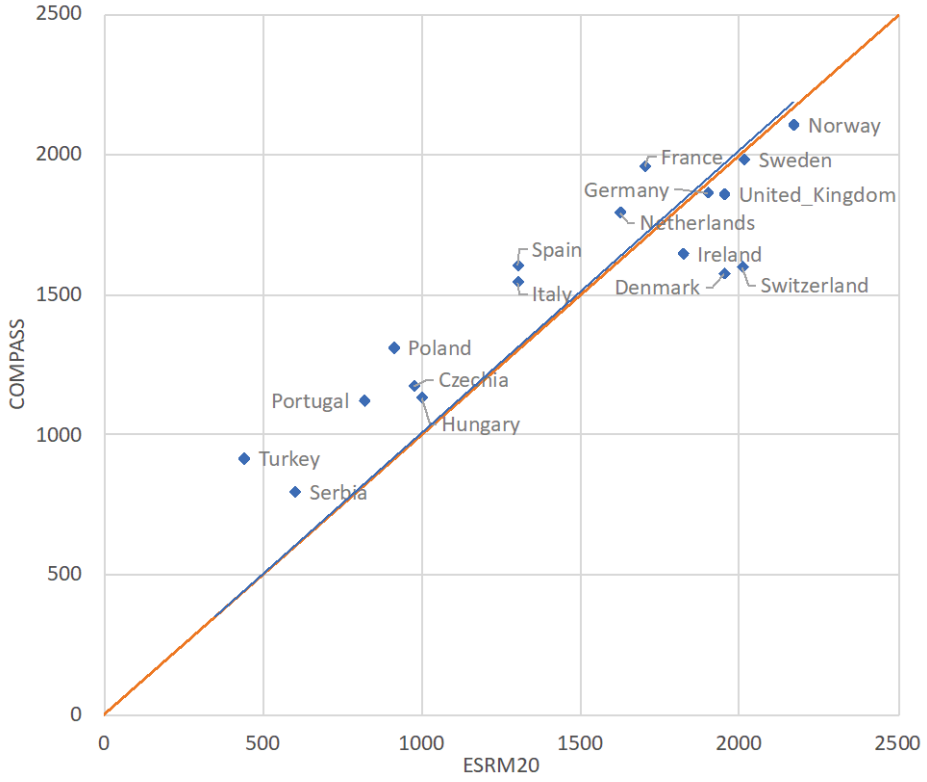

Fig A.2 Comparison of residential reconstruction cost per square metre in COMPASS (2020) and ESRM20

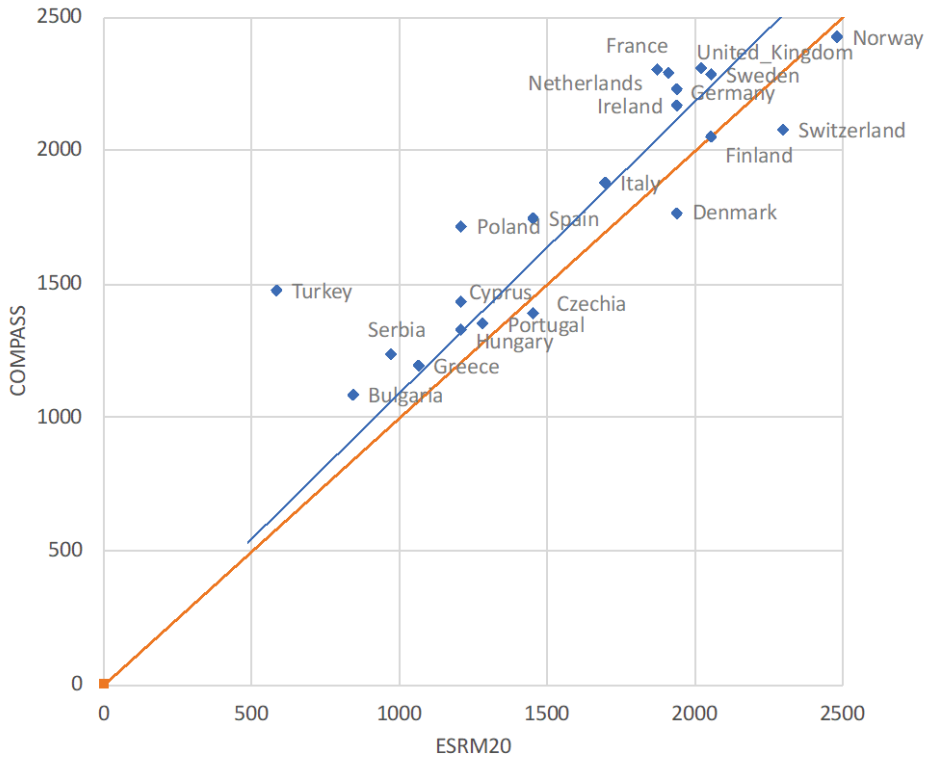

Fig A.3 Comparison of commercial reconstruction cost per square metre in COMPASS (2020) and ESRM20

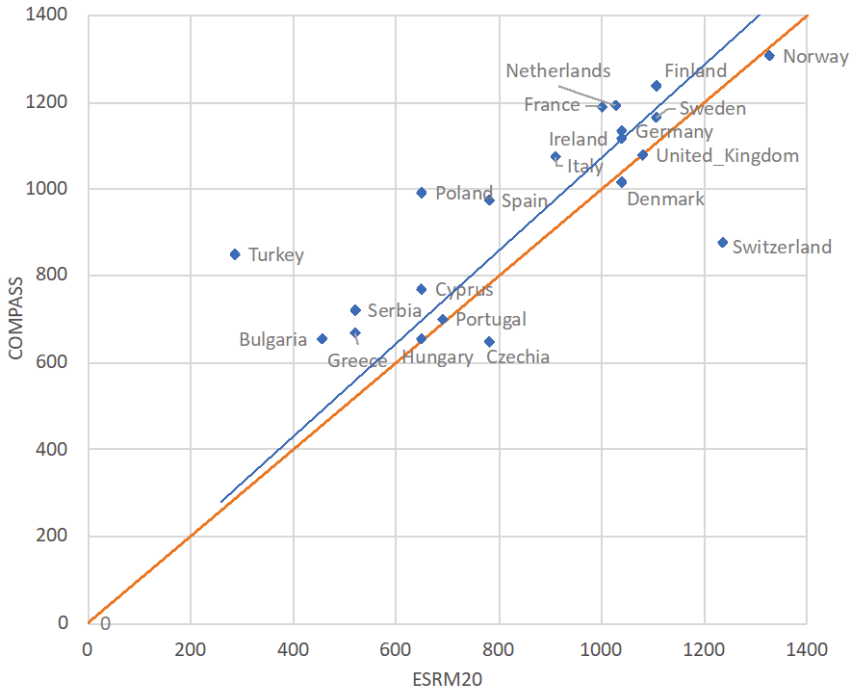

Fig A.4 Comparison of residential industrial cost per square metre in COMPASS (2020) and ESRM20

Table A.1 Data used to rank countries in terms of construction costs and to validate the ranking of reconstruction costs in ESRM20

Country	Residential cost index [1]	Non-residential cost index [1]	Construction cost index [2]	Cost group [3]
Albania	40	50.8	55.85	5
Andorra	-	-	74	-
Austria	118.6	111.5	100.67	1
Belgium	103.4	96	89.29	2
Bosnia and Herzegovina	35.8	44	56.41	5
Bulgaria	51.3	49.7	48.69	5
Croatia	44.1	49.2	55	4
Cyprus	64.6	63.6	60.29	3
Czechia	60.7	71.2	61.11	4
Denmark	127.8	136.3	145.38	1
Estonia	64.6	81.5	59.33	4
Finland	125.2	168.4	114.04	1
France	89.4	104.1	103.8	2
Germany	147	142.1	96.62	2
Gibraltar	-	-	-	-

Country	Residential cost index [1]	Non-residential cost index [1]	Construction cost index [2]	Cost group [3]
Greece	56.2	66.4	63.46	3
Hungary	52.7	62.8	53.24	4
Iceland	142.8	134.8	123.57	1
Ireland	100.8	118.4	79.18	2
Isle of Man	-	-	-	-
Italy	77.7	84.4	93.63	3
Kosovo	-	-	95	-
Latvia	58.5	76.1	57.9	4
Liechtenstein	-	-	-	-
Lithuania	60.6	68	58.72	4
Luxembourg	121.7	104.7	98.21	2
Malta	67	83.8	79.58	3
Moldova	-	-	48.72	-
Monaco	-	-	114	-
Montenegro	41.4	50.1	65	5
Netherlands	130.3	126	82	2
North Macedonia	29.9	40.3	48.18	5
Norway	148.7	172.7	160.74	1
Poland	53.5	67.2	65.61	4
Portugal	67.3	64.7	50.33	3
Romania	41.4	50.7	46.4	5
Serbia	40.1	52.1	38	5
Slovakia	62.3	81.8	51.68	4
Slovenia	48.7	70.1	80	4
Spain	76.5	82.1	70.52	3
Sweden	140.7	159	134.18	1
Switzerland	180.3	177.6	137.42	1
Turkey	31.7	39.4	68	5
United Kingdom	87.7	118	100	1

[1] https://ec.europa.eu/eurostat/statistics-explained/index.php?title=File:Price_level_indices_for_construction_and_its_components,_2019,_(EU-27%3D100)_v2.png

[2] http://constructioncosts.eu/cost-index/

[3] Cenk Budayan, Irem Dikmen & M. Talat Birgonul (2020) Construction cost map of European countries, The Engineering Economist, 65:2, 135-157, DOI: 10.1080/0013791X.2019.1668097

Fig. A.5 presents the comparison of the total replacement cost of the buildings per country with the total capital stock value in the GAR2015 exposure models. This plot shows that the ESRM20 exposure value is well correlated with the capital stock, but is lower which is expected given that public buildings and infrastructure are not included in the ESRM20 exposure. Similar plots are shown for residential, industrial and commercial buildings in Fig A.6 to A.8. Services and industrial sector GDP have been compared with the commercial and industrial replacement costs in ESRM20, as shown in Fig A.9 and A.10.

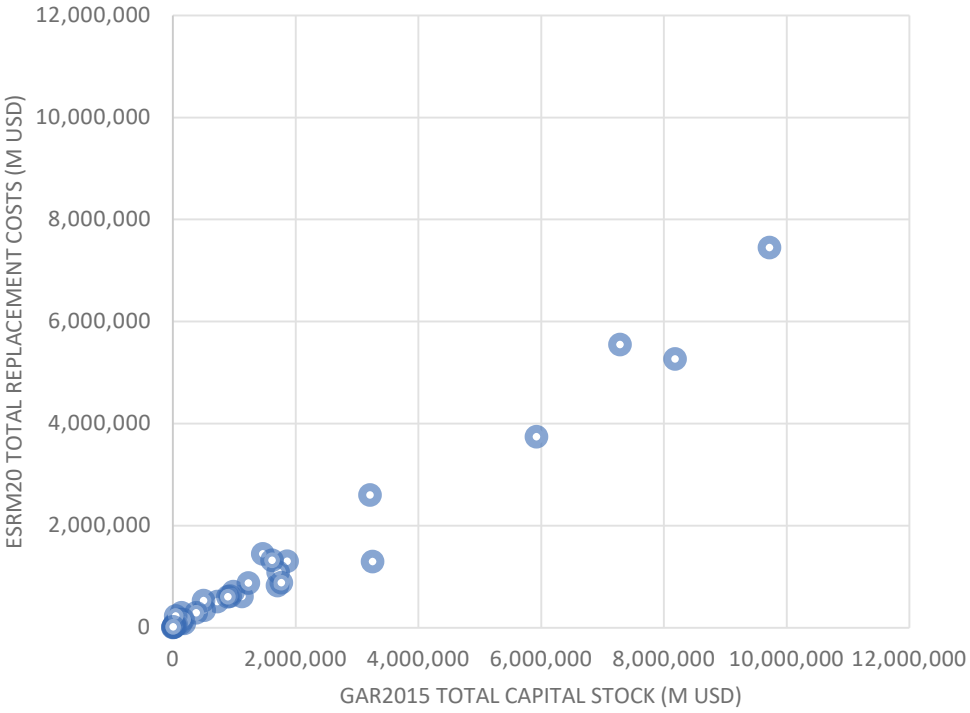

Fig. A.5 Comparison of total replacement cost per country with the total capital stock value of the GAR2015 exposure model

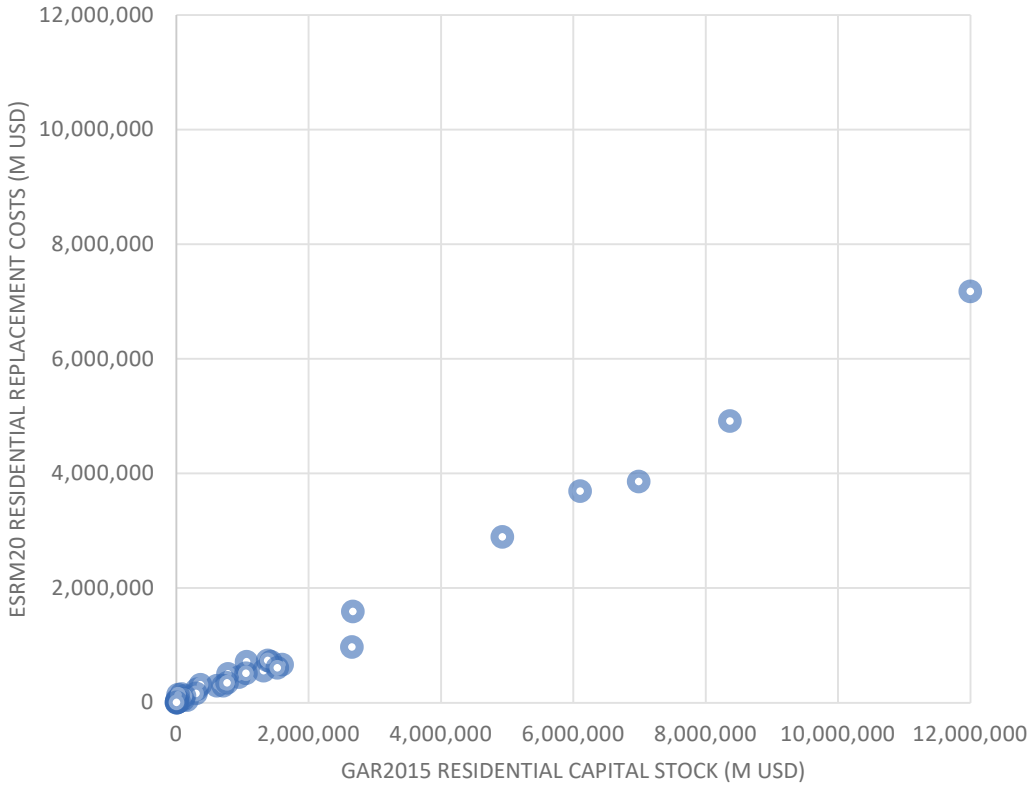

Fig A.6 Comparison of total replacement cost of residential buildings per country with the residential capital stock value of the GAR2015 exposure models

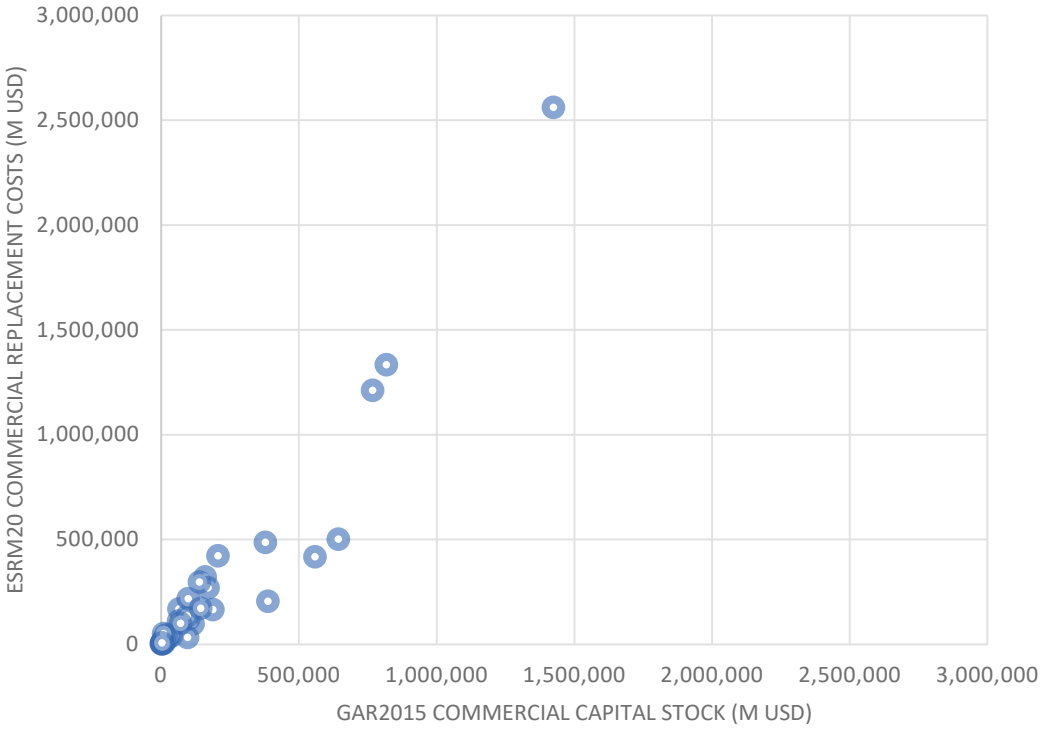

Fig A.7 Comparison of total replacement cost of commercial buildings per country with the commercial capital stock value of the GAR2015 exposure models

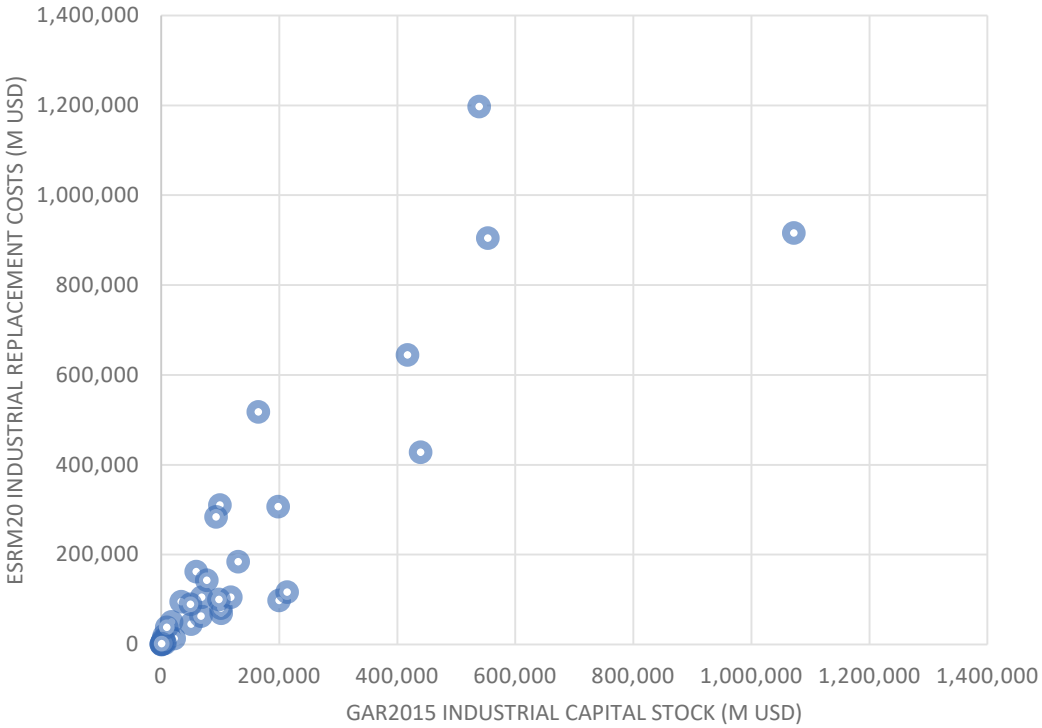

Fig A.8 Comparison of total replacement cost of industrial buildings per country with the industrial capital stock value of the GAR2015 exposure models

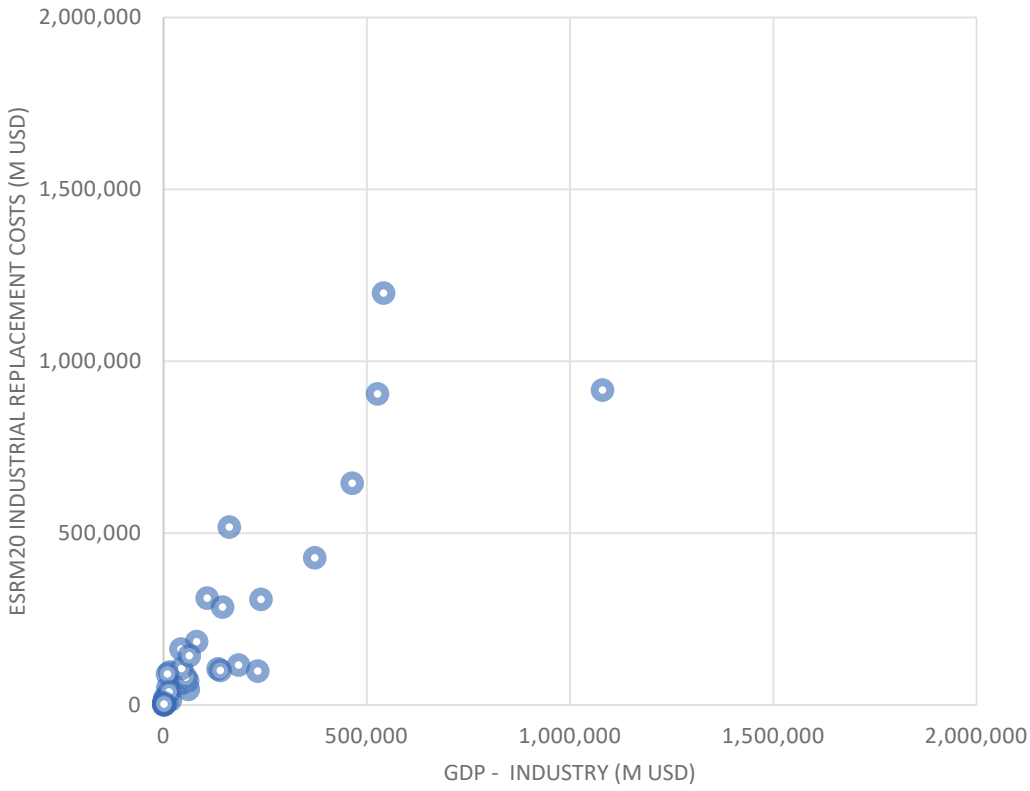

Fig A.9 Comparison of total replacement cost of industrial buildings per country with the GDP in industry

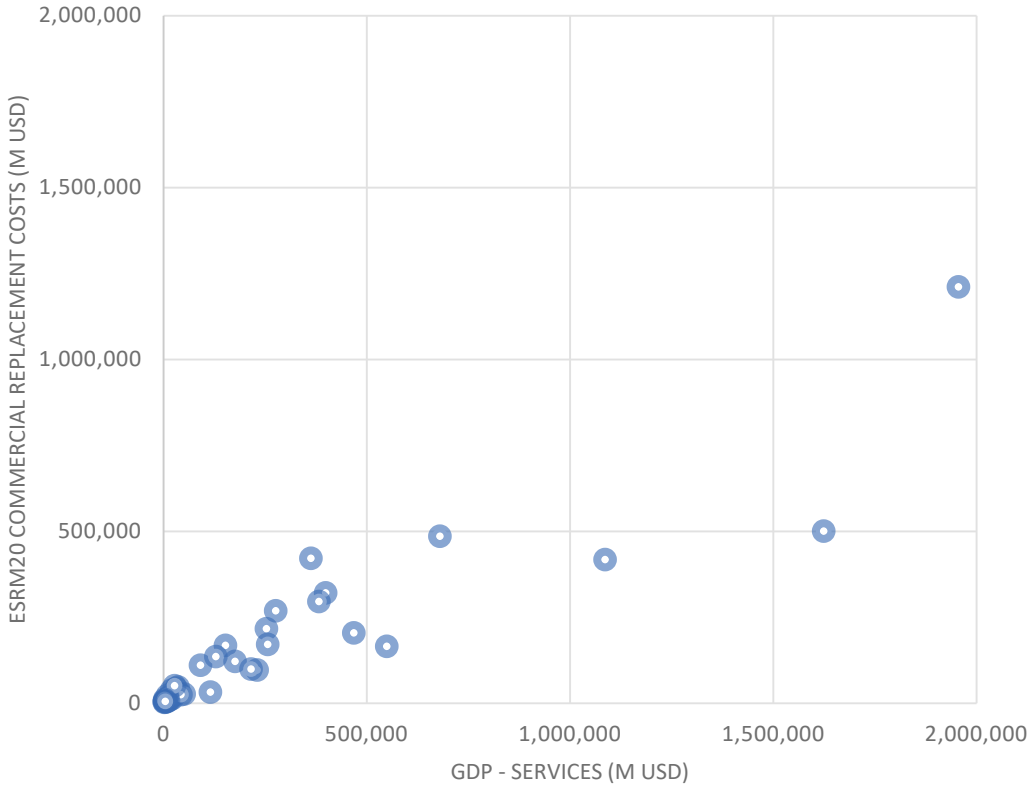

Fig A.10 Comparison of total replacement cost of commercial buildings per country with the GDP in services

A.2 Vulnerability Models

As described in Section 5.5, the losses predicted by the analytical vulnerability models have been compared with past losses observed in recent damaging earthquakes in Europe. The plots shown below compare the data from CRED's EMDAT database (EMDAT, n.d.) with the mean loss for each event (shown by a circle), together with the bounds given by the 5th and 95th percentile loss. A best-fit linear curve (shown by the black line) has also been fit to the modelled data. The comparison is shown on a country basis, with Greece shown in Fig. A.11, Italy shown in Fig. A.12, and Turkey shown in Fig. A.13.

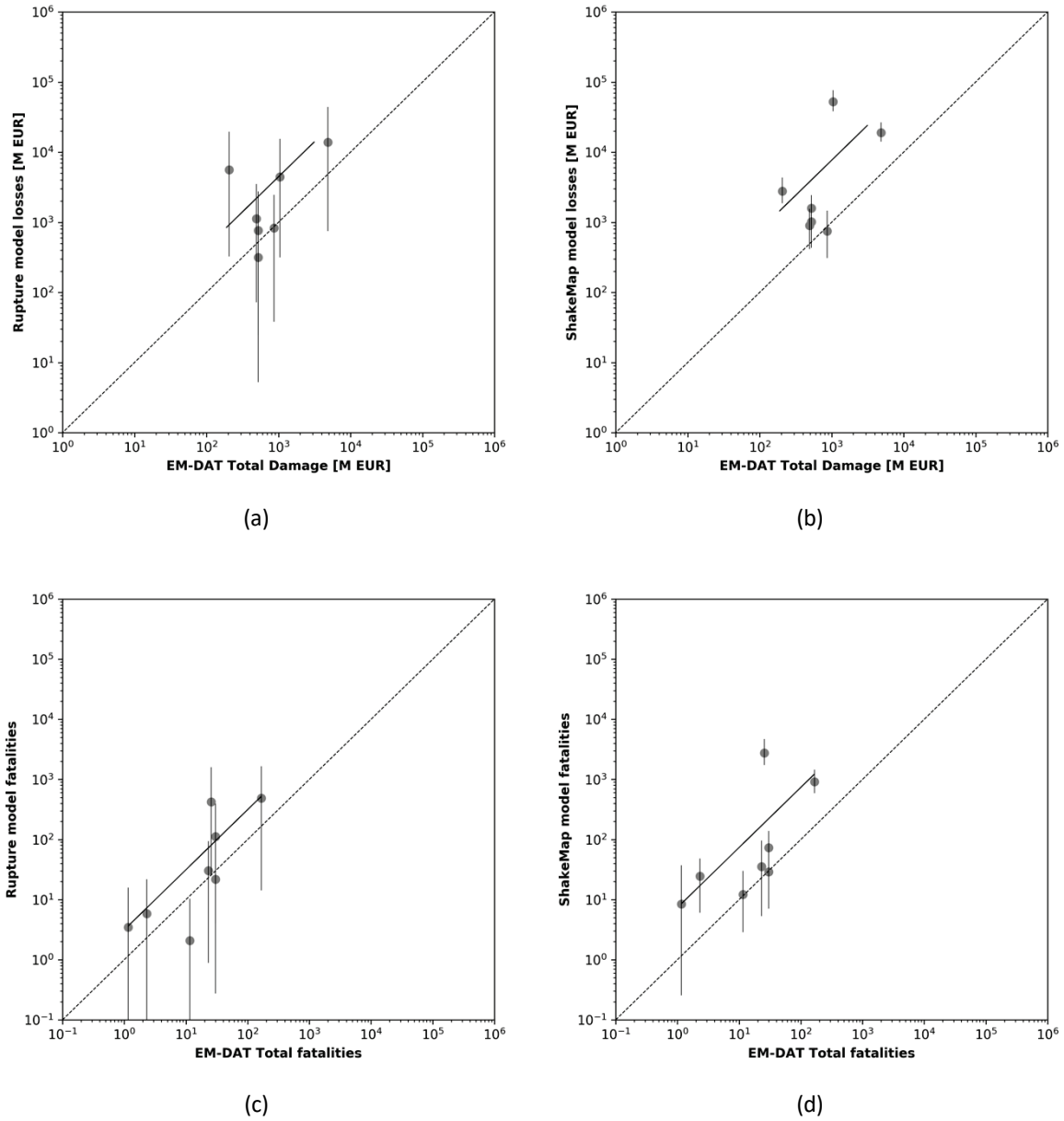

Fig A.11 Comparison of observed (horizontal axis) and modelled (vertical axis) losses for Greece (a) economic losses based on rupture model, (b) economic losses based on ShakeMap model, (c) fatalities based on rupture model, (d) fatalities based on ShakeMap model

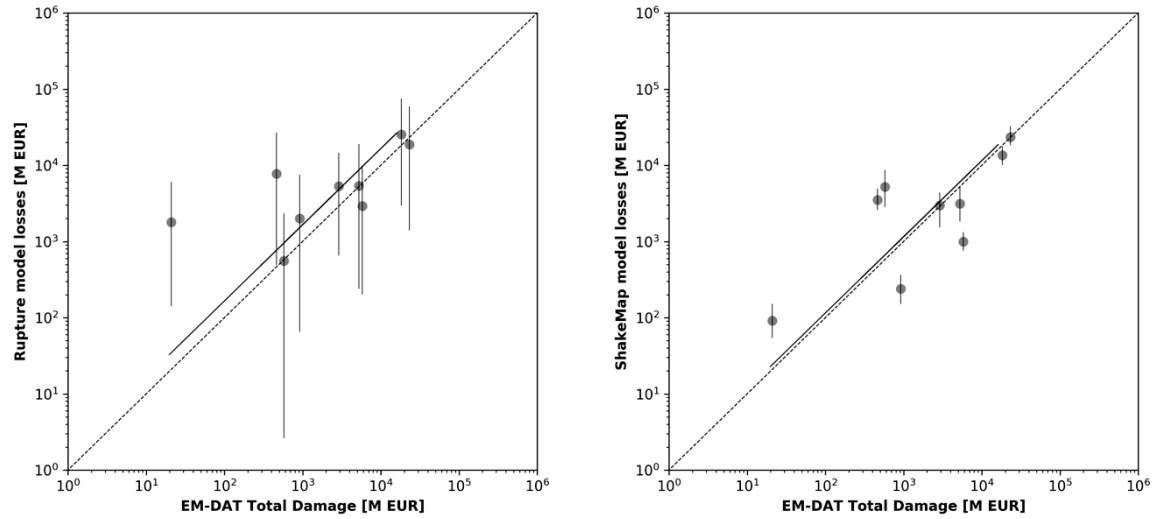

(a)

(b)

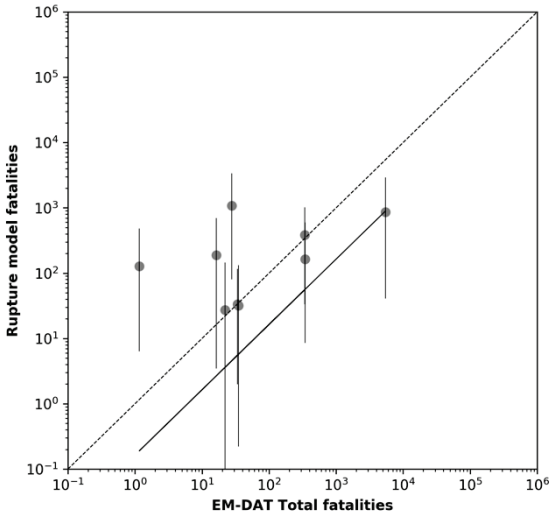

(c)

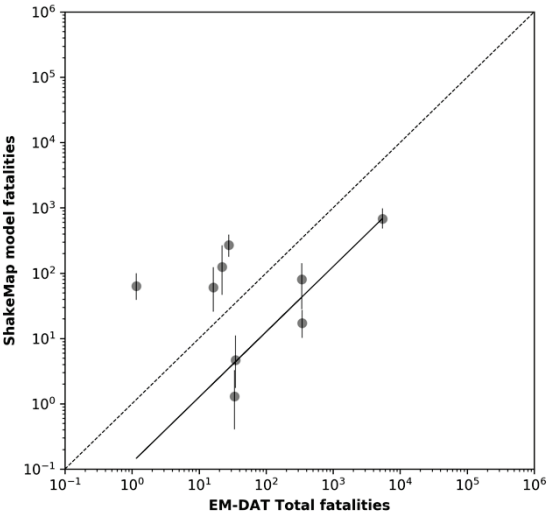

(d)

Fig A.12 Comparison of observed (horizontal axis) and modelled (vertical axis) losses for Italy (a) economic losses based on rupture model, (b) economic losses based on ShakeMap model, (c) fatalities based on rupture model, (d) fatalities based on ShakeMap model

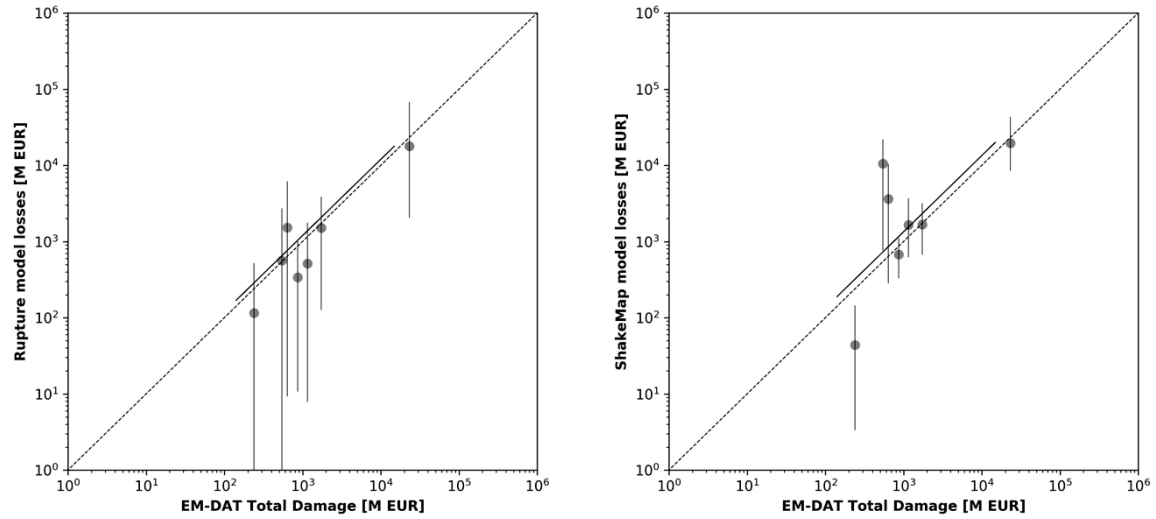

(a)

(b)

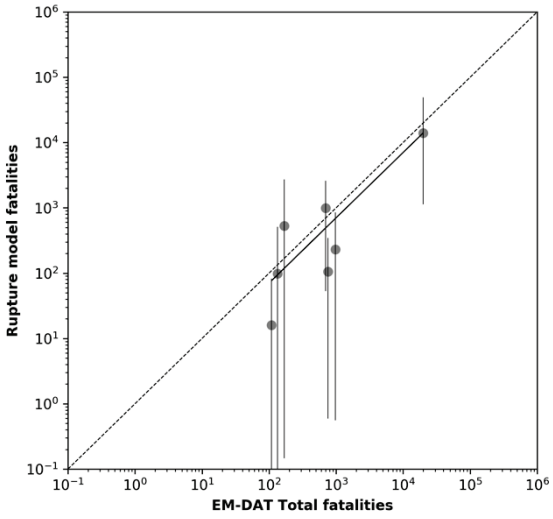

(c)

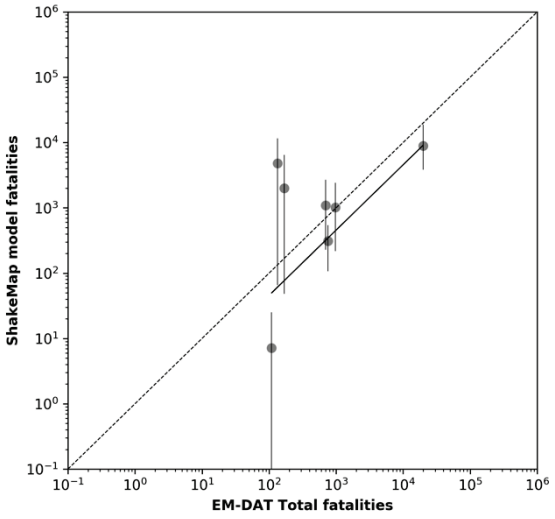

(d)

Fig A.13 Comparison of observed (horizontal axis) and modelled (vertical axis) losses for Turkey (a) economic losses based on rupture model, (b) economic losses based on ShakeMap model, (c) fatalities based on rupture model, (d) fatalities based on ShakeMap model

Appendix B: Additional Plots

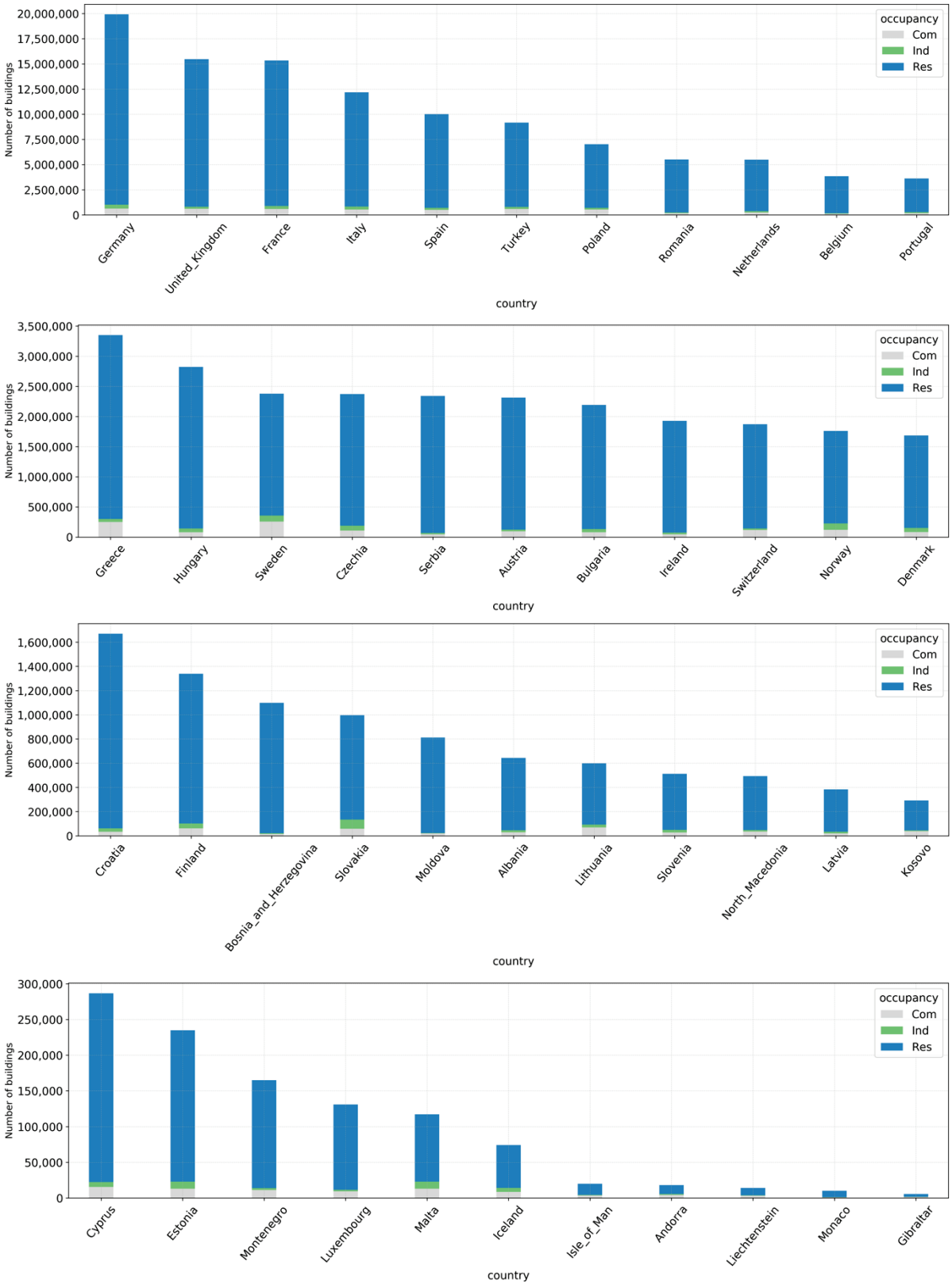

Fig. B.1 Number of occupants (average over a 24-hour period) in buildings in each country, and distribution between residential (Res), industrial (Ind) and commercial (Com) occupancy classes

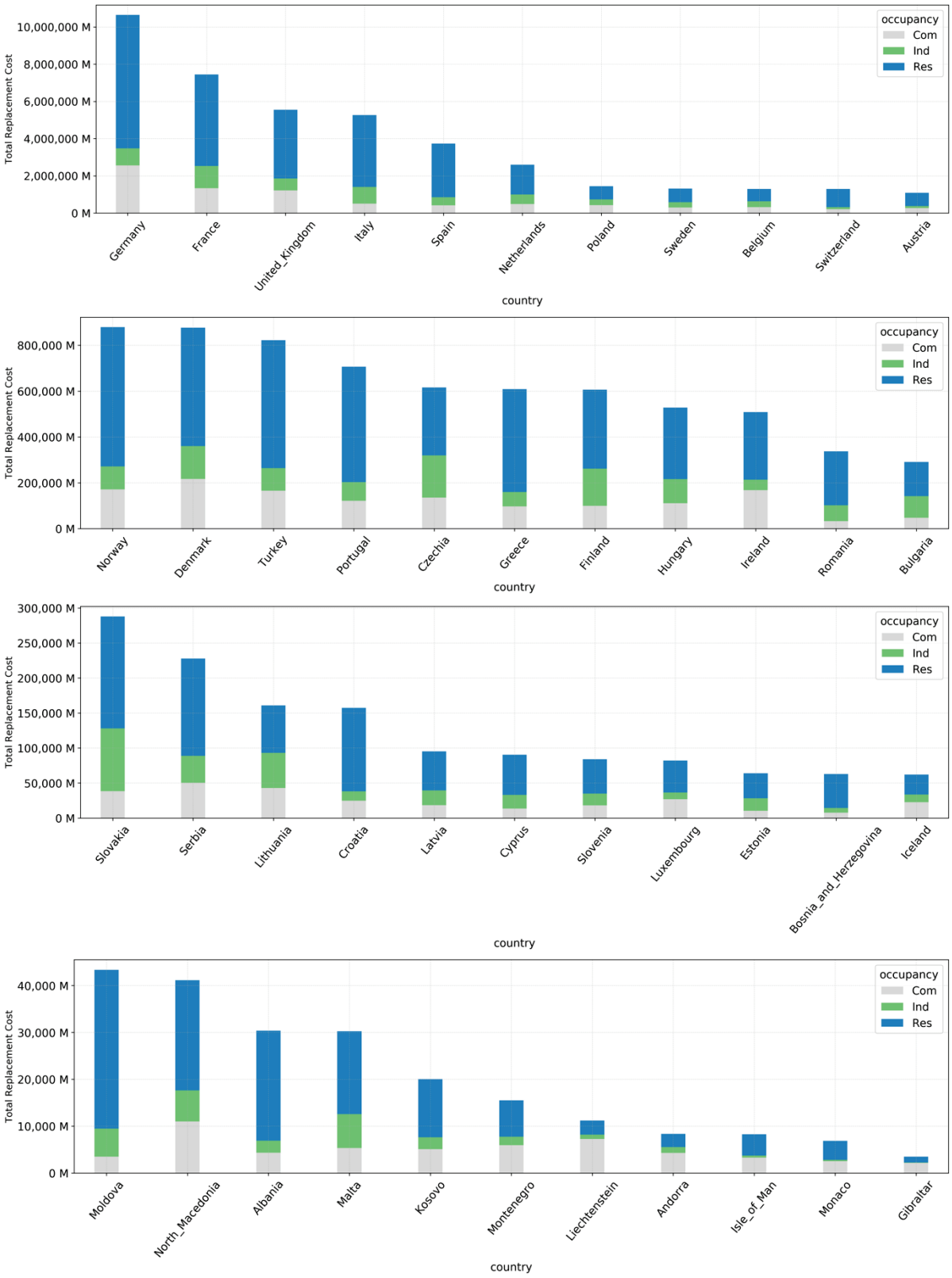

Fig. B.2 Total replacement cost of buildings (M EUR) in each country, and distribution between residential (Res), industrial (Ind) and commercial (Com) occupancy classes

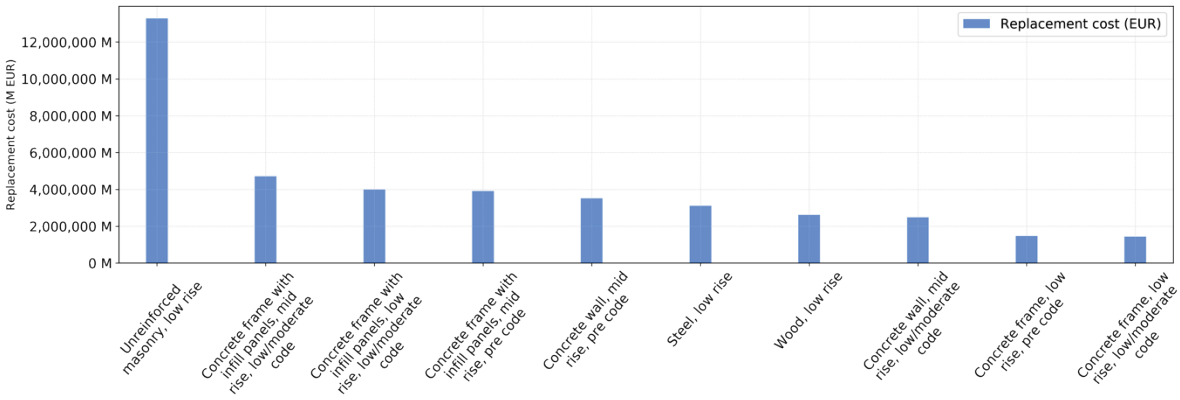

Fig. B.3 Top 10 building classes (according to the simplified taxonomy) in the European exposure model in terms of total replacement cost

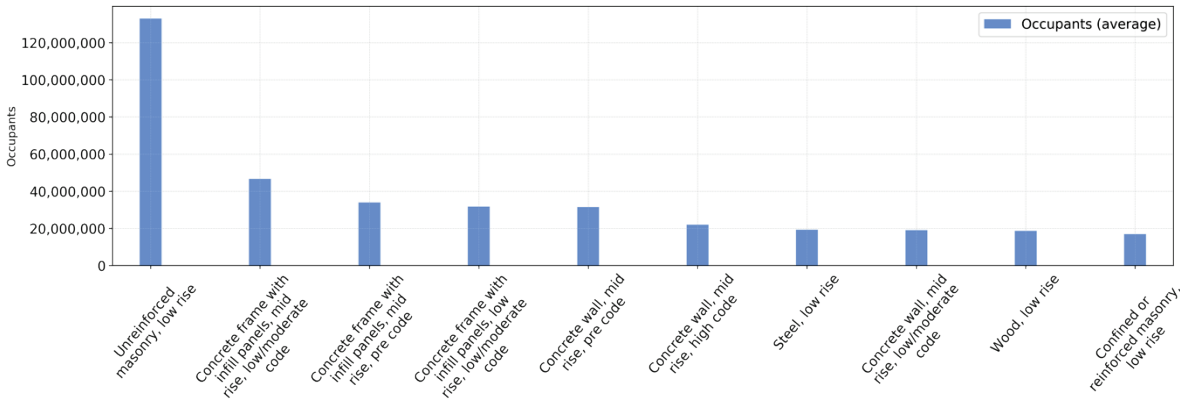

Fig. B.4 Top 10 building classes (according to the simplified taxonomy) in the European exposure model in terms of occupants